Integrated Project

ABSOLUTE - Aerial Base Stations with Opportunistic Links for Unexpected & Temporary Events

Contract No. 318632

Deliverable

FP7-ICT-2011-8-318632-ABSOLUTE/D4.2.1

System Capacity Assessments

Contractual date:	**03/2015**
Actual date:	**06/2015**
Authors/Editors:	**Karina Gomez (CNET), Leonardo Goratti (CNET), Kandeepan Sithamparanathan (RMIT), Qiyang Zhao (UoY), David Grace (UoY), Ales Svigelj, Kemal Alic, Andrej Vilhar, Tomaz Javornik (JSI), Mohit Thakur (DLR)**
Participants:	**DLR, UOY, CNET, JSI, FT, RMIT**
Work package:	**WP4 – T4.2**
Security:	**PU**
Nature:	**Report**
Version:	**V1.0**
Total number of pages:	**84**

Abstract

This deliverable aims to assess the system capacity leveraged by the ABSOLUTE architecture in both post disaster and temporary event scenarios. The ABSOLUTE network is characterized by the flexible and dynamic roll out and roll back phases of network elements to provide coverage and efficient transport of information for the public safety agencies over time and space, distinguishing whenever appropriate between the different scenarios typical of public safety. Simulations and analytical work are carried out in order to produce a realistic evaluation of the achievable ABSOLUTE system capacity. To accomplish this objective, several different aspects are hence taken into consideration including propagation models and different channel conditions, number and mobility of the users, type of traffic, network topology and terrain models. Furthermore, the different ABSOLUTE network constituents such as the Aerial eNB and the Portable Land Mobile Unit are considered both separately as well as in combination as prescribed by the ABSOLUTE system architecture to serve the Multi Mode User Equipment

Keywords

LTE System Capacity, Public Safety, Aerial eNB, Portable Land Mobile Unit, Multi Mode User Equipment, Aerial-Terrestrial, Scheduling, Learning, Wireless Sensor Networks.

Table of Contents

List of Figures

List of Tables

Abbreviations

3GPP	Third Generation Partnership Project
AAA	Authentication, Authorization and Accounting
ABSOLUTE	Aerial Base Stations with Opportunistic Links For Unexpected & Temporary Events
AeNBs	Aerial eNodeB
BAN	Body Area Network
BCQI	Best CQI
CQI	Channel Quality Indicator
CS	Combined Scheduler
DL	Downlink
DSA	Diversity Slotted Aloha
eNB	Evolved NodeB
EPC	Evolved Packet Core
FDD	Frequency Division Duplexing
FME	Flexibility Management Entity
FTP	File Transfer Protocol
ICIC	Inter-Cell Interference Coordination
LAP	Low Altitude Platforms
LTE	Long Term Evolution
MAC	Medium Access Control
MCS	Modulation and Coding Scheme
MIMO	Multiple Input- Multiple Output
MM	Maximum Minimum
MME	Mobility Management Entity
MM-UE	Multi Mode User Equipment
OFDMA	Orthogonal Frequency Division Multiple Access
PDCP	Packet Data Control Protocol
PDN	Packet Data Network Gateway
PF	Proportionally Fair
PHY	Physical Layer
PLMU	Portable Land Mobile Unit
PS	Public Safety

QCI	QoS Class Identifier
QoS	Quality of Service
RA	Ransom Access
RB	Resource Block
REM	Radio Environment Map
RF	Resource Fair
RR	Round Robin
RRH	Remote Radio head
RSRP	Reference Signal Received Power
RSRQ	Reference Signal Received Quality
RSSI	Received Signal Strength Indicator
SA	Slotted Aloha
SGW	Serving Gateway
SIC	Successive Interference Cancellation
SINR	Signal-to-Interference-plus-Noise-Ratio
SISO	Single Input Single Output
SNR	Signal-to-Noise-Ratio
SRS	Sounding Reference Signals
TDD	Time-Division Duplexing
TTI	Transmission Time Interval
UE	MM-UE Equipment
UG	User Group
UL	Uplink
WSN	Wireless Sensor Network

Executive summary

The goal of this deliverable is to evaluate the system capacity of the Aerial Base Stations with Opportunistic Links for Unexpected & Temporary Events (ABSOLUTE) network providing a complete view, discussion and meaningful results which can provide realistic figures on the capacity achievable by the ABSOLUTE system. Therefore, this includes not only the Aerial eNodeB (AeNB) installed on the Low Altitude Platforms (LAP) but also the other network components such as the Portable Land Mobile Unite and clearly the Multi-Mode User Equipment (MM-UE). The studies carried out are sufficiently general to include both post disaster and temporary event scenarios. The scenarios of public safety are characterized by sudden and temporary appearance and disappearance of an emergency, which render impossible any planning of the network in advance. Furthermore, the network could remain operatives for few days but even for a few weeks, hence demanding to optimize resources cognitively. In order to take all the advantages leveraged by the ABSOLUTE network, public safety users, or first responders, require efficient coordination on the field. This can be greatly improved by the monitoring of life and environment related parameters whereby wireless sensor networks connected directly to the PLMUs which behave as gateways in this case. The satellite signal is assumed always available to transport the traffic generated inside a cell to the command centre despite the delay introduced by a GEO satellite station

As it is will be shown hereinafter, it is crucial to take into consideration different operational conditions such as temperature, type of terrain or whether the ABSOLUTE system has to be deployed in a remote area or not. In addition, the scheduling discipline adopted to assign resources to the MM-UEs and load balancing and unbalancing techniques will show to be crucially important in the process of provisioning resources in the areas where they are mostly required. Also the type of service requested by the public safety users prove to largely affect the capacity which can be achieved either for a single user or within an entire cell covered by an aerial platform. Since the goal is to overcome most of the limitations of deployed radio technologies in the field of public safety such as TETRA, as it will be clear in the following chapters, 4G LTE can unfold the necessary capacity provided that all the network elements are deployed and satisfy the momentary requests of the MM-UEs. The central role is played by the AeNB as expected, since it is the pillar of the ABSOLUTE architecture.

1 Introduction

This deliverable shows the studies delving into the assessment of the ABSOLUTE system capacity in both post-disaster and temporary event scenarios. The objective of the ABSOLUTE project is to design a rapidly-deployable and resilient communication solution, capable of offering broadband connectivity to Public Protection & Disaster Relieve (PPDR) organizations and citizens in different situations. From the point of view of the network organization the pillars of the ABSOLUTE systems are: the Aerial evolved NodeB (AeNB), the Portable Land Mobile Unit (PLMU) and the Multi Mode User Equipments (MM-UEs), while the satellite link provisions backhaul connectivity to connect first responders with local and remote command centres or the Internet. An important additional set of nodes is constituted by the Wireless Sensor Network (WSN) devices, which can be worn by the first responders and for example can act as a body area network (BAN). Clear connection with ABSOLUTE use cases will be shown for each study.

Task 4.2 is devoted to investigate the capacity attainable with the different ABSOLUTE network components and provisioned to the MM-UEs when several options in terms of radio technologies are made available either individually or a combination thereof. In addition, since a GEO satellite can cover a wide geographical area, this link is assumed to be always present to enable backhaul connectivity. Indeed, the satellite connection could be the bottleneck for broadband services but it shall guarantee at least the presence of a radio signal. According to the hybrid system developed within ABSOLUTE, the goal is to study the system capacity at different levels:

a) **Network level:** The network capacity is evaluated taking into account all the communication links available in the different segments of the ABSOLUTE network. The results provide an overview of the overall system capacity.
b) **Link Level:** The link capacity is evaluated focusing on the different types of available technologies specifically LTE and WSN.

In the following chapters different scenarios and network configurations will be studied in order to reflect the needs of and the dangers experienced by first responders (e.g. wildfire in a forest) in predicting realistic values of the ABSOLUTE system capacity. Notice that different simulators (system and packet levels) are used to obtain the results presented in this deliverable. In this respect, more information can be found in D2.6.1 “System-Wide Simulations Planning Document”. It is important to remark that the present document, especially when i) reviewing the ABSOLUTE protocol architecture and its components, ii) the evolution of the ABSOLUTE architecture over time and iii) the uses cases and scenarios, shall be read in conjunction with D2.5.1 (Architecture Reference Model First version), D4.1.2 (Detailed Network and Protocol Architecture Second revision) and D2.1 (Use cases definition and scenarios description).

The capacity of the ABSOLUTE network depends on a number of volatile factors such as environment dependent, service dependent, location of the MM-UEs and more in general it varies over time. The achievable capacity of the ABSOLUTE system depends also on the efficiency of its main components, the AeNB and the PLMUs, and in particular how resources are scheduled. Furthermore, a cognitive approach shows to be beneficial to develop efficient resource allocation algorithms. From a more general perspective, the work presented in this deliverable will clearly show how the ABSOLUTE system can unfold capacity which outperforms existing communication technologies adopted by the public safety community.

The remainder of this document is organized as follows. Chapter 2 presents the studies carried out in LTE for AeNB and PLMU using different scheduling disciplines. Known strategies are compared with a scheduler tailored to public safety under different operational conditions of the first responders

and propagation models of the radio signal. Chapter 3 evaluates the capacity of the radio links between the AeNB and the MM-UEs as well as between the PLMUs and the MM-UEs during roll out and roll back phases. The approach is modular and cognitive with Q Learning and Transfer learning methods applied together with different scenario-dependent parameters. Chapter 4 shows an in-depth simulation study on the achievable capacity of the ABSOLUTE system in a large forest area affected by a wildfire. Radio Environment Map (REM) is used to evaluate coverage while at the same time different services such as VoIP and File Transfer Protocol (FTP) are simulated in case network resources are provisioned by the AeNB, PLMUs and the commercial network infrastructure of a telecom operator. In all cases the users are mobile over the incident area. Chapter 5 presents the study of sensor networks in which sensor traffic is generated by the MM-UEs and transmitted to multiple PLMU units. The sensor traffic could be aggregated by the MM-UE but generated by wearable sensors as well as it could be generated by sensors embedded directly in the MM-UE. Finally, Chapter 6 provides the conclusions of this deliverable.

2 LTE System Capacity Estimation of ABSOLUTE Network Components

ABSOLUTE project [1] incorporates LTE links in an innovative Aerial Terrestrial and Satellite network architecture. Both ABSOLUTE network components, AeNB and PLMU, support LTE technology for providing coverage and capacity in both post disaster and temporary event scenarios. The adoption of 3GPP LTE as candidate for public safety communications introduces a unique opportunity to improve the response of public safety MM-UEs and bring high-level applications to the MM-UE equipments (UEs) of the first responders. Indeed, the release 12 of 3GPP will enhance the features of LTE-Advanced, the starting point for future 5G communications systems, to meet the requirements of public safety communications [2][3]. Establishing common technical standards for commercial and public safety networks offers several advantages to both communities. So far, two major enhancements for public safety communications will be included in the release 12. These features include D2D communication for mobiles in physical proximity and group call.

In LTE an important function is the scheduling, which affects the system performance mainly in terms of achievable throughput and Quality of Service (QoS) of the MM-UEs. Since 3GPP does not define any specific uplink or downlink scheduling algorithm, several proposals can be found in the literature [4][5]. Schedulers that are often implemented in practice in LTE systems are best Channel Quality Indicator (BCQI), Proportionally Fair (PF) and Round Robin (RR) [6]. These schedulers have different objectives that include i) the best utilization of the available resources for increasing network performance in terms of fairness, throughput and bandwidth utilization and ii) assign the available resources more promptly and faster to the MM-UEs.

Emergency and commercial systems typically are designed and deployed to satisfy different needs and have different requirements, which are directly affecting the QoS of the communications. The unique and vital nature of public safety also affects the technical decisions that are necessary to guarantee connectivity and minimum bit-rate for everyone, anywhere and anytime, albeit this could imply decreasing the overall system utilization. On the other hand, the unpredictable nature of disaster scenarios is accompanied by adversarial changes of channels conditions and unexpected variation of the traffic. Public safety officers inside destroyed buildings or tunnels can experience poor channel conditions affecting the quality of the communications and isolating the officers from the group. Hence, it is mandatory to design smarter resource allocation schemes for distributing them between all the MM-UEs and guarantee connectivity also to those with bad channels since they are the most vulnerable.

In this chapter, we propose a simple and effective uplink and downlink scheduler for emergency communications, namely Public Safety (PS) scheduler that relies on the channel condition sub-grouping policies for scheduling MM-UEs. The sub-grouping policies classify the MM-UEs based on their channel quality similar to the multicast channel scheduling used in [7]. Our approach prioritize public safety MM-UEs with poor channel conditions while trying to maximize the user's throughput. By means of simulations of the proposed scheduler, we quantify the average achievable cell throughput and fairness and we compare the results of different schedulers. We demonstrate that the PS scheduler is capable to distribute more evenly the resources to the users, though at the cost of introducing a penalty in the system's capacity utilization.

We also provide a comparative study of different scheduling disciplines in ABSOLUTE network focusing on both post disaster and temporary event scenarios. The system capacity analysis focuses on AeNBs and PLMUs working under different uses cases and scenarios as described in D2.1 (Use cases definition and scenarios description). The system capacity analysis is also performed using the different LTE bandwidth and scenario dependent parameters in order to measure the maximum capacity achieved by the AeNBs and PLMUs under different configurations

2.1 Scheduling Schemes in LTE-based Networks

The way resources are scheduled in LTE is affected by both the radio and traffic conditions. An important indicator in LTE is the QoS Class Identifier (QCI), which denotes the traffic characteristics. The QCI defines the attributes of the bearer[1] such as guaranteed bit-rate, target delay and loss requirements. The base station translates the QCI attributes into logical channel attributes for the air-interface and the upper layers scheduler reacts accordingly to these attributes. Over time, LTE transmissions are organized in radio frames (each radio frame consists of 10 sub-frames of 1 ms each) and the resource blocks (RBs) over frequency (each RB consists of 12 sub-carriers with 15 kHz of spacing). The graphical representation of a RB is shown in the figure below.

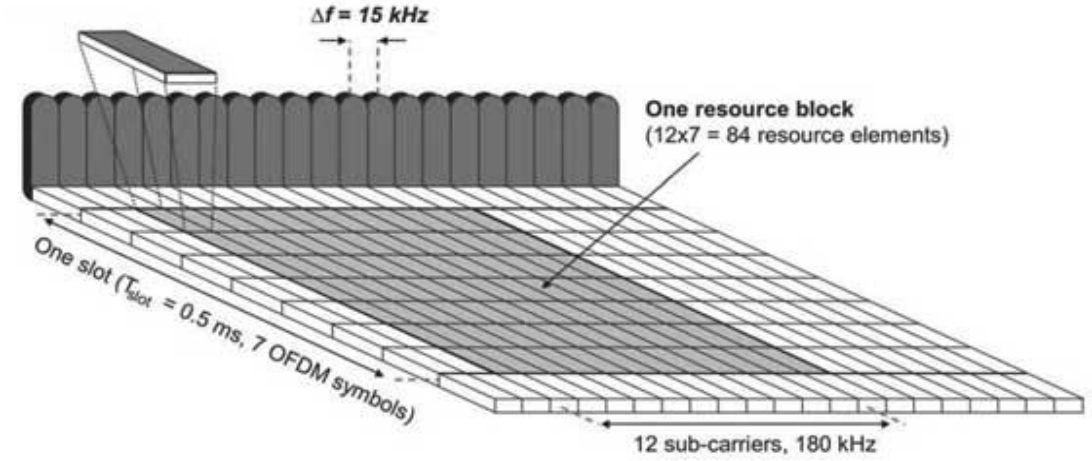

Figure 2-1: LTE resource block graphical representation.

In LTE systems each physical channel (resource block) has a corresponding quality indicator expressing channel conditions, which differs between the uplink and downlink transmissions. In practice, in the downlink case this information is provided by the UEs through the feedback of Channel Quality Indicators (CQIs). In the uplink, the base station may use Sounding Reference Signals (SRSs) or other signals transmitted by the UEs to estimate the channel quality. A higher CQI value denotes a better channel condition with the CQIs quantified by 16 standard values [8]. Since in LTE each physical channel has a corresponding quality indicator, the role of the resource scheduler in the MAC layer is to map the quality of a communication to the corresponding CQIs and SRSs.

2.1.1 LTE-Based Commercial Networks

The majority of the LTE-based scheduling schemes proposed in literature [5][6] are based on maximizing fairness and throughput. In [5], authors design an LTE downlink scheduler combining fast

[1] Bearer is a logical channel for data flows which requires specific QoS levels.

computing algorithms and resource scheduling. In order to study strengths and drawbacks of the different schedulers a comparison in terms of performance is presented in [6].

- **Best Channel Quality Indicator (BCQI):** The BCQI scheduler is an unfair scheduling scheme, which is based on the best channel condition strategy [6][9]. Only MM-UEs with the best channel conditions are scheduled across the available RBs. This scheduler aims to maximize the cell throughput but usually penalizes the MM-UEs with worse channel conditions.
- **Round Robin (RR):** To enhance the MM-UE fairness the RR scheduler can be used. The RR is a fair scheduling scheme simple and easy to implement [6]. In this case, MM-UEs are scheduled with the same amount of RBs without taking the CQI into account. Since the channel conditions of the MM-UEs are not considered, this scheduler usually decreases the cell throughput compared to BCQI but improves the fairness.
- **Proportionally Fair (PF):** A compromise between BCQI and RR scheduler is achieved by PF [10][11]. The PF is a scheduling scheme that is based on a balancing strategy. Each MM-UE is scheduled using a utility function that takes into account the CQI and the amount of RBs assigned. This scheduler tries to maximize the cell throughput while enhancing the fairness at the same time.
- **Resource Fair (RF):** Similar to PF, the RF scheduler [11] tries to maximize the sum rate of all MM-UEs while guaranteeing fairness with respect to the amount of RBs allocated to the MM-UEs.
- **Maximum Minimum (MM):** The MM scheduler [6] achieves the best fairness maximizing the minimum of the MM-UE throughputs. This scheduler guarantees equal throughput to all the MM-UEs. Notice that in MM scheduler the throughput of one MM-UE cannot be increased without decreasing the throughput of another device.

The schedulers mentioned above were designed for commercial networks and they are unable to catch all the peculiarities of public safety communications. On the other hand, our proposed PS scheduler is designed in the context of emergency communications with the explicit goal of providing fairness in the distribution of the LTE resources, prioritizing the MM-UEs with poor channels conditions, while at the same keeping the system utilization as high as possible.

2.1.2 LTE-Based Public Safety Networks

The schedulers described above were designed for commercial networks and they are not optimized to catch all the peculiarities of communications in the field of public safety. Since LTE is the next candidate technology for public safety networks, only few studies in the literature tackles on scheduling for public safety applications. In [12] MAC level resources allocation focusing on uplink/downlink real-time video transmissions is investigated. In the model proposed, MM-UEs are connected to Remote Radio Heads (RRH) deployed throughout the cell and connected to a central base station. The authors argue that distributing RRHs in the cell enhances the channel gains of all the MM-UEs and reduces the negative effects due to the MM-UE with degraded channel conditions. However this consideration is not valid for disaster scenarios where part of the communication infrastructures can be destroyed. In such scenarios, survived or temporarily deployed base stations can provide coverage to the MM-UEs with both good and bad channel conditions, a topic which we address in this chapter.

Scheduling at the upper layers level is discussed in [13] and [14]. In [13] the advantages of using commercial networks for public safety purposes are discussed. The authors remark that LTE

technology provides a wide range of capabilities to support priority, specifically CQI, which can be used for resource allocation decisions. Similarly in [14], a LTE-based architecture for public safety applications is proposed. Authors discuss how the LTE radio admission control mechanisms and allocation-retention priority scheme can be adapted to the public safety MM-UEs for differentiating with commercial MM-UEs. Such mechanisms used at the upper layers can be complemented with the schedulers proposed and studied in this chapter.

2.2 Scheduler for Public Safety Communications

The intervention of first responders can be greatly improved making available a communication system capable of offering broadband wireless access to interconnect different devices to local and remote control centres in a quick and reliable manner. In Figure 2-2, the high-level architecture adopted in ABSOLUTE project (Hybrid Aerial-Terrestrial Architecture) is depicted. The architectural components are designed as standalone ground and aerial platforms that can be rapidly deployed in areas where physical access is impeded to first responders. Thus, low altitude platforms are deployed using helikites equipped with an LTE payload and capable of acting as base stations, the AeNB. Furthermore, PLMUs equipped with an LTE interface are also deployed to provide additional capacity and coverage to first responders. Both AeNBs and PLMUs embed a satellite modem and antenna for connectivity to a GEO satellite module, enabling both inter-AeNBs and back-hauling services. Finally, MM-UEs equipped with LTE and satellite interfaces are used as handhelds. The role of each network component is to improve availability and reliability of the communications for the PS MM-UEs.

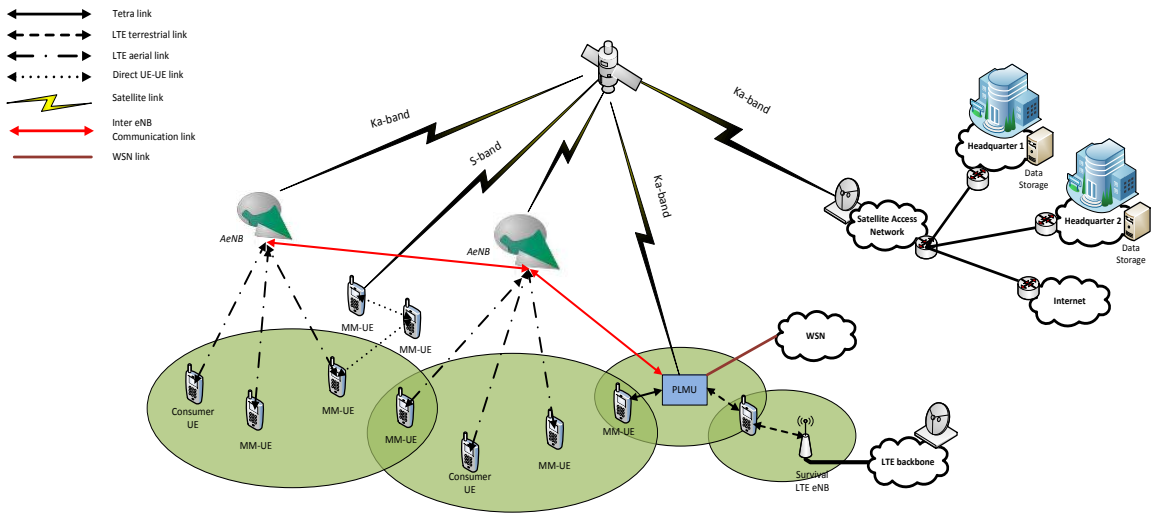

Figure 2-2: Overall ABSOLUTE architecture.

We analyse the scenarios (either during special events or post-disasters) in which some MM-UEs experience poor channel conditions. Figure 2-3 shows the scenario that we deem to investigate for the schedulers. In this scenario, the communication of public safety MM-UEs inside buildings, tunnels or even building on fire are affected by bad channel conditions. Therefore, the scheduling is done at the MAC layer and MM-UEs with bad channels conditions are prioritised by the scheduler. In this context, it worth to emphasize that poor channel conditions exclude the case of isolated UEs (i.e. CQI=0) since in this case there is no scheduling discipline which can be applied. A critical aspect that we need to take into account is that the channel state information of the UEs available at the AeNB side must be up-to-date. In this work, we assume that the CQI value of each RB on a per MM-UE basis is available at the AeNB in each Transmission Time Interval (TTI).

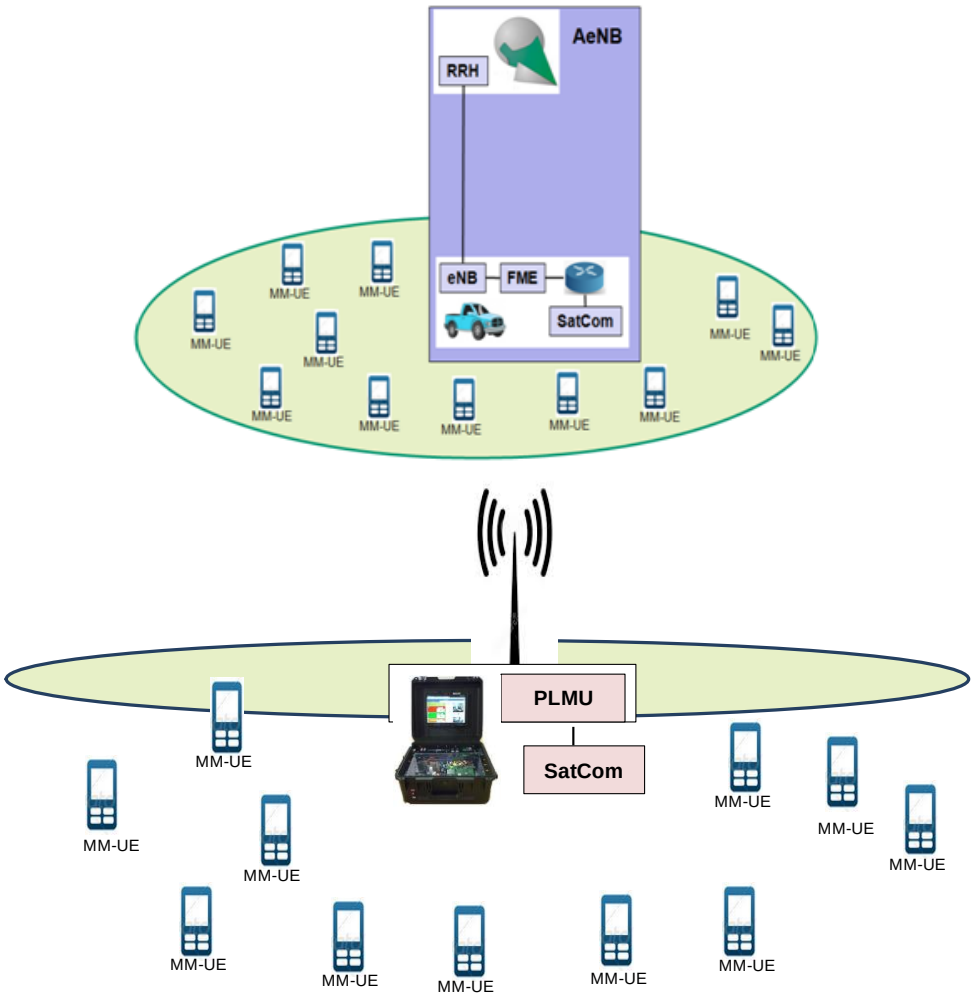

Figure 2-3: Scenarios considered for LTE resource scheduling (AeNB and PLMU).

As mentioned, in ABSOLUTE, the assessment of the LTE system capacity is valid in both post-disasters and temporal event scenarios. Specifically, Table 2-1 summarizes the scenarios and the use cases with the involved LTE equipments/subsystems, explicitly referring to those identified in *D2.1 (Use cases definition and scenarios description)*.

Table 2-1: Scenarios and use cases with involved equipment/subsystems (LTE systems on board).

	Use case	Primary equipment	Secondary equipment	Description
Public Safety	ABS.UC.01	AeNB, PLMU	MM-UE	Unitary call and data transfer
	ABS.UC.02	AeNB, PLMU	MM-UE	Unitary call with a terrestrial backhaul
	ABS.UC.03	PLMU		Enabling a new First-Responder user
	ABS.UC.04	PLMU		Media upload to the PLMU
	ABS.UC.05	PLMU	MM-UE	Unified group call
	ABS.UC.10	MM-UE	AeNB, PLMU, Ka-band satellite	Communication from MM-UEs to a remote peer through satellite

				link
	ABS.UC.11	MM-UE	AeNB, PLMU, Ka-band satellite	Inter-cell communications via the MM-UE's Ka-band links
	ABS.UC.17	AeNB		Roll-out phase of an AeNB in the context of a disaster
	ABS.UC.18	AeNB		Roll-back phase of an AeNB in the context of a disaster
	ABS.UC.22	MM-UE		Direct communications with MM-UEs in relay-mode
Temporary Event	ABS.UC.12	MM-UE	AeNB, PLMU, Ka-band satellite	Inter-cell communications via the MM-UE's Ka-band links for temporary events
	ABS.UC.15	PLMU/WSN	MM-UE	WSN-assisted crowd monitoring and staff coordination
	ABS.UC.16	PLMU/WSN	MM-UE	Use of body area wireless sensor network in moving events
	ABS.UC.19	AeNB		Roll-out phase of an AeNB in the context of a temporary event
	ABS.UC.20	AeNB		Roll-back phase of an AeNB in the context of temporary event

2.2.1 PS Scheduler in LTE

We consider an LTE-based cellular network where one base station is serving a set of i UEs (i=1, 2,..., m). The downlink bandwidth is divided into a set of maximum j RBs (j=1, 2,..., n), which will be fed in input to the scheduling vector $\Delta(1, 2, ...,n)$. We assume that the base station has always at least one packet waiting for transmission to each UE (traffic saturation conditions). In terms of scheduled resources, a UE can be assigned with a minimum of one RB in frequency and one TTI (simple denoted by t hereinafter) over time. We now define the matrix Γ, whose values α_{ij} denote the CQI corresponding to UE i and RB j. In the base station each α_{ij} is represented by 16 standard values as specified in [2] and shown in Table 2-2.

Table 2-2: Channel quality indicator.

CQI (α)	Modulation	Approximate Code Rate	Information bits per symbol
0	no transmission	–	–
1	QPSK	0.076	0.1523
2	QPSK	0.120	0.2344
3	QPSK	0.190	0.3770
4	QPSK	0.300	0.6016
5	QPSK	0.440	0.8770
6	QPSK	0.590	1.1758
7	16-QAM	0.370	1.4766
8	16-QAM	0.480	1.9141
9	16-QAM	0.600	2.4063
10	64-QAM	0.450	2.7305

11	64-QAM	0.550	3.3223
12	64-QAM	0.650	3.9023
13	64-QAM	0.750	4.5234
14	64-QAM	0.850	5.1152
15	64-QAM	0.930	5.5547

At time *t*, we compute the average CQI ($\bar{\alpha}_i$) for the i_{th} UE, where we take the values in Γ and we average with respect to the *j* RBs. After that, the scheduling priority of the UEs in the proposed scheduler is done organizing the $\bar{\alpha}_i$ in descending order. The lower the average CQI value, the higher the scheduling priority. The average CQI value is computed as follows:

$$\bar{\alpha}_i(t) = \frac{1}{n}\sum_{j=1}^{n} \alpha_{ij}(t). \quad (2\text{-}1)$$

Each value of α corresponds to a specific modulation and coding scheme (MCS), determining in this way the maximum capacity of a RB. Therefore, the information carried by the RBs depends on α_{ij}. The value of α maximizing the capacity of the UE *i* per RB *j* in each time t is the following

$$\alpha_i * (t) = \max_j\{\alpha_{ij}(t)\}, \quad (2\text{-}2)$$

where α_i* is the best available RB for each UE *i* at each time *t*. In order to distribute equally the *n* RBs among the set of *m* UEs, the maximum number of RBs assigned to UE *i* is denoted by β and calculated as follows

$$\beta(t) = \begin{cases} 1 & \text{if } \frac{n}{m} \leq 1 \\ \left\lfloor \frac{n}{m} \right\rfloor & \text{if } \frac{n}{m} > 1 \end{cases}, \quad (2\text{-}3)$$

2.2.1.1 **LTE Scheduling in Downlink**

The PS scheduler makes use of equations (2-2) and (2-2) for scheduling the UEs in the best available RBs as illustrated in **Algorithm 1**. The proposed PS algorithm schedules the UEs as described in the steps below:

- **Step 1:** UEs in Γ are scheduled with a priority decreasing as $\bar{\alpha}_i$ increases. In this way, the UEs with poor channel conditions are scheduled first using the best available RBs in terms of CQI (see line 5 in **Algorithm 1**).
- **Step 2:** For each UE in Γ, the highest α_{ij} value across the *n* available RBs is selected (α_i*). Thus, the best RB *j* for allocating the UE is identified (see lines 7, 8 and 9 in **Algorithm 1**).
- **Step 3:** The RB *j* is allocated to UE *i* and marked in the scheduling vector Δ (see lines 10 and 11 in **Algorithm 1**). Then the RB *j* is deleted from the set of available RBs and it will not be available at the next iteration (see line 12 in **Algorithm 1**).

The PS scheduler iterates steps 2 and 3 until all RBs have been assigned to the UEs (see line 5 in **Algorithm 1**).

Algorithm 1: LTE Scheduling in Downlink.

1	Let Γ be the matrix with dimension [*m*,*n*],
2	Let α_i* be the maximum α_{ij} value of UE *i*,
3	Let β be the maximum number of RBs assigned to UEs,

```
4  Let Δ be the scheduler vector of n RB,
5  While {∃ Δ(j) = Ø} do RBs are still available
6      For all m UE Є Γ do
7          UE i is being scheduled
8          αi* ←max_j{α_ij},
9          select highest α_ij value across the all n RBs of UE i
10         pick the RB j, which contains α_i*
11         Δ(j)← i, assign RB j to UE i
12         Γ[ :, RB(j)]=0, remove the α_j values of RB j
13         (next round) the RB j will not be considered as available
14     End for
15 End while
```

2.2.1.2 LTE Scheduling in Uplink

The PS uplink scheduler takes into account the constraint that in LTE only RBs that are consecutive in frequency can be allocated to the same UE. Thus, the RBs are divided in groups of β RBs each (a group of RBs is indexed by k). The total number of non-overlapping groups that can be created with n RBs is equal to the integer part of (n/β). The α_{ij} values[2] of each group of RBs are aggregated in the variable Φ_{ik} as follow $\Phi_{ik}=[\alpha_{ij}(t)+\alpha_{i(j+1)}(t)+...+\alpha_{i(j+\beta)}(t)]$. The value of Φ maximizing the capacity of UE i in each time t is the following:

$$\Phi_i^* = \max_k\{\Phi_{ik}(t)\}, \tag{2-4}$$

where Φ_i^* is the best available group of RBs for each UE i at each t.

Algorithm 2: LTE Scheduling in Uplink.

```
1  Let Φ_i* be the maximum Φ_jk value of UE i,
2  While {∃ Δ(k) = Ø} do groups of RBs are still available
3      For all m UE Є Γ do
4          If UE i is unscheduled then
5              select highest Φ value across the groups of RBs of UE i
6              Φ_i* ←max_{Φ⊂Γi} {Φ_ik}
7              pick the group of RBs k, which contains Φ_i*
8              If Δ(k)←Ø then This group of RBs is unassigned
9                  assign group of RBs k to UE i, Δ(k)← i
10                 mark UE i as scheduled
11             End if This group of RBs is already assigned
12             Φ_i*=0, remove the maximum Φ_ik value
13             (next round) select the next highest Φ_ik value for UE i
14         End if
15
```

[2] Notice that we assume that CQIs may be used as indicators also for the uplink channel conditions since using SRSs or CQIs will not affect the general purpose of the proposed uplink PS.

16	**End for** **End while**

The PS scheduler relies on equation (2-4) for scheduling the UEs across the group of best available RBs as described in **Algorithm 2** and summarized below.

- **Step 1:** As before, the scheduling priority of the UEs in Γ is organized with respect to $\bar{\alpha}$i and in particular assigning a higher priority to UEs with lower $\bar{\alpha}_i$. UEs with poor channel conditions are scheduled first (see line 3 in **Algorithm 2**).
- **Step 2:** For each (unscheduled) UE in Γ, the highest Φ_i value across the available group of RBs is selected (Φ_i*). Thus, the best group of RBs for allocating the UE is identified (see lines 5, 6 and 7 in **Algorithm 2**).
- **Step 3:** If the group of RBs k is unassigned, this group is allocated to UE i in the scheduling vector Δ and the UE i is marked as scheduled (see lines 9 and 10 in **Algorithm 2**).
- **Step 4:** If the group of RBs *k* is already assigned, this group is deleted from the set of available RBs. Thus, the next group of RBs with the highest Φ_{ik} will be selected at the next iteration (see lines 12 and 13 in **Algorithm 2**).

The PS scheduler iterates steps 2, 3 and 4 until all the groups of RBs have been assigned to the UEs. Figure 2-4 shows an illustrative example of downlink and uplink scheduling of UEs with bad and good channel conditions, respectively. For clarity the example is limited to a set of 3 UEs camping in a single cell with 6 available RBs. The green coloured cells highlight the RBs selected following the policies of a-b) BCQI, c-d) RR and f-g) PS schedulers. The figure highlights that the proposed PS scheduler provides a compromise in distributing the available RBs among UEs with good and bad channel conditions. Simulation results are obtained whereby the Matlab LTE simulator presented in [17][18].

CQI		Resource Block						
		1	2	3	4	5	6	Mean
UE	3	6	2	1	3	4	8	4.00
	1	8	9	9	7	11	6	8.33
	2	10	11	14	12	10	9	11.00
BCQI		UE2	UE2	UE2	UE2	UE1	UE2	
CQI		10	11	14	12	11	9	
∑(CQI)		67						

(a) Downlink BCQI Scheduler

CQI		Resource Block						
		1	2	3	4	5	6	Mean
UE	3	6	2	1	3	4	8	4.00
	1	8	9	9	7	11	6	8.33
	2	10	11	14	12	10	9	11.00
BCQI		UE2	UE2	UE2	UE2	UE2	UE2	
CQI		10	11	14	12	10	9	
∑(CQI)		66						

(b) Uplink BCQI Scheduler

CQI		Resource Block						
		1	2	3	4	5	6	Mean
UE	3	6	2	1	3	4	8	4.00
	1	8	9	9	7	11	6	8.33
	2	10	11	14	12	10	9	11.00
RRS		UE3	UE1	UE2	UE3	UE1	UE2	
CQI		6	9	14	3	11	9	
∑(CQI)		52						

(c) Downlink RR Scheduler

CQI		Resource Block						
		1	2	3	4	5	6	Mean
UE	3	6	2	1	3	4	8	4.00
	1	8	9	9	7	11	6	8.33
	2	10	11	14	12	10	9	11.00
RRS		UE3	UE3	UE1	UE1	UE2	UE2	
CQI		6	2	9	7	10	9	
∑(CQI)		43						

(d) Uplink RR Scheduler

CQI		Resource Block						
		1	2	3	4	5	6	Mean
UE	3	6	2	1	3	4	8	4.00
	1	8	9	9	7	11	6	8.33
	2	10	11	14	12	10	9	11.00
PSS		UE3	UE1	UE2	UE2	UE1	UE3	
CQI		6	9	14	12	11	8	
∑(CQI)		60						

(e) Downlink PS Scheduler

CQI		Resource Block						
		1	2	3	4	5	6	Mean
UE	3	6	2	1	3	4	8	4.00
	1	8	9	9	7	11	6	8.33
	2	10	11	14	12	10	9	11.00
PSS		UE1	UE1	UE2	UE2	UE3	UE3	
CQI		8	9	14	12	4	8	
∑(CQI)		55						

(f) Uplink PS Scheduler

Figure 2-4: Example for the scheduler using different policies.

2.3 LTE-level Capacity Evaluation

To compare the different schedulers, a MATLAB-based LTE simulator is used [15]. The comparison is done in terms of achievable throughput and fairness with MM, RR, PF, RF and BCQI schedulers [15]. The fairness is quantified using Jain's fairness index [16], denoted by $\mathcal{J}$, which measure the fairness among the MM-UEs. The index $\mathcal{J}$ is a set of values for the m MM-UEs as shown below:

$$\mathcal{J}(T_1, T_2, \dots, T_m) = \frac{\left(\sum_{i=1}^{m} T_i\right)^2}{m.\sum_{i=1}^{m} T_i^2}, \quad (2\text{-}5)$$

where, T_i is the throughput for the i_{th} MM-UE. The ideal case of fairness is achieved when the index $\mathcal{J}$ is equal to 1 reflecting the situation in which all MM-UEs receive an equal amount of resources. While decreasing fairness is reflected by the decreasing value of the $\mathcal{J}$ index.

2.3.1 Simulation Description and Parameters

In this section, the LTE system capacity of the AeNB is analyzed and also in this case the evaluation we carry out applies to post-disasters and temporal events scenarios.

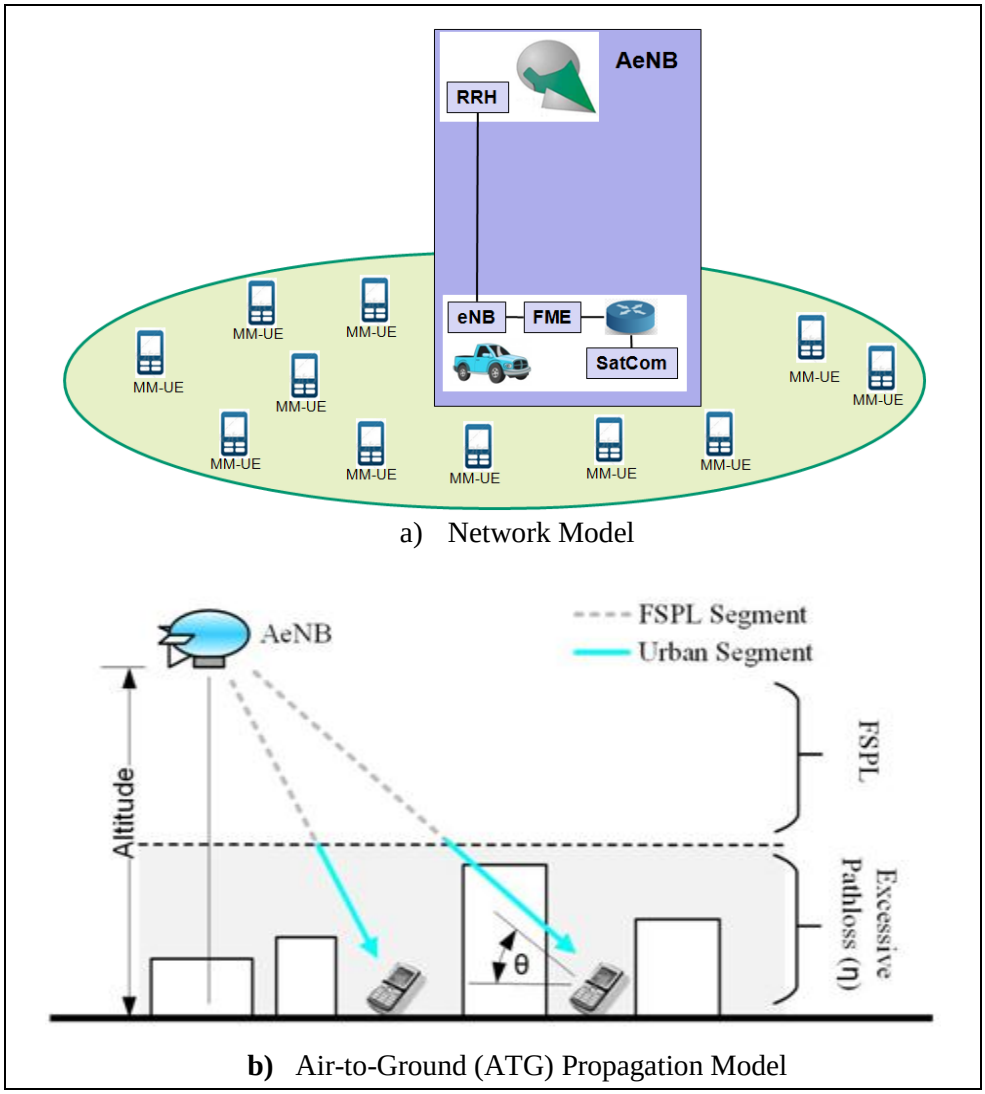

Figure 2-5: Simulation scenario considered for the LTE resource scheduling for AeNB.

Specifically, **Erreur ! Source du renvoi introuvable.** summarizes the scenarios and use cases with involved LTE equipment/subsystems. For more details refer to *D2.1 (Use cases definition and scenarios description)*. Table 2-3 shows the simulation parameters used in the LTE simulator based on the 3GPP specifications [8]. The simulation setup consists of a single cell, where one AeNB or PLMU with an omni-directional antenna is located at the centre of the cell and SISO discipline is applied. The targeted area is a square of 5000 meters x 5000 meters. Figure 2-5 shows the simulation scenario and the way the Air-To-Ground (ATG) propagation model is adopted in order to obtain the AeNB performance evaluation. The cell is configured in Frequency-Division Duplex (FDD) mode in uplink and downlink directions. Bandwidth values used are 1.4, 3, 5, 10, 15 and 20 MHz in both downlink and uplink considering QPSK, 16-QAM and 64-QAM modulations. These bandwidths are equivalent to 6, 15, 25, 50, 75, and 100 RBs, respectively. In the simulation, an increasing number of UEs is assumed [5, 10, 20, 30, 40, 50], with the terminals uniformly distributed inside the cell. A statistical propagation model is used to predict the ATG path-loss between the AeNB and MM-UEs [19]. On the other hand, the Ericsson channel model is used to evaluate the path-loss between the PLMU and MM-UEs [20].

Table 2-3: Simulation parameters and assumptions.

Parameter	Value
AeNB Altitude	1000 m for the LAP 3 m for the PLMU
Duplex Mode	Frequency-Division
System bandwidths (*W*)	[1.4, 3, 5, 10, 15, 20] MHz
Number of RBs	[6, 15, 25, 50, 75, 100]
Carrier frequency (*f*)	2600 MHz
RB bandwidth	180 kHz
TTI	1 ms
Modulation	QPSK, 16–QAM, 64–QAM
Transmission Power (P_{TX})	23 [dBm] (including antenna Gain)
Elevation angle between the MM-UEs and the AeNB	15^{o} for the LAP
Temperature (*T*)	20 ºC
Channel Model	ATG Channel Model for AeNB [19] Ericson channel model for PLMU [20]
Environment Properties	Dense–urban
Antenna configuration	1 transmit, 1 receive (1x1)
Receiver sensitivity	-107.5 [dBm] (20ºC, 50 RB)
Noise figure of the MM-UE (*N*)	-7 [dB]
MM-UE distribution	Uniform
Served MM-UEs	[1, 25]
Traffic model	Infinite backlogged
Schedulers	BCQI, PF, RF, RR, MM,PS

The licensed carrier frequency is fixed to 2.6 GHz, which is the choice of ABSOLUTE project for public safety communications. To map the channel conditions of the users, CQI values are generated as specified in [15]. The MM-UEs receiver sensitivity is set to -107.5 dBm (for 20°C and 50 RBs). Based on the receiver sensitivity, it is assumed that the communication between MM-UEs and AeNBs or PLMUs is possible only with SNR values higher than -5 dB. Traffic is modelled with an infinite backlog of packets in which nodes are assumed in saturation conditions. The simulation results are averaged over 1000 different simulations (however 95% confidence interval is too small to be identified in the figures).

2.3.2 AeNB-level Capacity Evaluation

In this section the LTE system capacity of the AeNB is analyzed for the scenarios identified in **Erreur ! Source du renvoi introuvable.**, which involves AeNB as primary or secondary equipment

(for more details refer to *D2.1, Use cases definition and scenarios description)*.

2.3.2.1 **Effect of the SNR on the AeNB Capacity**

We focus on the AeNB network and consider that the commercial infrastructure could be destroyed or temporarily overloaded. The coverage area of the AeNB as well as the SNR is computed using the free space and the ATG propagation models for a 10 MHz LTE bandwidth. Figure 2-6 shows the received power P_{RX} and the SNR distribution across the coverage area of the AeNB.. As it can be seen, the SNR is distributed between 1 and 25 dB and we notice that the AeNB can achieve a good coverage area over the targeted region. Thus, in order to show how the CQI values affect the AeNB system capacity, we run preliminary experiments using the average received SNR distributed in the range between 1 dB and 25 dB (in steps of 1dB) for 25 MM-UEs which have been deployed in the cell. The objective of this set of simulations is to show how the SNR and the CQI values associated to the MM-UEs affect the capacity of the ABSOLUTE system. In addition, this experiment gives a clear view about the behaviour of the different scheduling disciplines.

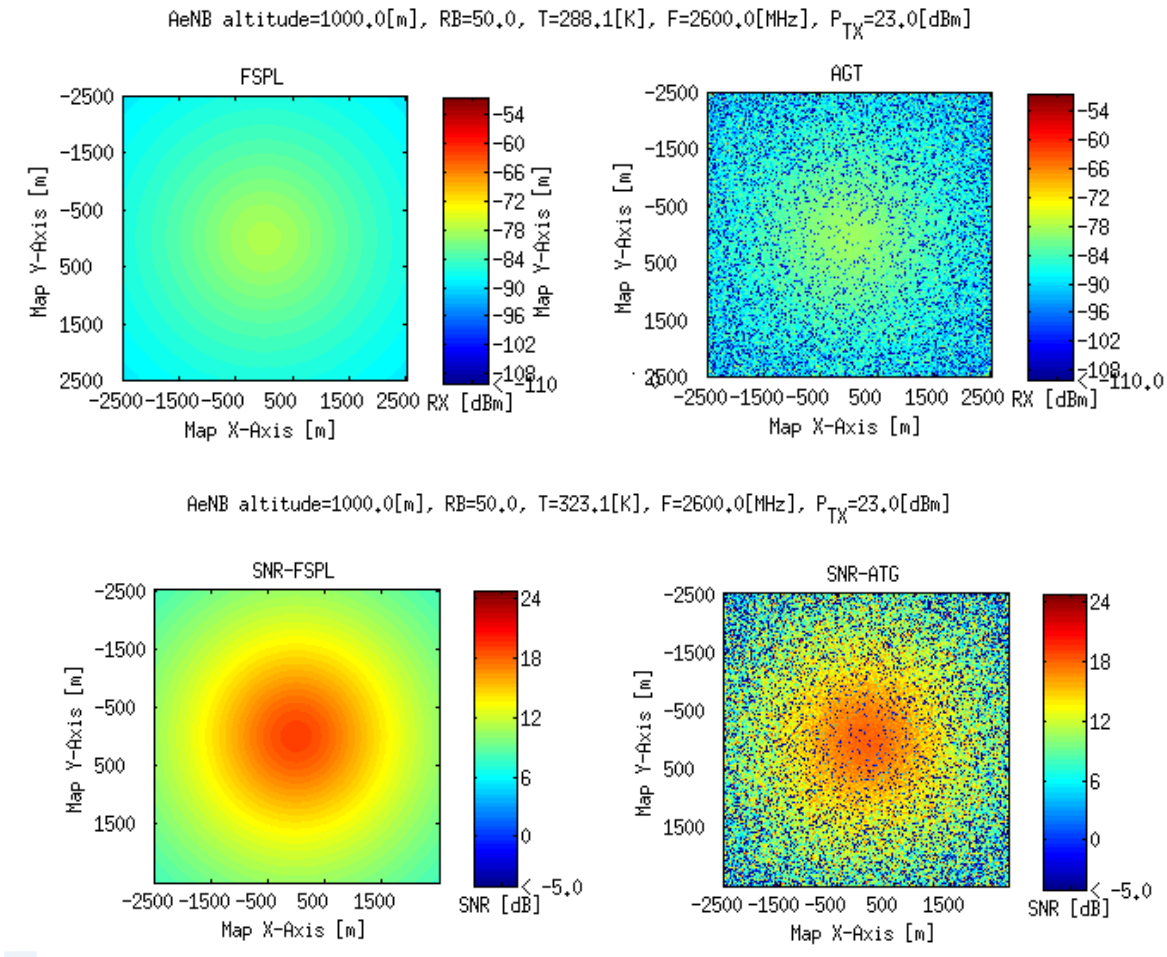

Figure 2-6: P_{RX} and SNR distribution over the coverage area of the AeNB. (P_{TX}=23 dBm, W=10 MHz, Dense–urban Scenario, f=2.6 GHz).

Figure 2-7 shows the performance of different schedulers in terms of user's throughput versus SNR. The cell is configured with 10 MHz bandwidth (the 25 MM-UEs experience an average SNR ranging from 1 to 25 dB for all cases of interest showed with a granularity of 1 dB). The results were obtained for BCQI, PF, RF, RR, MM and PS schedulers, respectively. Along this line, Figure 2-8 shows the comparison of the user's throughput achieved with the different schedulers.

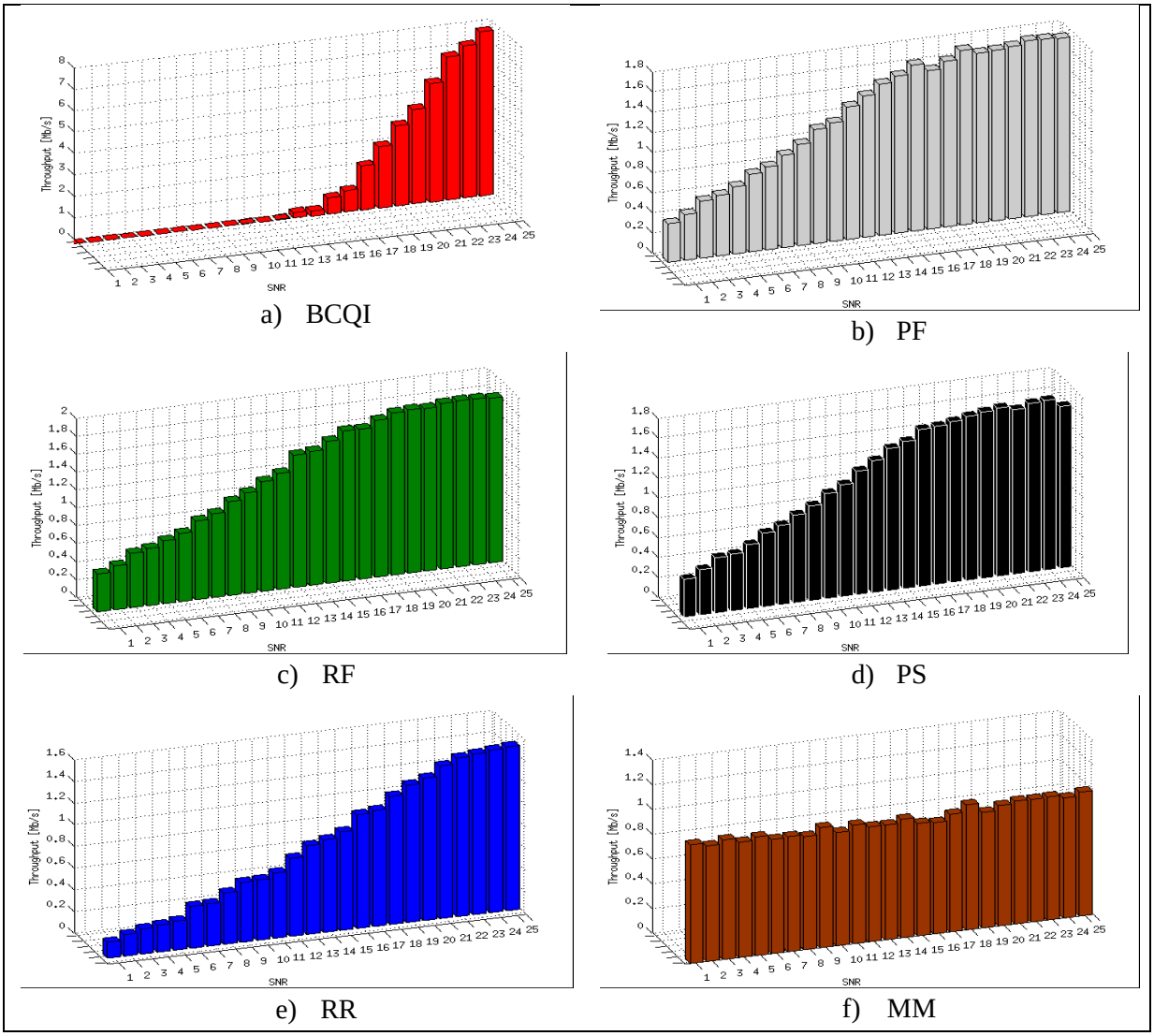

Figure 2-7: MM-UE average throughput achievable within a cell configured with 10 MHz bandwidth vs. SNR. The cell is serving 25 users with average SNR from 1 to 25 dB in steps of 1 dB (organized by the scheduler).

From Figure 2-7 and Figure 2-9, we are able to do the following observations:

- The highest cell throughput is achieved using the BCQI scheduler since it serves only MM-UEs with good channel conditions, which corresponds to UEs with SNR ranging from 13 dB up to 25 dB. In terms of fairness, the worst fairness is achieved with the BCQI scheduler as expected.
- A compromise is achieved using PF, RF and PS schedulers since the channel conditions of the MM-UEs are taken into account for allocating the resources. Good fairness is also achieved with the PF, RF and PS schedulers complementing the good performance achieved in terms of throughput.
- The lowest cell throughput is achieved using the RR scheduler since it allocates the resources without taking into account the channel conditions of the MM-UEs. The figure shows clearly the behaviour of the scheduler, the throughput is directly proportional to the SNR (channel conditions). In terms of fairness, the RR scheduler performs better than BCQI but worse than PF, RF and PS.

- Similar cell throughput is achieved using the MM scheduler since it maximizes the minimum of the users' throughput. As it can be seen, all the MM-UEs have equal throughput. In terms of fairness, the best is achieved with the MM scheduler since it divides the resources equally amongst the MM-UEs.

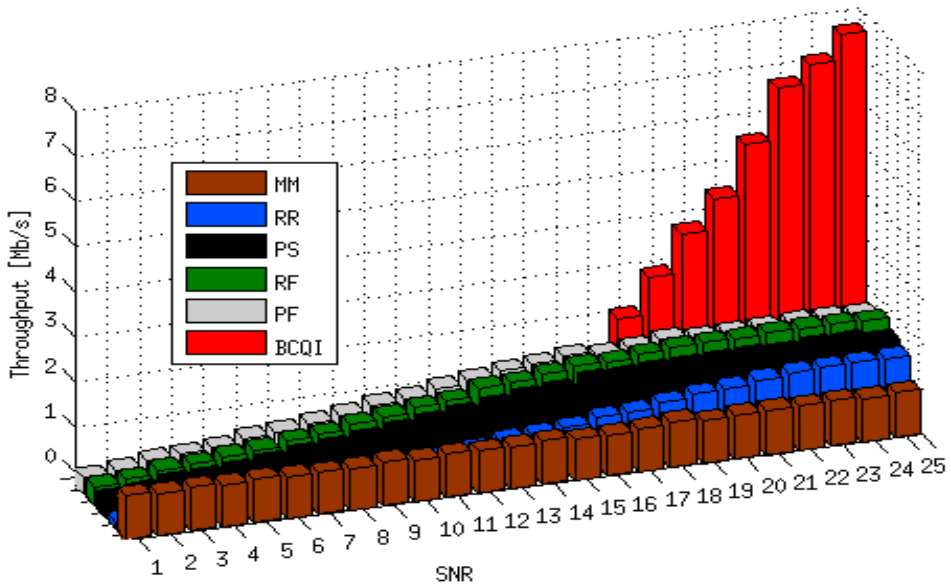

Figure 2-8: MM-UE average throughput achievable within a cell configured with 10 MHz bandwidth versus SNR. The cell is serving 25 users with average SNR from 1 to 25 dB in steps of 1 dB.

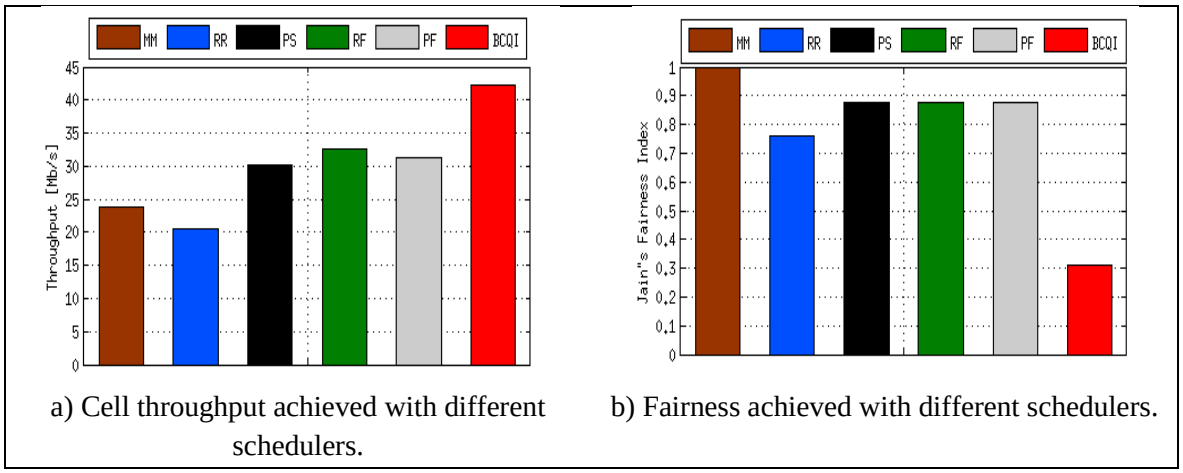

a) Cell throughput achieved with different schedulers.

b) Fairness achieved with different schedulers.

Figure 2-9: Performance of different schedulers in a cell configured with 10 MHz bandwidth. The cell is serving 25 users with average SNR from 1 to 25 dB in steps of 1 dB.

2.3.2.2 Effect of the Number MM-UEs on the AeNB Capacity

Here we focus on the effect of the number MM-UEs on the AeNB capacity running simulations with an increasing number of served terminals. We further assume that the average received SNR is distributed in the range of i) 2 dB to 4 dB for 50% of the users, and ii) 18 dB to 36 dB for the remainder of the MM-UEs.

Figure 2-10 shows the performance of different schedulers in terms of cell throughput and fairness versus the number of served MM-UEs. The cell is configured with 10 MHz bandwidth (50% of the MM-UEs experience an average SNR lower than 4 dB in all studied cases). We can observe that

similar results in terms of cell throughput and fairness are achieved as the number of MM-UEs increases. Observations done before for the different schedulers are also valid in case of Figure 2-10. Notice that the results of fairness and cell throughput prove the effectiveness of the proposed PS scheduler for distributing the available resources amongst the users, though at the cost of a moderately lower the cell throughput in comparison to other policies other than BCQI. This is due to the fact that the PS scheduler prioritizes first the MM-UEs with poor channel conditions during resources assignment.

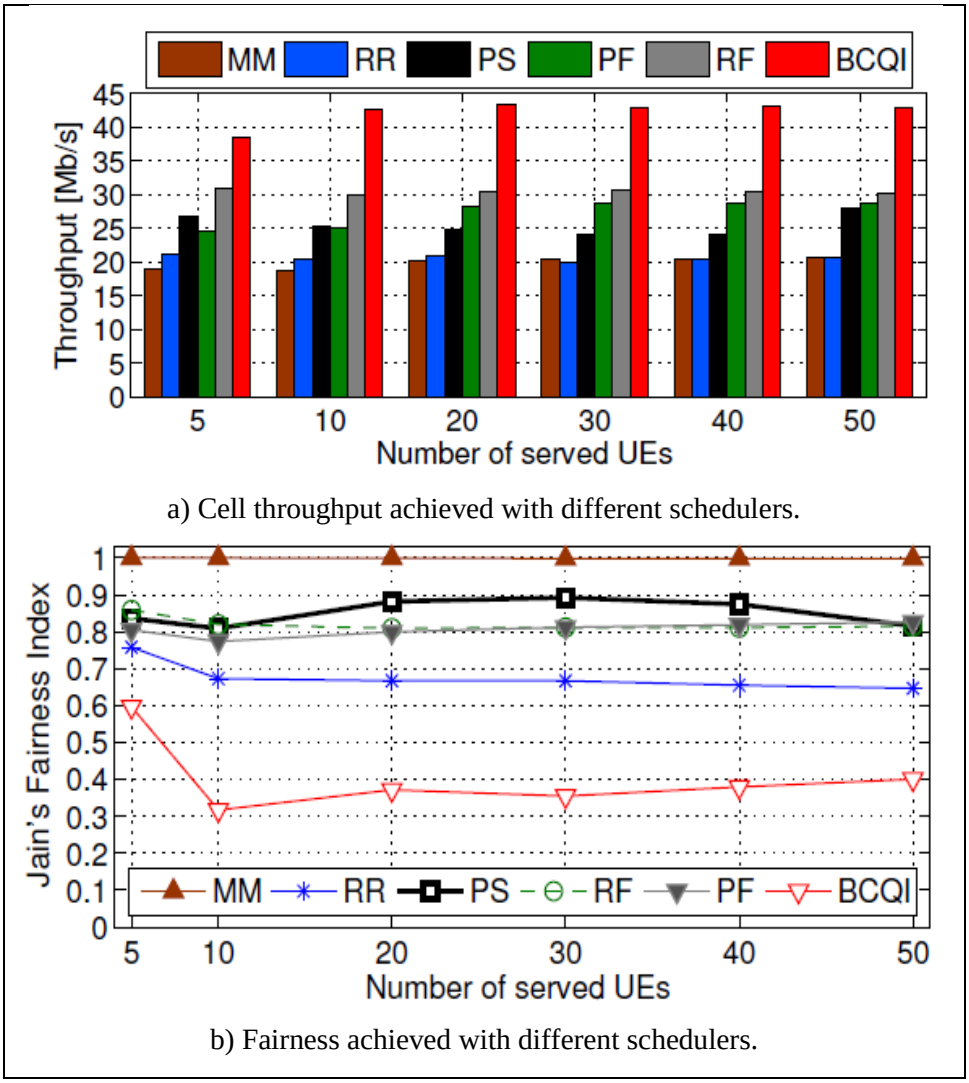

a) Cell throughput achieved with different schedulers.

b) Fairness achieved with different schedulers.

Figure 2-10: Performance of different schedulers versus number of served MM-UEs in a cell configured with 10 MHz bandwidth (50% of the MM-UEs experience an average SNR lower than 4 dB).

2.3.2.3 Effect of the LTE Band on the AeNB Capacity

We now focus on studying the effect of the LTE bandwidth on the AeNB capacity. The coverage area of the AeNB is calculated using the ATG propagation model for all the LTE bands. In order to understand the effect of the system bandwidth on the AeNB cell coverage and capacity, Figure 2-11 shows the SNR distribution across the coverage area of the AeNB using different LTE bandwidth values in the dense–urban scenario. As it can be seen in Figure 2-11.a-f, the system bandwidth has considerable effect on the AeNB coverage area. Based on the results of Figure 2-11, Figure 2-12 shows the lower and upper bounds of the cell-level capacity versus the LTE bandwidth. For this study

we have assumed that the cell is serving 1 MM-UE with an average SNR equal to i) -5 dB for the lower bound, and ii) 24 dB for the upper bound. As expected, the AeNB capacity depends on the amount of RBs in each LTE bandwidth.

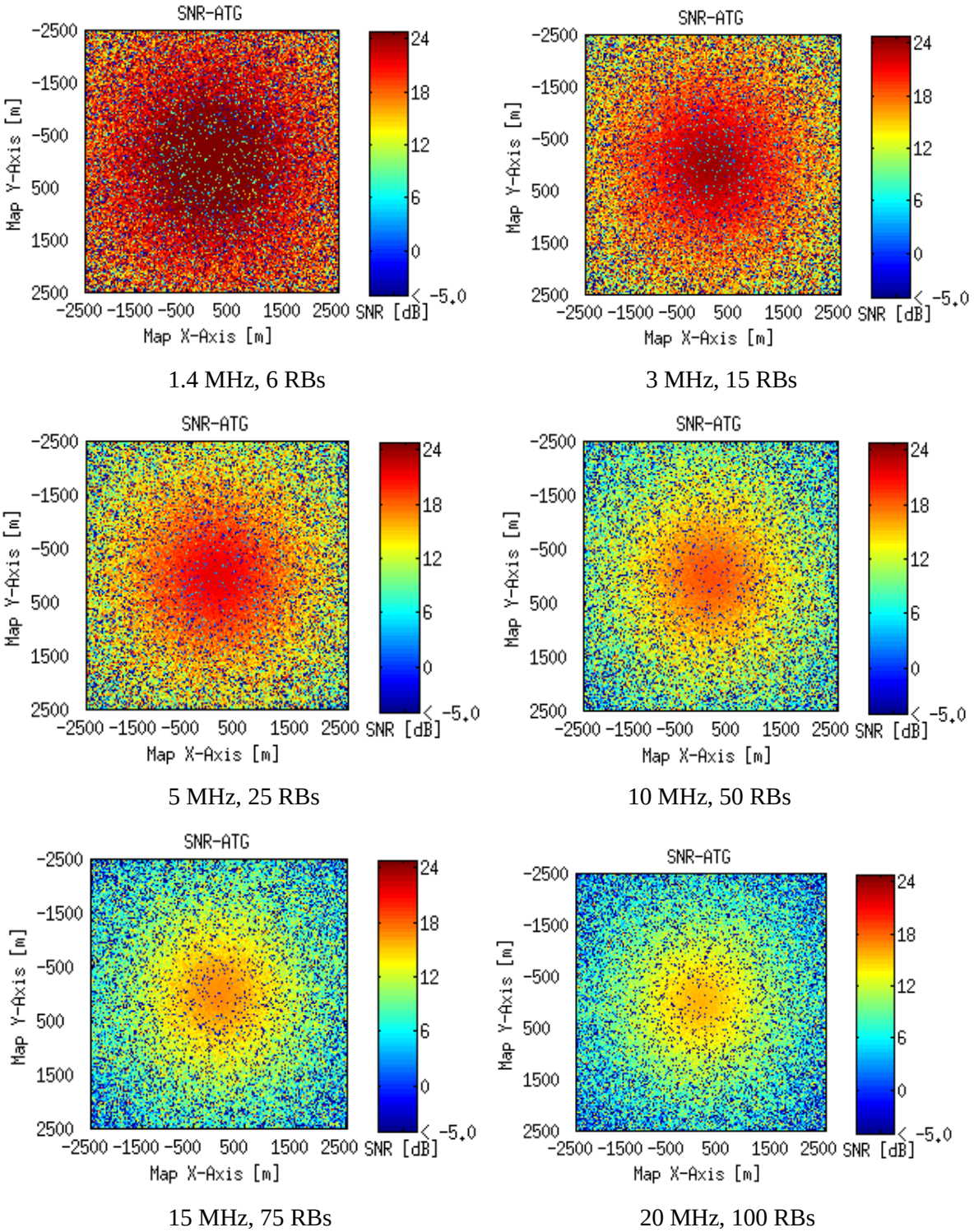

1.4 MHz, 6 RBs

3 MHz, 15 RBs

5 MHz, 25 RBs

10 MHz, 50 RBs

15 MHz, 75 RBs

20 MHz, 100 RBs

Figure 2-11: SNR distribution over the AeNB coverage area versus LTE bandwidth (P_{TX}=23 dBm, Dense–urban scenario, T=20 °C, f =2.6 GHz, ATG propagation model).

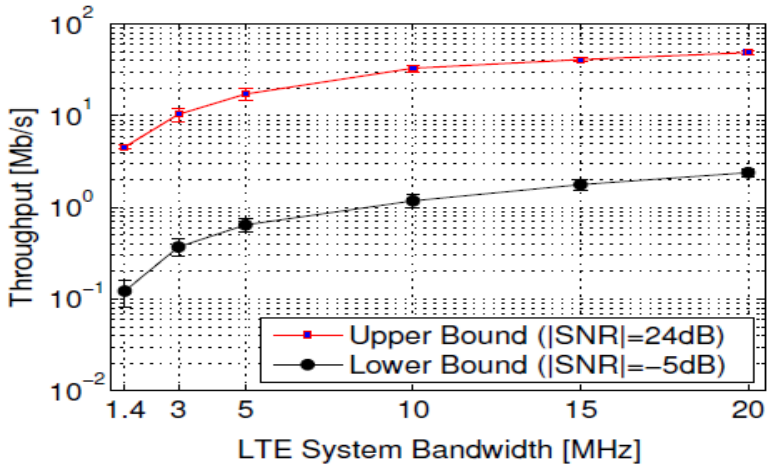

Figure 2-12: Lower and upper bounds of the AeNB capacity versus LTE system bandwidth (P_{TX}=23 dBm, Dense–urban scenario, T =20 ˚C, f =2.6 GHz, ATG channel model, UE=1).

In another set of simulations, we have assumed that the average received SNR is distributed in the range between i) 2 dB and 4 dB for 50% of the users, and ii) 18 dB to 36 dB for the remaining MM-UEs (20 MM-UEs in total). Figure 2-13 shows the performance of different schedulers in terms of cell throughput and fairness versus the LTE system bandwidth. The figures show the results we obtained for BCQI, PF, RF, RR, MM and PS schedulers while assuming different bandwidth values equal to 1.4, 3, 5, 10, 15 and 20 MHz, respectively. Notice that for the 1.4 and 3 MHz bandwidths, which corresponds to 6 and 15 RBs respectively, the number of resources is lower than the number of MM-UEs (β<1). Figure 2-13.a allows to derive the following general conclusions:

- For all LTE bandwidths, the highest cell throughput is achieved using the BCQI scheduler since it serves only MM-UEs with good channel conditions.
- The lowest cell throughput is instead achieved using the RR scheduler since it allocates the resources without taking into account the channel conditions of the MM-UEs.
- Similar cell throughput is achieved using the MM scheduler since it maximizes the minimum of the users' throughput.
- A compromise is achieved using PF and RF schedulers since the channel conditions of the MM-UEs are taken into account during the allocation of the resources.
- The cell throughput achieved using PS scheduler is lower than PF and RF since the scheduler prioritizes the MM-UEs with bad channel condition.
- The PS scheduler performs better than RR and MM schedulers for the LTE bandwidths equal to 5, 10, 15 and 20 MHz in which the number of resources are larger than the number of MM-UEs (β>1).

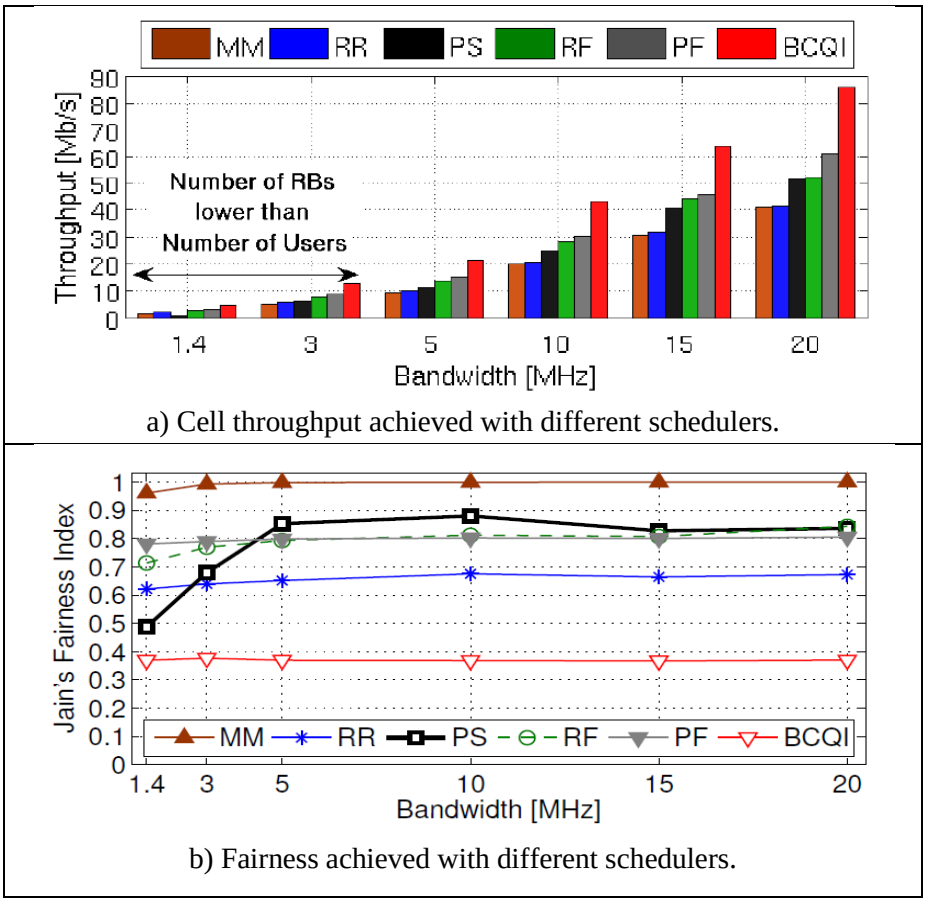

a) Cell throughput achieved with different schedulers.

b) Fairness achieved with different schedulers.

Figure 2-13: Performance of different schedulers versus LTE bandwidth. The cell is serving 20 MM-UEs (50% of the MM-UEs have average SNRs lower than 4 dB).

Focusing on fairness, the best is achieved with the MM scheduler since it divides the resources equally amongst the users, whereas the worst fairness is achieved with the BCQI scheduler as expected. The RR scheduler performs better than BCQI but worse than PF, RF and PS. Out of this three scheduling policies the PS scheduler has better fairness than PF and RF when the system has not exhausted the resources, which is advantageous for the MM-UEs with bad channel conditions. Good fairness is also achieved with the PF and RF schedulers complementing the good performance achieved in terms of throughput.

2.3.2.4 Effect of the Combined Schedulers on the AeNB Capacity

It is worth pointing out that the combinations of PS and PF schedulers can be a good option for systems serving both PS and commercial MM-UEs. In the following example, we simulate an LTE cell configured with 10 MHz bandwidth, when 40 MM-UEs are uniformly distributed within the cell coverage. Out of the total users, 20 are first responders (10 MM-UEs experience an average SNR lower than 4 dB) and other 20 are commercial MM-UEs. We perform simulations for PS and PF individually as well as combining them. The combined scheduler (CS) is created assigning 50% of the RBs for scheduling the PS MM-UEs according to the PS discipline and the other 50% of the RBs for scheduling the commercial MM-UEs according to the PF discipline. Figure 2-14 shows the performance of PF, PS and CS. As it can be seen, the figures highlight that the combinations of PS and PF schedulers can be beneficial for both cell throughout and fairness.

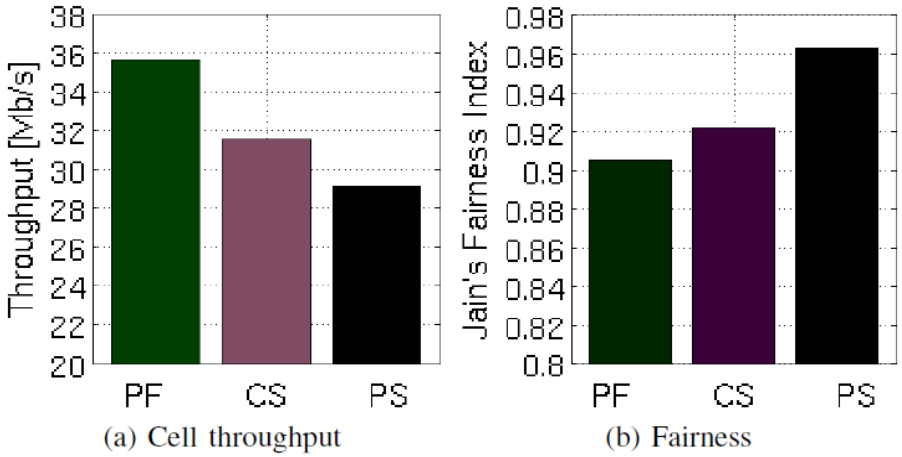

Figure 2-14: Performance of different schedulers in a cell configured with 10 MHz bandwidth.

2.3.3 PLMU-level Capacity Evaluation

In this section the LTE system capacity of the PLMU is analyzed. Notice that the analysis applies to the post-disasters and temporal events scenarios explained in **Erreur ! Source du renvoi introuvable.**, which involves PLMU as the primary (or secondary) equipment. For more details refer to D2.1 (*Use cases definition and scenarios description*). Simulation scenario and Ericsson channel model characterization considered for PLMU performance evaluation is shown in Figure 2-15.

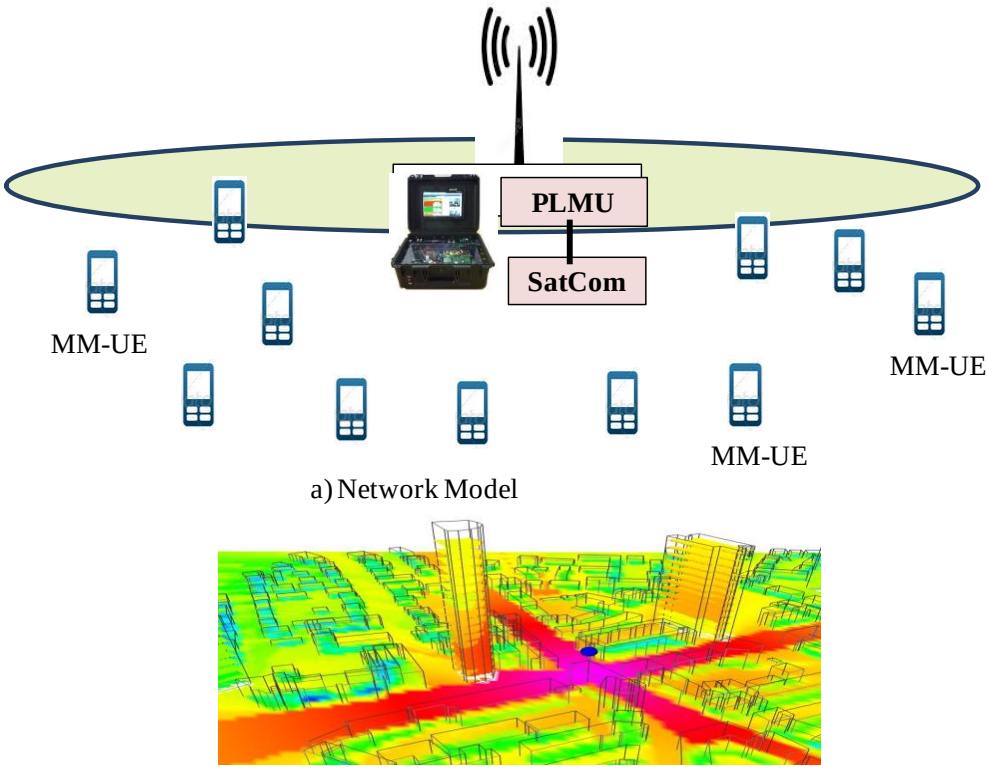

a) Network Model

b) Typical urban propagation scenario

Figure 2-15: Simulation scenario considered for the LTE resource scheduling with the PLMU.

The main objective of the PLMU is to provision coverage extension and additional capacity for specify areas. The LTE equipment used in the PLMU is the same that the used in the AeNB but the

altitude of the antenna is different. The PLMU is deployed on the ground and the PLMU antenna will be placed 30 meters high. Ericsson channel model is used to evaluate the path-loss between the PLMU and MM-UEs [20]. This channel model is appropriate for simulating cellular networks in urban environments with parameters used for modelling the PLMU simulation scenarios shown in Table 2-4.

Table 2-4: Simulation parameters and assumptions for PLMU.

Parameter	Value
PLMU Antenna Altitude	3 m for the PLMU
System bandwidths (W)	10 MHz
Carrier frequency (f)	2600 MHz
Channel Model	Ericson channel model for PLMU [20]
Receiver Antenna altitude	1.5 m
a0, a1, a2, a3	39.1, 36.4, -12, 0.1
MM-UE distribution	Uniform
Served MM-UEs	[1, 25]
Traffic model	Infinitely backlogged
Schedulers	BCQI, PF, RF, RR, MM,PS

The coverage area of the PLMU is calculated using the free space and the Ericsson channel model for an LTE system of 10 MHz bandwidth. Figure 2-16 shows the received P_{RX} and the SNR distribution across the coverage area of the PLMU. The SNR was also computed whereby the free space and the Ericsson channel model. As it can be seen, the SNR is distributed between 1 and 25 dB over a circular area of 500 m of radius. Furthermore, the PLMU achieves a coverage area lower than the AeNB as expected due to the different antenna altitudes. Figure 2-17 shows the performance of different schedulers in terms of user's throughput versus SNR. The cell is configured with 10 MHz bandwidth (the 25 MM-UEs are uniformed distributed over the PLMU coverage area). Figures show results obtained for BCQI, PF, RF, RR, MM and PS schedulers. While Figure 2-18 shows a comparison of the user's throughput achieved with the different schedulers.

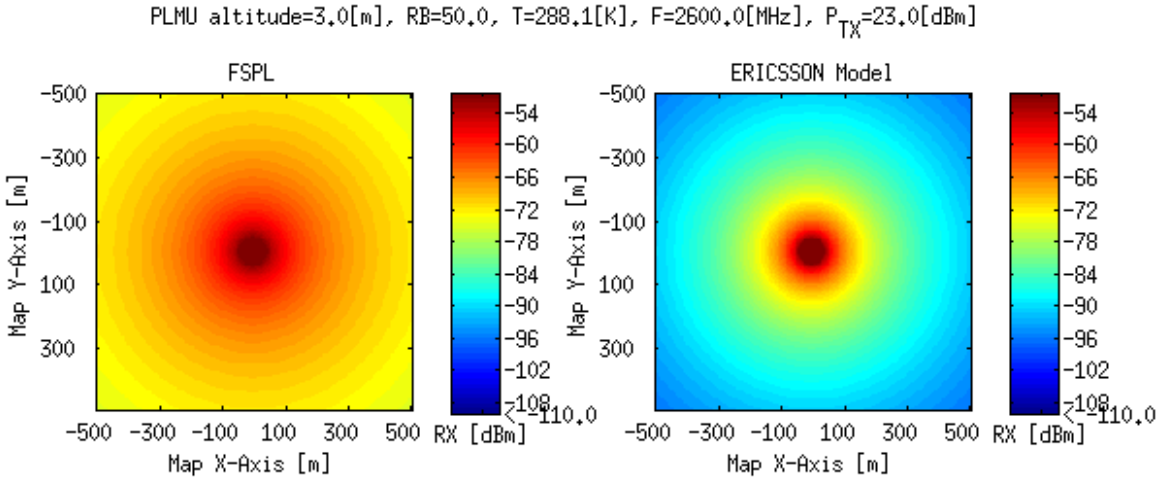

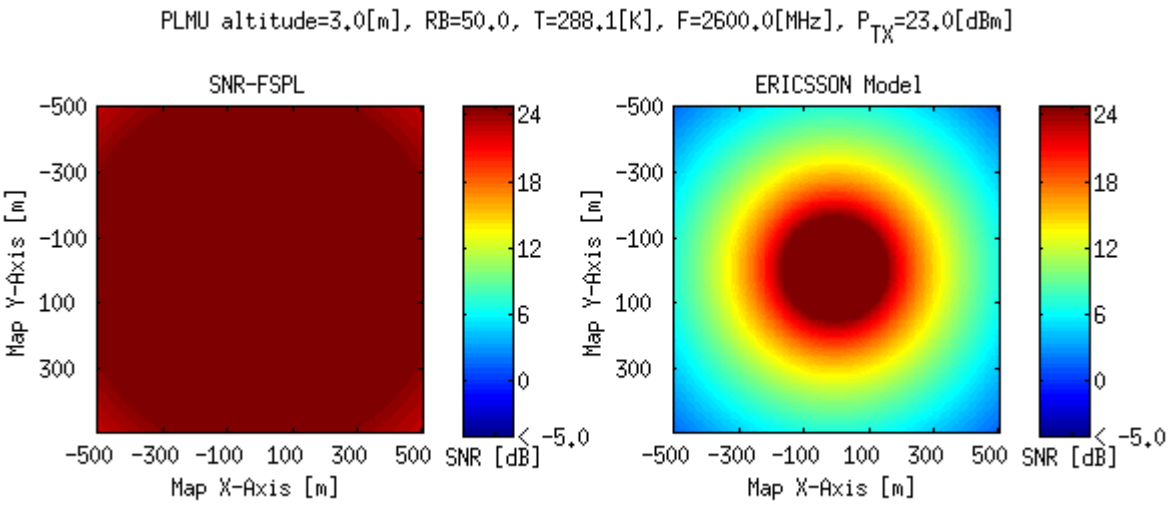

Figure 2-16: P_{RX} and SNR distribution over the coverage area of the PLMU. (P_{TX}=23 dBm, W=10 MHz, Dense–urban Scenario, f=2.6 GHz).

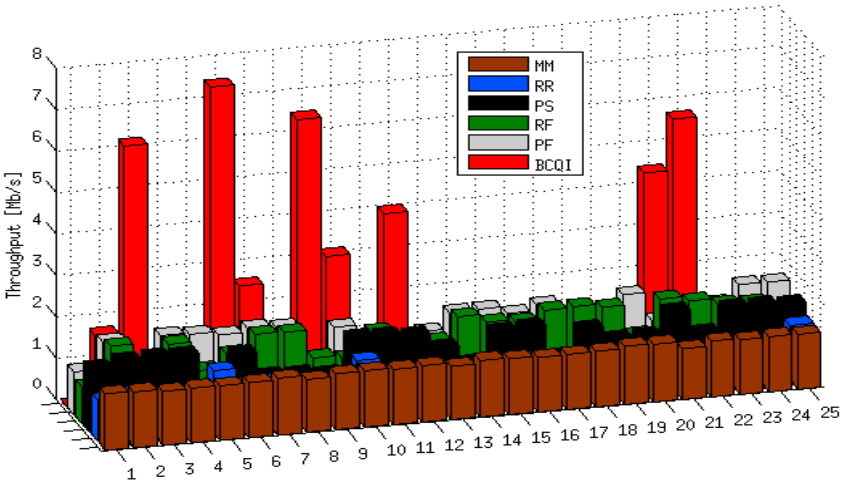

Figure 2-17: MM-UE average throughput achievable in a cell configured with 10 MHz bandwidth versus MM-UE identifiers. The cell serves 25 users with average SNRs distributed over the PLMU coverage area.

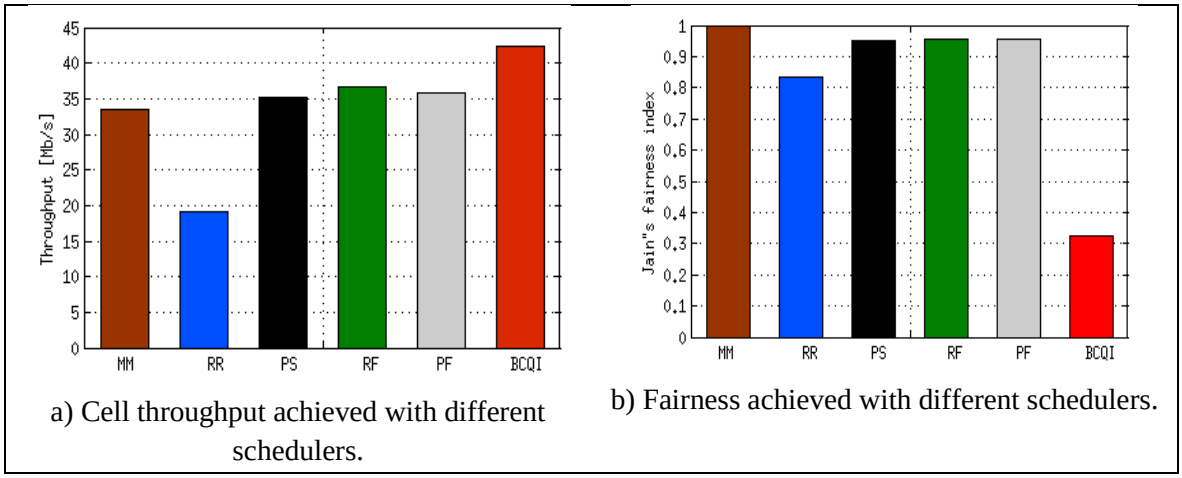

a) Cell throughput achieved with different schedulers.

b) Fairness achieved with different schedulers.

Figure 2-18: Performance of different schedulers in a cell configured with 10 MHz bandwidth. The cell is serving 25 users with average SNRs distributed over the PLMU coverage area.

From the Figure 2-17 and Figure 2-18, we can do the following observations:

- Also in this case, the highest cell throughput is achieved using the BCQI scheduler since it serves only MM-UEs with good channel conditions. In terms of fairness, the worst fairness is achieved with the BCQI scheduler as expected.
- A compromise is achieved using PF, RF and PS schedulers since the channel conditions of the MM-UEs are taken into account for allocating the resources. Good fairness is also achieved with the PF, RF and PS schedulers complementing the good throughput performance.
- The lowest cell throughput is achieved using the RR scheduler. In terms of fairness, the RR scheduler performs better than BCQI but worse than PF, RF and PS.
- Similar cell throughput is achieved using the MM scheduler since it maximizes the minimum of the users' throughput. In terms of fairness, the best is attained by the MM scheduler since it divides the resources equally amongst the MM-UEs.
- As it can been seen, the throughput achievable at the MM-UE level larger than 1Mb/s, which is clearly suitable for multimedia applications like for example streaming of HD video.

Figure 2-19 shows the performance of different schedulers in terms of individual user's throughput versus SNR. The cell is configured with 10 MHz bandwidth. The cell is serving 25 users, with average SNR values distributed in the proximity of the PLMU coverage area (from 100 m until 300 m away from the PLMU). Different results have been obtained for BCQI, PF, RF, RR, MM and PS schedulers. On the other hand, Figure 2-20 shows a comparison of the aggregate cell average throughput achieved with the different schedulers. As it can be seen in the figures, PLMU provides good capacity for the MM-UEs.

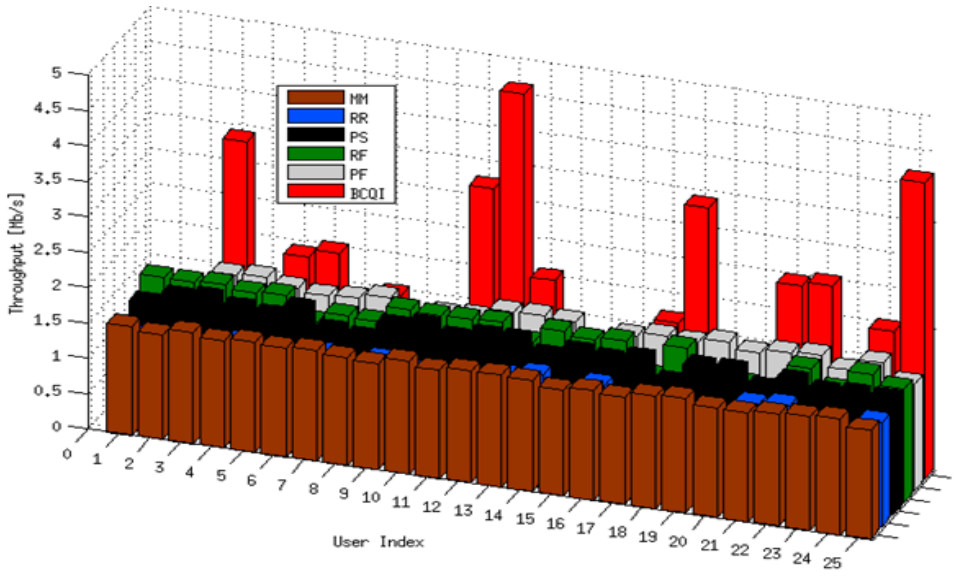

Figure 2-19: MM-UE throughput achieved in a cell configured with 10 MHz bandwidth versus MM-UE identifiers. The cell is serving 25 users, with average SNRs distributed in the proximity of the PLMU coverage area (from 100m until 300m away from the PLMU).

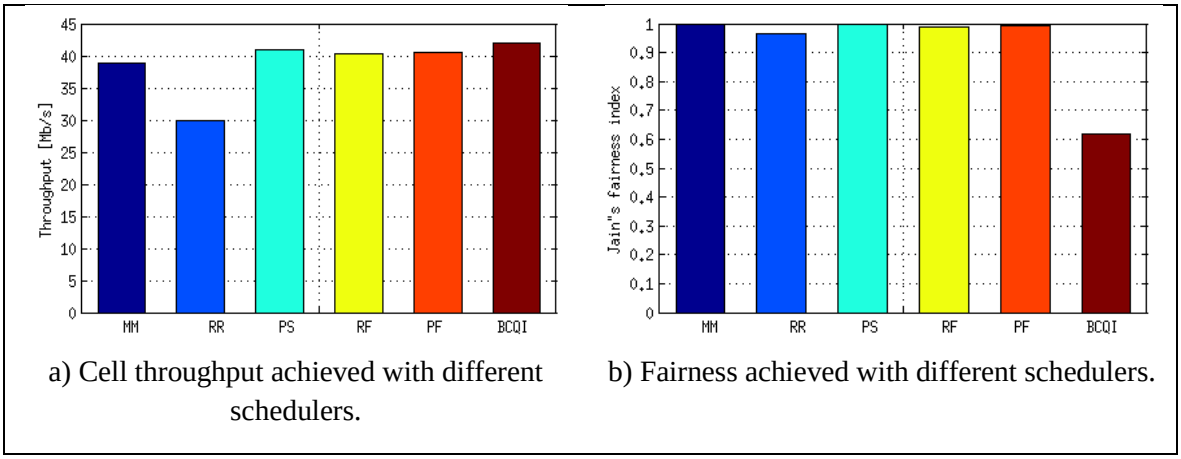

a) Cell throughput achieved with different schedulers.

b) Fairness achieved with different schedulers.

Figure 2-20: Performance of different schedulers in a cell configured with 10 MHz bandwidth. The cell is serving 25 users, with average SNRs distributed in the proximity of the PLMU coverage area (from 100m until 300 m away from the PLMU).

2.4 Conclusions

In this chapter, we provided a comparative study of different scheduling disciplines that can be used in ABSOLUTE system when deployed in both post disaster and temporary event scenarios. We further proposed and studied the performance of a simple yet effective uplink/downlink PS scheduler for LTE-based emergency communications. The proposed scheduler uses the channel condition sub-grouping policies for scheduling MM-UEs with bad channel conditions. The proposed scheduler assigns higher scheduling priority to MM-UEs with poor channel conditions while trying to achieve a cell throughput as high as possible. Simulation results show the effectiveness of the different scheduling disciplines by comparing them in terms of cell throughput and fairness. Based on the results we obtained, we are able to conclude that the proposed PS scheduler well compromises throughput and fairness. We also proved that the combinations of PS and PF schedulers can be beneficial for both cell throughout and fairness when serving public safety and commercial MM-UEs at the same time.

We analyzed the LTE system performance of the AeNB and PLMU in terms of capacity and fairness using six different scheduler schemes. Based on the results we obtained, we remark the following:

- **BCQI** scheduler is not recommended for emergency communications. The scheduling excludes MM-UEs with poor channel conditions, which is optimal for commercial networks but not for emergency communications in which fairness is crucial.
- **MM** scheduler is also not recommended for emergency communications where severe propagation conditions of the radio signal are challenging. In these cases, the MM scheduler penalizes the MM-UEs with good channel conditions in terms of throughput since the goal is to maximize the minimum of the users' throughput.
- **RR** scheduler does not take into account channel conditions for resources allocation. It penalizes throughput and fairness. The main advantage of RR scheduler is simplicity of implementation in assigning the available resources to the MM-UEs in a practical system.
- **PF** and **RF** schedulers maintain a good balance between the objective of maximizing cell throughput and fairness. These schedulers represent a good compromise in both emergency and commercial communications.

- **PS** scheduler provides the best trade-off in terms of cell throughput and fairness in all cases of several MM-UEs with bad channel conditions. Another advantage of PS scheduler is that of a reduced implementation complexity and faster assignment of the resources.
- **Combined Schedulers** combinations of PS and PF schedulers can be beneficial for both cell throughout and fairness.

3 Capacity Evaluation in Hybrid Aerial-Terrestrial Access Network

In this chapter, we evaluate the system capacity of a generic heterogeneous aerial-terrestrial access network. The case scenario of Callania presented in D2.1.1 has been modelled for the deployment of ABSOLUTE public safety communications, which supports capacity demanding from first responders and commercial users affected by the damages of infrastructures in a large disaster area. System level simulations of a practical radio environment in the city of Ljubljana have been conducted. The simulator validates capacity enhancement of the dynamic spectrum and topology management technologies developed in Task 3.3 and 4.1. Furthermore, mathematical analysis of the capacity was carried out using Markov modelling to provide theoretical proof of the performance gain.

3.1 Problem definition

The framework of network capacity assessment is based on the concept of flexible roll out and roll back of AeNBs and PMLUs over a large disaster area, which has been defined in D4.1.4. This section presents the E-UTRAN network performance which mainly considers the radio links between AeNB and MM-UE and PLMU and MM-UE. System level modeling and simulation is used as the main evaluation approach, which investigates PHY, MAC, RLC and RRM layers, such as antenna and propagation, channel capacity, terrain profile, users distribution, base station placement, coverage and service area, traffic density, spectrum and radio resource allocation, base station user association, etc. In this context, this work complies with and supports the satellite backhaul link and network layer capacity assessed in Chapter 4.

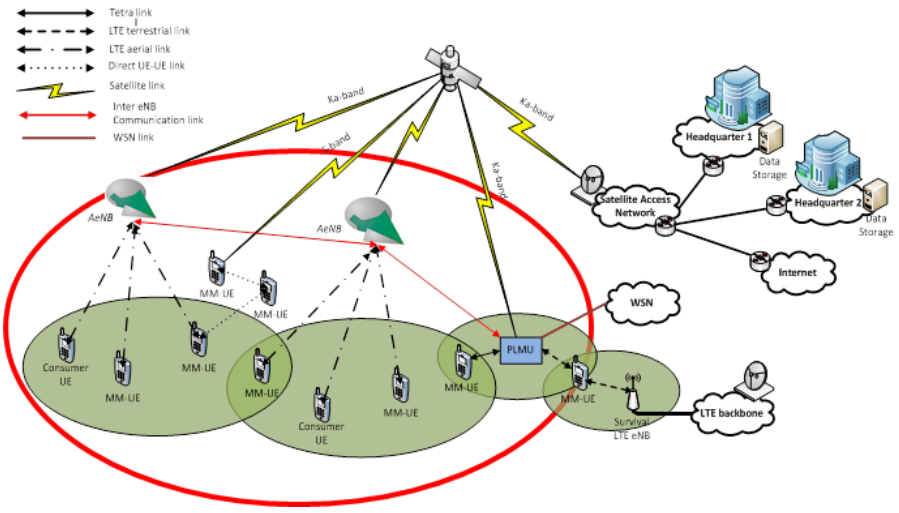

Figure 3-1: ABSOLUTE access network capacity assessment.

We emulate the roll out and roll back process in the disaster relief scenario and demonstrate the overall system throughput in AeNBs and PLMUs, as well as the achievable perceived throughput by the UEs. The relevant scenarios and use cases with involved LTE equipment/subsystems are listed below, which have been detailed in *D2.1 (Use cases definition and scenarios description)*. In particular, the following use cases have been identified: ABS.UC 01 and ABS.UC 02 (AeNB, PLMU and MM-UE for Unitary call and data transfer and Unitary call with a terrestrial backhaul, respectively), ABS.UC 03 and ABS.UC 04 (PLMU for Enabling a new First-Responder user and Media upload to the PLMU, respectively), ABS.UC 05 (PLMU and MM-UE for Unified group call),

ABS.UC 017 and ABS.UC 018 (AeNB for Rolling-out an AeNB in the context of a disaster and Rolling-back an AeNB in the context of a disaster, respectively)

3.2 System simulation

In this section, we evaluate the capacity through system level simulations of the aerial-terrestrial network in a practical scenario. The system, scenario and QoS parameters are based on the definitions in D2.6.2 and D4.2.3. Spectrum and topology management technologies developed in D3.3.3 and D4.1.4 are used for performance validation.

3.2.1 Simulator setup

A customized system and link level simulator has been developed using Matlab, with the purpose of evaluating the technologies developed in Task 3.3 and 4.1, such as spectrum allocation, base station placement, switching operation, user association and load balancing. The simulator comprises the following modules capturing different functionalities, namely: system module, traffic module, spectrum management module, topology management module and physical module.

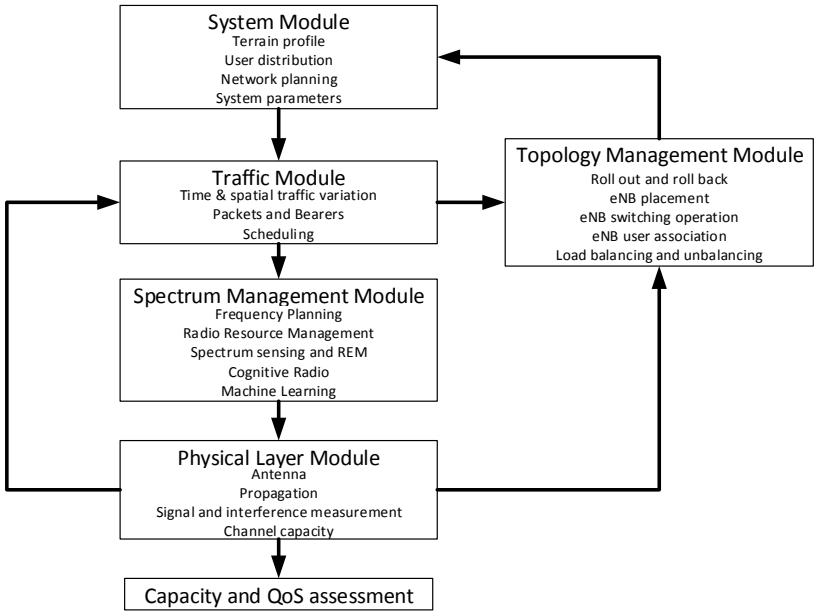

Figure 3-2: System level simulator architecture.

The system module is responsible for defining the scenario including terrain profile and user distribution. It also conducts preliminary network planning, which provides the number, location and service areas of AeNBs and PLMUs. This process is performed by the public safety headquarter in phase 1 through capacity assessment in satellite random access network and incumbent operators' networks. The module also provides input of all system parameters defined in Task 2.6, such as antenna beam width, transmit power and channel bandwidth. The network topology and system parameters can be dynamically adjusted by the topology management module during simulation.

The traffic module describes the traffic variation in both spatial and time domain, which characterizes user requirements in different phases of the disaster relief process. The data packets and message bears are generated following the characteristics of traffic distribution. It also defines the format of frequency bands, radio carriers and resource blocks following LTE specifications and regulatory

bodies. The Monte-Carlo method is used in this simulator, which generates a large number of repeatedly sampled events from random distributions.

The topology management module is designed to dynamically control the network topology based on the traffic level. This module manages the location of network elements and connection between them, namely the placement of AeNB/PLMUs and the association with UEs. The aim is to best match the network capacity with user traffic and guarantee the QoS level specified in system requirement. This will change the initial network planning preliminarily defined in the system module. Moreover, the module supports dynamic AeNB/PLMUs switching operation to reduce power consumption and load management mechanisms to improve resources utilization.

The spectrum management module is responsible for enabling spectrum sharing and coexistence, interference control and radio resource management. Cognitive radio technology is developed to intelligently assign frequency bands to AeNB/PLMUs and schedule message bearers onto resource blocks. It improves the standard inter-cell interference coordination protocol in opportunistic network scenario by considering flexible roll out/back and dynamic topologies. Spectrum sensing and REM information have been integrated in the cognitive radio engine to improve performance.

The physical layer module handles radio transmissions over wireless links. It implements various types of antennas on AeNBs and PLMUs and models different propagation environments on aerial and terrestrial links. Channel capacity is measured using the models from physical layer technologies including advanced modulation and coding, MIMO, interference cancellation, etc. The module evaluates various link level parameters such as RSSI, RSRP, RSRQ, SINR, data rate, resource utilization, which will be used for spectrum and topology optimization. Capacity and QoS assessment will be conducted based on these output parameters.

In system simulation, the throughput is evaluated from the average amount of data bits delivered in unit time. A file transfer traffic model is used to emulate data packets transmitted in the network. The generation of data files follows different types of statistical distributions and arrival rates, depending on the scenarios and user requirements. The transmission time of a file is determined by the channel bandwidth, channel capacity and SINR. A Truncated Shannon model [21] is used as a representative of data rates that can be achieved in practice give an Adaptive Modulation and Coding code-set. The achievable data rate for a specific user on a channel can be expressed as

$$C = \begin{cases} 0 & \gamma < \gamma_{\mathrm{MIN}} \\ \alpha W \log_2(1+\gamma) & \gamma_{\mathrm{MIN}} \le \gamma \le \gamma_{\mathrm{MAX}}, \\ \alpha W \log_2(1+\gamma_{\mathrm{MAX}}) & \gamma > \gamma_{\mathrm{MAX}} \end{cases} \quad (3\text{-}1)$$

where W is the channel bandwidth, $\alpha$is the implementation loss of Shannon bound, γ_{MIN} is the minimum SINR requirement of a communication link and γ_{MAX} denotes the SINR that contributes to the maximum data rate. The SINR at a receiver is given by

$$\gamma = \frac{P_{Tx} G_{Tx} G_{Rx} (PL_{TxRx})^{-1}}{n + \sum_{Tx'=0, Tx' \neq Tx}^{N} P_{Tx'} G_{Tx'} G_{Rx} (PL_{Tx'Rx})^{-1}} \quad (3\text{-}2)$$

where Tx and Rx are the transceiver pair and$T_{X'}$denotes other transmitters in the system that cause interference. P_{Tx} is the transmitted power, which is allocated equality on each channel, n is the thermal noise, G is the antenna gain and PL is the path-loss.

In the file transfer traffic model [22], a blocked or interrupted file can be retransmitted until it is successfully delivered. In this context, the delay of a file consists of the duration for transmission and possible back off. Transmission delay is the time required to push all the bits of a file into the wireless link, which mainly depends on the channel capacity. The back off delay is the time consumed by a file waiting in the queue for retransmissions. The use perceived throughput can be calculated from the amount of delivered bits averaged by delay as follows

$$\overline{S} = \sum_{i=1}^{N_{File}} \left(\frac{N_{bit}(i)}{C} + \sum_{j=1}^{N_B(i)+N_I(i)} D_r(j) \right) \Bigg/ \sum_{i=1}^{N_{File}} N_{bit}(i) \quad , \tag{3-3}$$

This equation includes the time consumed to deliver files with N_{bit} bits, as well as the time spent to back off N_B blocked files and N_I interrupted files.

3.2.2 Scenario

The simulation is based on a practical scenario of the city of Ljubljana in Slovenia. The geographical terrain profile is measured based on the resolution of 100m. The user traffic volume, density and distribution are presented as normalized units, which can be mapped onto practical traffic variations in different phases of the disaster relief. A total number of 4 AeNBs and 30 PLMUs are available to be deployed in the 12 km by 9 km urban area, coexisting with commercial operator networks. A base station placement scheme using evolutionary algorithms developed in D4.1.4 has been applied as preliminary setup of the network. The algorithm maximizes the coverage and network capacity according to statistical information of the terrain and traffic distribution. The Hata-DEM propagation model developed by the GRASS-RaPlaT project [23] is used to calculate the path-loss between transceivers, which is an extended Okumura-Hata model taking into account the terrain profile, clutter data and shadowing.

Erreur ! Source du renvoi introuvable. (a) presents the elevation in the urban area. The MM-UEs are distributed following the traffic density map presented in **Erreur ! Source du renvoi introuvable.** (b). The key simulation parameters are listed in **Erreur ! Source du renvoi introuvable.**.

Table 3-1: Simulation Parameters

Parameters		**Values**
Carrier Frequency		900 MHz
Bandwidth		AeNB: 10 MHz; TeNB: 10 MHz
Number of channels		AeNB: 20; TeNB: 20
Transmit Power P_{Tx}		AeNB/TeNB: 47 dBm; UE: 33 dBm
Thermal Noise		-174 dBm/Hz
Traffic Model	Inter-arrival time	Pareto distribution: $\alpha = 4$
	File size	100 kB
Antenna profile		Omni-directional
Height		AeNB: 250 m; TeNB: 15 m; UE: 1.5 m
QoS parameter		Retransmission probability $QoS_{thre} = 5\%$, $QoS_{bound} = 2.5\%$
Learning rate λ		0.1
Cluster size k		3
Effective SINR $[\gamma_{\text{MIN}}, \gamma_{\text{MAX}}]$		[1.8, 21]
Transceiver Chains N_{TRX}		6
Load dependent slope Δ_P		2.8
Maximum output power P_{out}		20 W

Power without RF P_0	84 W

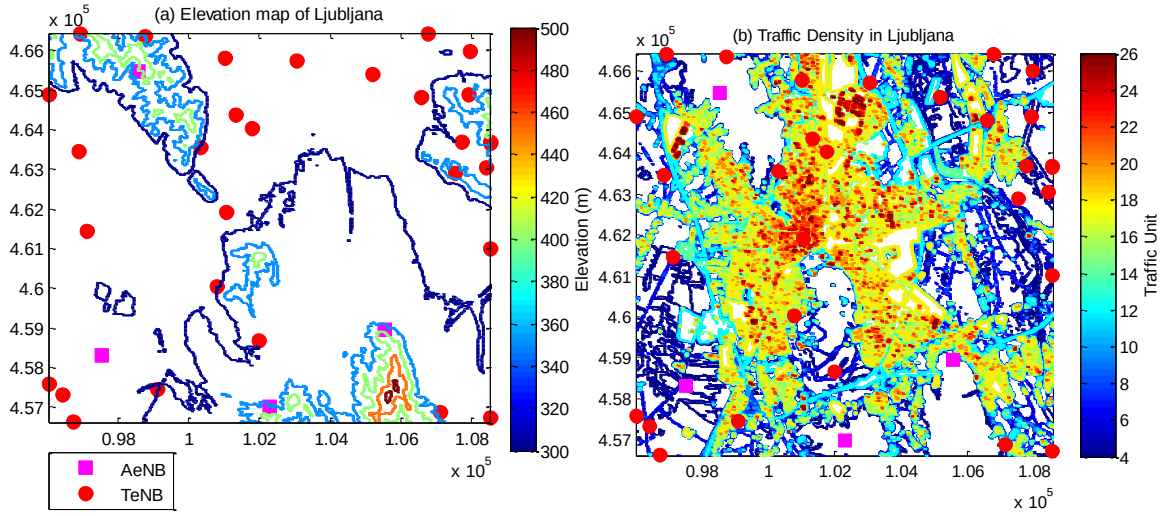

Figure 3-3: Ljubljana city scenario.

3.2.3 Enabling technologies

In this section, we briefly present some selected spectrum and topology management technologies used to do the network capacity assessment. The detailed algorithms can be found in Task 3.3 and 4.1 deliverables. In addition, we will evaluate both co-channel and multi-carrier spectrum assignment strategies for AeNB and PLMU deployment.

3.2.3.1 Spectrum Management

The spectrum management function handles the assignment of resource blocks to generated data files for transmission. Cognitive dynamic spectrum access technologies have been adopted here to improve spectrum utilisation and control interference. This is enabled by a number of machine learning algorithms. Specifically, we have selected the transfer learning and single state Q learning [24][25] algorithms developed in D4.2.3 for capacity assessment. A cognitive engine is implemented in the resource manager in the AeNB and PLMU, which conducts the intelligent algorithms for resource allocation. This can be referred to the eNB protocol architecture in D4.1.4.

Single State Q learning

The single state Q learning algorithm applies a knowledgebase (Q-table) on the learning agent to store and update the environment information. Each resource block is associated with a Q value, which is updated every learning iteration triggered by a file arrival on either the uplink or downlink. The AeNB/PLMUsmakes decision on channel assignment according to a defined decision making policy:

$$a_k = \pi(a) \in \arg\max Q_a\,(t), \tag{3-4}$$

where the channel a_k with maximum Q value in the spectrum pool a is selected at iteration t. A successfully selected channel is then assigned to the file for data transmission. In the event of a failure selection, this process will be carried out iteratively until no channel is available. A learning function is then used to update the Q array in the event a file is either delivered or rescheduled for transmission:

$$Q(t) = (1-\lambda)Q(t-1) + \lambda R(t), \lambda \in (0,1)\ , \tag{3-5}$$

where λ is the learning rate controlling the convergence speed. R is the reward that reinforces the Q array based on the outcome of decision making:

$$R_k(t) = \begin{cases} 1 \text{ (positive reinforcement): Success Iteration} \\ -1 \text{ (negative reinforcement): Failure Iteration'} \end{cases} \quad (3\text{-}6)$$

Transfer learning (TL)

The motivation of transfer learning is to exploit prior learning by transferring knowledge from a set of selected and established *Source Tasks* to the naïve and newly established *Target Task*. The Source Tasks are the learning tasks that have been learnt in the past, where the Target Task is the one that an agent is currently learning. The objective of spectrum assignment is to partition channel sets to users in different locations. In this context, a cognitive agent is expected to optimize its preferred channel set by appropriately transferring the learning policy from neighboring agents.

Transfer learning is triggered before the resource allocation process is carried out. The UE obtains a cluster of neighboring AeNB/PLMUs by evaluating the RSRP level. The objective of transfer learning is to train the Q-table on the connected AeNB/PLMUs by transferring the knowledge learnt on other AeNB/PLMUs. Clustering of cells from network topologies is used to manage the capability for frequency reuse between cells in most frequency planning systems. A reuse cluster is designed to be the smallest number of cells required to include all frequencies, thus avoiding co-channel interference among any cluster members. In this case, the channel information exchanged between agents in a cluster can mitigate interference and reuse channels provided from other agents outside. However,instead of directly applying channel usage information in interference coordination, transfer learning is designed to integrate the effects of cluster topology into the Q-table. This will allow the single state Q learning to exploit more accurate environment information in the following iterations.

The channel prioritization process is conducted iteratively by all the cluster members until achieving Pareto efficient conditions. The idea is to exchange channel priority information throughout multiple agents in a defined reuse cluster, to partition the channel orders learnt by each agent. The source agents are the cluster members which provide spectrum priority information to the target agent that uses transfer learning. The priority table P is obtained from sorting the Q-table in descending order:

$$[Q^{(S)}, P^{(S)}] = Sort(Q): Q_{P^{(S)}(i)} \geq Q_{P^{(S)}(i+1)}, Q^{(S)}(i) > Q^{(S)}(i+1), \quad (3\text{-}7)$$

In the decision making process, the intelligent agent effectively assigns channels in the order of P.

Once the channel-weight-priority information is exchanged collectively throughout the entire cluster, each target agent then generates a new priority table $P^{(T)}$, which is sorted differently from those of multiple source agents $P^{(S(k))}$:

$$\bigcap_{k=1}^{|K|} (P^{(T)}, P^{(S(k))}) = \varnothing, \quad (3\text{-}8)$$

where $|K|$ is the cluster size.

The priority table should then be applied to the Q-table, in order to reinforce the knowledge base with TL information. A value association scheme is designed to assign weights from the priority table, which effectively combines the information from transfer learning and distributed learning.

$$Q^{(S)}(i) \xrightarrow{Assign} Q(P^{(T)}(i)), \quad (3\text{-}9)$$

The transfer learning policy $T^{(p)}$ is then completed. Single state Q learning is then conducted for resource allocation and Q value updates.

3.2.3.2 **Topology Management**

A network topology in general is defined as the arrangement of the various elements, including the location of nodes and the interconnections between them. In Task 4.1, we have studied dynamic network planning and load management aspects in supporting roll out/back and QoS optimization. This section specifically investigates a base station user association approach to achieve load balancing in the heterogeneous network.

In the ABSOLUTE network, AeNBs are deployed for coverage provision while the PLMUs are used for capacity enhancement. In this context, the PLMUs have effective spectrum reuse because of less interference and dense deployment. The loading on AeNBs should be effectively controlled to avoid traffic congestion. Load balancing scheme can significantly improve the overall resource utilization and network capacity, which in turns reduce the number of AeNB/PLMUsand energy consumption.

In Task 4.1, we have developed an intelligent base station user association algorithm to improve load balancing [26]. It allows the UEs to select appropriate AeNB/PLMU based on the Q tables updated from reinforcement and transfer learning. Specifically, we have developed a transfer learning function that transfers the expert knowledge learnt from the **source domain (spectrum management)** to the **target domain (load management)**.The Q values in spectrum assignment contain the information of success or failure file transmission on each channel. By aggregating a Q array appropriately, we can have a new Q value that provides the QoS information of the whole cell.

A transfer learning function is developed to normalize the Q values updated by Q learning and aggregating them proportionally based on their number of iterations, which is expected to differentiate the learnt information. By defining the number of iterations as *N*, a Q value in the load management domain, associated with eNB$b(i)$, can be calculated from:

$$\forall k \in a : Q_{b(i)}^{UA} = \sum Q_{b(i)}^{SA}(k) \frac{N_{b(i)}^{SA}(k)}{\sum N_{b(i)}^{SA}(k)}, \tag{3-10}$$

Upon the arrival of a file, the UE collects Q^{UA} from multiple AeNB/PLMUs with RSRP satisfying the SINR threshold, and makes decisions on AeNB/PLMUsselection based on the newly formulated Q array. Q learning is then carried out for spectrum assignment. This algorithm uses one cognitive engine to solve two different learning tasks, which effectively reduces system complexity.

3.2.4 Results and discussions

The ABSOLUTE network is required to be rapidly deployable after the disaster. In this context, spectrum sharing is a critical methodology to avoid complex frequency planning before operating the network. The AeNBs has significant wide coverage with up to 30 km radius. In this context, it is likely that the PLMUs and UEs receive severe interference when sharing the same spectrum. There are two possible spectrum deployment strategies: multi-carrier and co-channel deployment. In the multi-carrier scenario, the AeNBs and PLMUs are allocated with two different spectrum bands to eliminate aerial terrestrial interference. However, since the PLMU has much smaller coverage and can be densely deployed, the system capacity can be largely constrained by the AeNB which provides significantly lower spectrum reuse. In the co-channel scenario, a wideband spectrum is shared between AeNBs and PLMUs, meaning that all the AeNB/PLMUshave access to the entire spectrum allocated for public

safety service. The inter-cell interference could be a severe issue but the capacity constraints on AeNBs can be largely reduced.

In this section, we evaluate the system capacity in both multi-carrier and co-channel deployment scenarios. Specifically, the load balancing scheme is critical in multi-carrier deployment to reduce traffic congestion, while the transfer learning scheme plays a key role in reducing interference in co-channel deployment. We here present the performance of Q learning, transfer learning and load balancing schemes.

The system capacity is presented as the perceived user throughput, namely the actual data rate on the UE taking into account both transmission and back-off delay. The system throughput is demonstrated in Figure 3-4 below. First it can be observed that the overall user throughput reduces from 3.5 Mb/s down to below 1 Mb/s as the network traffic becoming congested. The co-channel deployment achieves significant higher throughput than the multi-carrier deployment, meaning that the cognitive dynamic spectrum access technology (both Q learning and transfer learning) provides effective interference control between AeNBs and PMLUs. Specifically, transfer learning achieves slightly higher throughput than Q learning in both spectrum deployment scenarios. This validates that transfer learning effectively assists Q learning to identify and avoid interference with adjacent AeNB/PLMUs, by appropriately trains the Q table using expert knowledge.

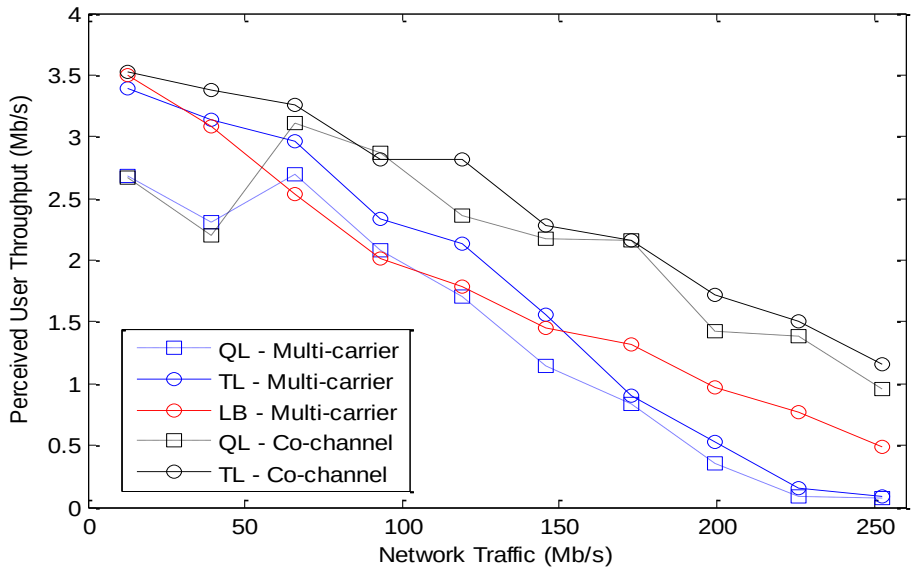

Figure 3-4: Overall Perceived User Throughput.

From the same figure we can see that, the load balancing scheme plays a key role in the multi-carrier deployment scenario. It achieves significant higher perceive throughput than the standard highest RSRQ cell selection scheme at high traffic levels. However, a worse performance is presented at low traffic levels compared to transfer learning. This is because the load balancing scheme extends the cell ranges which causes more inter-cell interference. Figure 3-5 below compares the AeNB and PMLU throughput of these three schemes. In the load balancing scheme, the AeNB and PLMU achieves similar throughput performance. Traffic congestion on AeNB is effectively reduced, while the PLMU has lower throughput because it offloads more traffic. However, the system capacity can be effectively enhance by improving spectrum utilization on PLMUs. On the other hand, transfer learning also significantly improves the PLMU throughput by reducing the inter-cell interference. However, its performance decreases quickly as the network traffic becoming congested.

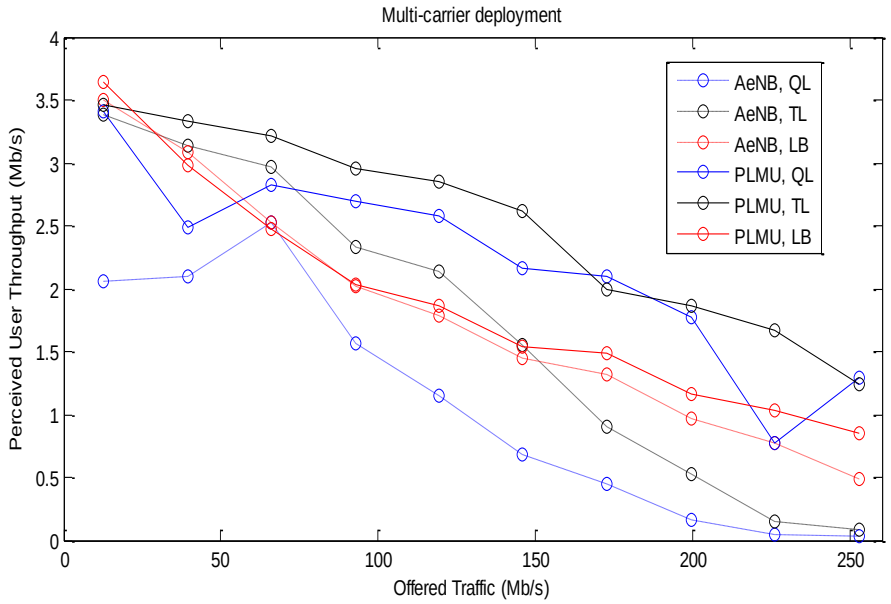

Figure 3-5: Perceived Throughput in Multi-carrier deployment.

In Figure 3-6 below, we present the temporal throughput performance in the multi-carrier deployment scenario showing the convergence of the intelligent algorithms. First we can see that the load balancing scheme improves the AeNB throughput by reducing PLMU throughput as presented in the overall performance. On the other hand, transfer learning achieves higher PLMU throughput at the initial stage compared to Q learning, which effectively reduces the harmful impact from random exploration in learning algorithms at the initial stages, and provides more reliable performance.

A similar throughput comparison of transfer and Q learning in the co-channel deployment scenario is presented in Figure 3-7. We can observe that transfer learning achieves significant higher throughput than Q learning on both AeNBs and PLMUs. This validates that transfer learning effectively controls interference between aerial and terrestrial links. Moreover, transfer learning is shown to largely improve the PLMU throughput at the initial stage. This is achieved from improved decision making policy, by using inter-cell coordination to improve the Q table. On the other hand, Q learning is shown to gradually improve performance from a long term trial and error process.

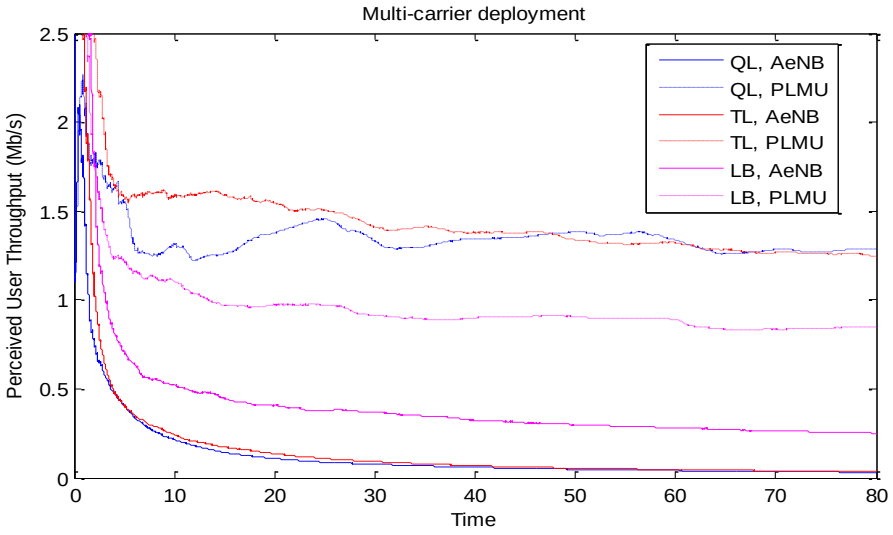

Figure 3-6: Convergence Performance – Multi-carrier Scenario.

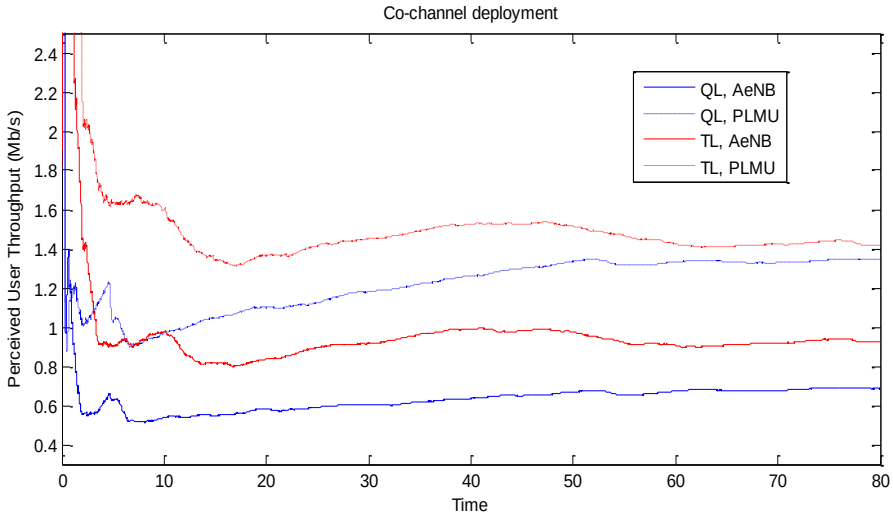

Figure 3-7: Convergence Performance – Co-channel deployment.

3.3 Numerical Analysis

In this section, we evaluate the system capacity based on a purely mathematical approach. Specifically, multi-dimensional Markov analysis is used based on queuing theory to model a network of one AeNB and *D* PLMUs. A set of RRM techniques including load balancing and load unbalancing are carried out under a generic traffic distribution model. Furthermore, we validate the capacity enhancement from AeNBs when deploying the ABSOLUTE network.

As the work presented here assesses a range of RRM solutions under different scenarios and network topologies, design parameters need to be used in such a way that a fair comparison is carried out. The first is the number of accessible AeNB/PLMUsthat a given UE can access at any given time. This is denoted as Ψ. This parameter is fixed and equal for all modelled scenarios and network architectures. Ψcan be also thought of as the degree of overlap between neighbouring nodes. The greater the overlap between neighbouring nodes, the more AeNB/PLMUsa given UE can access. Another design constraint is the use of cell-wrapping for allaying the edge effect and converting the finite simulated area into an unbounded surface. Cell-wrapping is essential to limit the number of

AeNB/PLMUsrequired to model the system. Interference is undoubtedly an important design constraint of cellular networks. However, since this study assesses and compares the optimal operation of the aforementioned techniques and deployment strategies from the occupancy standpoint, interference is not taken into account.

3.3.1 System model

In this section we introduce a generic model for a traffic distribution that is used to model all the RRM schemes assessed in this work. For a network with DAeNB/PLMUs, assuming that λ_1, λ_2, and λ_{D} $[s^{-1}]$ are the arrival rate for users whose only candidate AeNB/PLMUs is eNB_1, eNB_2, and eNB_{D} respectively, which depends on the design constraints and occupancy. Similarly, λ_{12} is the arrival rate for users capable of accessing eNB_1, and eNB_2, where the order of subscripts inλ_{12} indicates the preferred eNB (i.e., users of λ_{12} only access eNB_2 if eNB_1 is not capable of providing service and vice-versa for λ_{21}). Hence, the total arrival rate for users whose set of candidates is $\{eNB_1,\ eNB_2\}$ is denoted as $\lambda_{\{12\}}$, where $\lambda_{\{12\}} = \lambda_{12} + \lambda_{21}$. All other combinations of $\binom{D}{1}$, $\binom{D}{2}$,…,$\binom{D}{D}$ eNBs are calculated similarly, where D is the number of eNBs in the system. Hence, by denoting E as the set of size D representing the eNBs in the network, the overall arrival rate of users into the system (Λ) can be calculated as:

$$\Lambda = \sum_{i=1}^{D} \sum_{k=1}^{\binom{D}{i}} \lambda_{ik} \quad ; \quad \lambda_{ik} = \left\{ \lambda_{\{E\}} \middle| E \subset \{1, \dots, D\}, |E| = i \right\}. \tag{3-11}$$

The system state model of a generic state $(j_1, j_2, \dots, j_D)$ is illustrated in Figure 3-8 where μ is the user departure rate and $\gamma_n(j_1, j_2, \dots, j_D)$ means the fraction of Λ that is directed to eNB_n when the system is in state $(j_1, j_2, \dots, j_D)$.

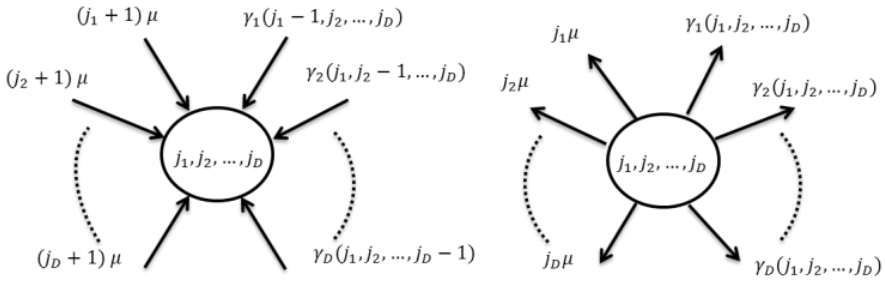

Figure 3-8: System state-transition-rate diagram.

The values of $\gamma_n(j_1, j_2, \dots, j_D)$are dependent on the scenario as well as on the deployment strategy. Thus a set of non-negative traffic coefficients, denoted by ρ, are defined to compute $\gamma_n(j_1, j_2, \dots, j_D)$ as follows:

$$\gamma_n(j_1, j_2, \dots, j_D) = \sum_{i=1}^{D} \sum_{k=1}^{\binom{D}{i}} \rho_{n,\{ik\}}(j_1, j_2, \dots, j_D)\, \lambda_{ik}, \tag{3-12}$$

where $\rho_{n,\{ik\}}(j_1, j_2, \dots, j_D)$ is the portion of λ_{ik} that is served by eNB_n when the system is in state $(j_1, j_2, \dots, j_D)$. λ_{ik} and $\rho_{n,\{ik\}}$ are calculated as follows

$$\gamma_n(j_1, j_2, \dots, j_D) = \sum_{i=1}^{\binom{D}{\Psi}} \rho_{n,\{E\}}(j_1, j_2, \dots, j_D)\ \lambda_{\{E\}} |\ E \subset \{1, \dots, D\},\ \ |E| = \Psi, \tag{3-13}$$

The system model is based on multidimensional Markov chains. Using queuing theory terminology, an AeNB/PLMUcan be modelled as a system with no queue but having m servers (i.e., it can serve m simultaneous users). The model has been developed along with the traffic model described in the

previous subsection, to assess the performance of different RRM mechanisms. The model is first introduced for a particular scenario of five AeNB/PLMUs and subsequently generalised to any number of eNBs. The state of the system of five eNBs is described as $(j_1, j_2, j_3, j_4, j_5)$where $j_i$denotes the number of occupied channels in $eNB_i | i = 1, 2, 3, 4, 5$. Given that AeNB/PLMUsare of equal capacity m, the number of possible states is $S = (m+1)^5$. We define $\frac{1}{\mu}[s]$ as the mean service time, which is equal for all $eNBs$, and $\mu_i = u\mu\,; u = 1, 2, \dots, m$ where $u$is the number of users being served by the i^{th} eNB. γ_i $[s^{-1}]$ is the arrival rate of users into eNB_i.

A system state model of a generic state $(j_1, j_2, \dots, j_D)$ is illustrated in Figure 3-9. The values of $\gamma_n(j_1, j_2, j_3, j_4, j_5)$ $(n = 1, 2, 3, 4, 5)$ are dependent on the scenario and are calculated using the set of non-negative coefficients (ρ) computed in the previous sub-section. These are calculated as shown in equation (3-13). As we cannot have a departure if there are no users in the system, $\mu_0 = \mu_{-1} = \mu_{-2} = \gamma_{-1} = \gamma_{-2} = \gamma_{-3} = \dots = 0$. Also, since it is logical that we cannot have a negative number of users in the system or more users than the system capacity, we can use the condition that $P(-1) = P(-2) = P(m+1) = P(m+2) = 0$. Let $P(j_1, j_2, j_3, j_4, j_5)$ be the equilibrium probability that there are j_n users being served by eNB_n. We can derive the corresponding conservation-of-flow equation as follows:

$$\begin{gathered}(\gamma_1 + \gamma_2 + \gamma_3 + \gamma_4 + \gamma_5 + j_1\mu_1 + j_2\mu_2 + j_3\mu_3 + j_4\mu_4 + j_5\mu_5)P(j_1, j_2, j_3, j_4, j_5) = \\ \gamma_1 P(j_1 - 1, j_2, j_3, j_4, j_5) + \gamma_2 P(j_1, j_2 - 1, j_3, j_4, j_5) + \gamma_3 P(j_1, j_2, j_3 - 1, j_4, j_5) + \\ \gamma_4 P(j_1, j_2, j_3, j_4 - 1, j_5) + \gamma_5 P(j_1, j_2, j_3, j_4, j_5 - 1) + (j_1 + 1)\mu_1 P(j_1 + 1, j_2, j_3, j_4, j_5) + \\ (j_2 + 1)\mu_2 P(j_1, j_2 + 1, j_3, j_4, j_5) + (j_3 + 1)\mu_3 P(j_1, j_2, j_3 + 1, j_4, j_5) + \\ (j_4 + 1)\mu_4 P(j_1, j_2, j_3, j_4 + 1, j_5 + (j_5 + 1)\mu_5 P(j_1, j_2, j_3, j_4, j_5 + 1),\end{gathered} \tag{3-14}$$

As the system must be in one of the states described by the conservation-of-flow equation (3-14), the state probabilities must satisfy the normalisation equation:

$$\sum_{j_1=0}^{m}\sum_{j_2=0}^{m}\sum_{j_3=0}^{m}\sum_{j_4=0}^{m}\sum_{j_5=0}^{m} P(j_1, j_2, j_3, j_4, j_5) = 1\,, \tag{3-15}$$

The system state probability vector can be obtained by solving the $(m+1)^5$ equations derived from equation (3-15) in conjunction with the normalization equation. Let A be the $(m+1)^5 \times (m+1)^5$ coefficient matrix, P the $(m+1)^5 \times 1$state probability vector and B the $(m+1)^5 \times 1$ constant vector. We can obtain the state probability vector P by solving the matrix equation as:

$$P = A^{-1}B, \tag{3-16}$$

It is arduous to present a closed form solution for the problem described above, thus we use numerically derived results in subsequent sections. Due to space constraints a detailed description of the method used is omitted and can be found in [27]. The generalisation of the five-dimensional Markov model derived for the five-eNB network is straightforward. Figure 3-8 illustrates the state transition diagram for the corresponding D-dimensional Markov model of$D$-eNB network.

$$\sum_{i=1}^{D}(\gamma_i + j_i\mu_i)\,P(j_1, j_2, \dots, j_D) = \sum_{i=1}^{D}\begin{bmatrix}\gamma_i P(j_i - 1, j_j, \dots, j_D) \\ +(j_i + 1)\mu_i P(j_i + 1, j_j, \dots, j_D)\end{bmatrix}, \tag{3-17}$$

As the system must be in one of the states described by conservation-of-flow equation (3-15), the state probabilities must satisfy the normalisation equation

$$\sum_{j_1=0}^{m}\sum_{j_2=0}^{m}\dots\sum_{j_D=0}^{m} P(j_1, j_2, \dots, j_D) = 1\,, \tag{3-18}$$

The system state probability vector can be obtained by solving the $(m+1)^D$ equations derived from equation (3-18) in conjunction with the normalization equation. Each state is described by the $(j_1, j_2, \dots\dots, j_D)$coordinates, where $j_x(n = 1, 2, \dots . D)$is the number of users being served by eNB_x, and $\gamma_x$is the total user inter arrival rate into eNB_x.

3.3.2 Scenario

In this section, we present two different network topologies: homogeneous network having terrestrial network only and heterogeneous network including both AeNBs and PLMUs. This is used to validate the importance of AeNBs in supporting disaster relief network and load management scheme handling traffic offloading of the AeNBs.

3.3.2.1 Homogenous terrestrial deployment strategy

As detailed in the previous sub-sections and in order to give a fair chance for the users of both deployment strategies to access the network, each MM-UE has three accessible AeNB/PLMUs out of the five available. The first modelled network is a traditional homogenous network as seen in Figure 3-9. This can be considered as a PLMU small-cell network with no AeNB overlay.

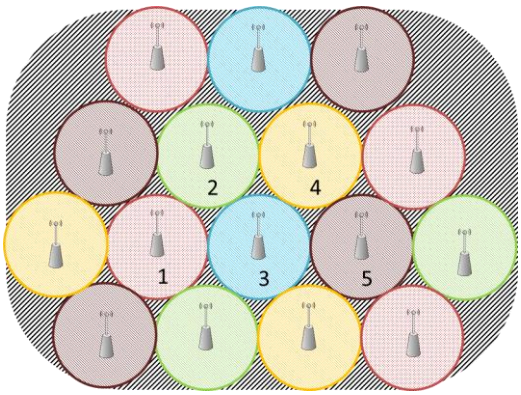

Figure 3-9: Homogeneous terrestrial network model.

Following the design constraints and parameters, each UE has three accessible PLMUs. By applying the cell-wrapping technique, the whole network can be accurately abstracted into a limited number of PLMUs forming a *D*-dimensions Markovian model with $\mathrm{C} = \binom{D}{\Psi}$ User Groups (UGs), each group accessing a different set of PLMUs. In our model, $D = 5$, and $\Psi = 3$, hence 10 UGs are formed.

- *Blocking probability and coverage limitations*

In this deployment and since each UG can access Ψ eNBs, UEs experience blocking only if Ψ or more eNBs have no free RBs. **Erreur ! Source du renvoi introuvable.** illustrates the coverage limitations of one and two PLMUs in a 5-PLMUs network and $\Psi = 3$ (when the other PLMUs have no free RBs).

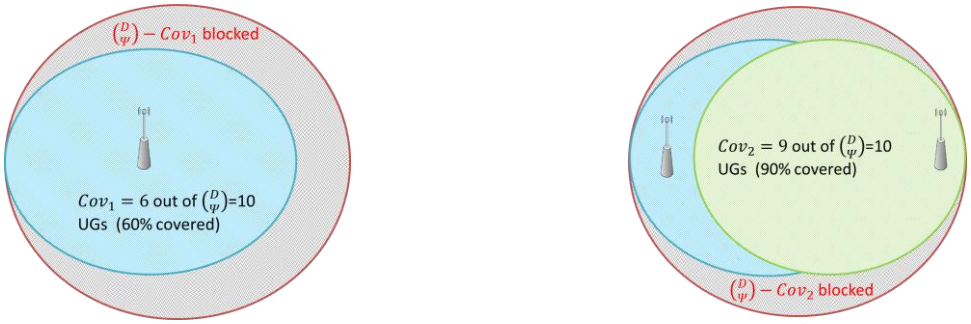

a. Coverage of a single PLMU b. Coverage of two PLMUs

Figure 3-10: Homogeneous coverage model.

The coverage limitation of any given number of PLMUs (n) is calculated as follows:

$$Cov_n = \sum_{i=1}^{n} Cov_{eNB_i} - \sum_{i<j} \left(Cov_{eNB_i} \cap Cov_{eNB_j}\right) \tag{3-19}$$

$$+ \sum_{i<j<k} \left(Cov_{eNB_i} \cap Cov_{eNB_j} \cap Cov_{eNB_k}\right) - \cdots + (-1)^{n-1} \bigcap_{i}^{n} Cov_{eNB_i}$$

$$\cap_i^n Cov_{eNB_i} = (\mathrm{D} - \mathrm{i})\mathrm{C}(\Psi - i), \tag{3-20}$$

where xCy is the combination function of subset of length y out of a set of length x, Cov_n is the service area that is covered by n eNBs in terms of number of User Groups (UGs). Given the fact that each UE is served by Ψ eNBs, hence blocking only happens if there are Ψ or more PLMUs with no free RBs (i.e., all RBs are taken hence the eNB is full). In the case when any Ψ eNBs are full, the blocking probability is calculated as

$$PB_\Psi = \sum_{n=1}^{\mathrm{DC}\Psi} P\,(j_I) \quad | \quad I \subset \{1, \ldots, D\}, |I| = \Psi, j_I = m, \tag{3-21}$$

where the sum runs over all subsets I of the indices 1,…, D that contain Ψ elements and has the value of m, and m is the number of resource block groups available at each eNB.

$$j_I := \cap_{i \in I} j_i \,. \tag{3-22}$$

This denotes the intersection of all j_i with index I. Hence, the system blocking (PB_{sc1}) can be calculated as

$$PB_{sc1} = \sum_{i=\Psi}^{n} \frac{BK_i \lambda_{UG}}{\lambda} PB_{\mathrm{i}}, \tag{3-23}$$

$$BK_i = N_{UG} - Cov_{D-i}, \tag{3-24}$$

whereBK_i is the number of blocked UGs when any i eNBs are full, N_{UG} is the total number of user groups in the system, Cov_n is the number of user groups served by any n eNBs which is calculated from equation **Erreur ! Source du renvoi introuvable.**, λ_{UG} is the UG arrival rate into the system and λ is the arrival rate of all UGs in the system (i.e., the system arrival rate).

3.3.2.2 Heterogeneous aerial-terrestrial deployment strategy

In this scenario, an AeNB overlay exists which covers the entire service area with a second tier of small-cell PLMUs. This type of scenario is becoming increasingly interesting and the subject of intense research and is seen as a way to boost capacity density and enhance spectrum efficiency [28][29]. A heterogeneous deployment strategy is also considered for providing high speed connectivity and 4G technology globally [29], or even as disaster relief architecture [28]. Again, for fairness, all UEs have Ψ accessible eNBs. Given the fact that the AeNBs covers the whole service area, all UEs can access $\Psi - 1$ PLMUs and the AeNB.

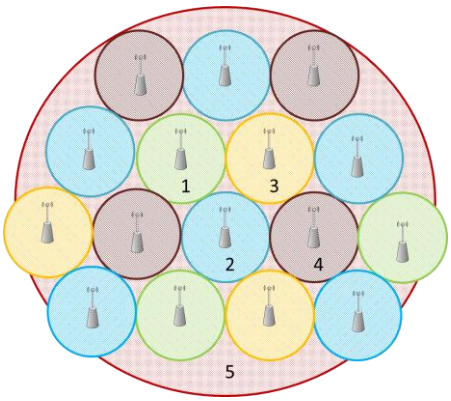

Figure 3-11. Heterogeneous Aerial-Terrestrial Network Model.

Also for this deployment strategy, the whole network is abstracted into a limited number of PLMUs forming a D-dimensional Markovian model with $\mathrm{C} = \binom{D}{\Psi}$ UGs, with each group accessing a different set of PLMUs. This was done following the design parameters and by applying the cell-wrapping technique. The number of UGs is changed given the presence of AeNB overlay to only $\mathrm{C} = \binom{D-1}{\Psi-1}$. The number of AeNBs needs to be subtracted also when calculating the coverage limitations of a given PLMUs. By keeping the parameters $D$and Ψ constant, six user groups are formed.

- *Blocking probability and coverage limitations*

In this case, a UE is blocked if any $\Psi - 1$ of the PLMUs have no free RBs and the AeNB is full. Figure 3-12 illustrates the coverage limitations of one and two PLMUs (when the other PLMUs have no free RBs).

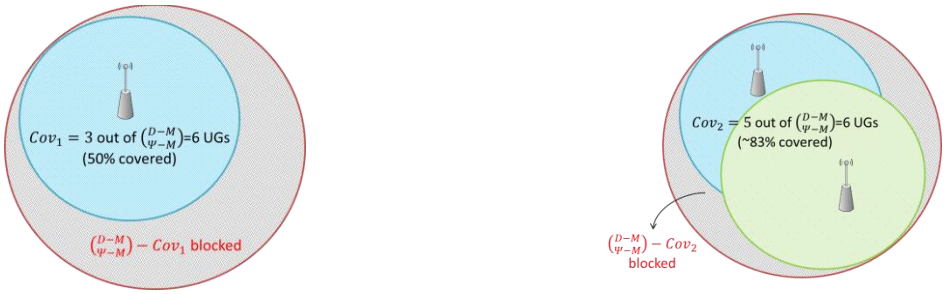

Coverage of one PLMU Coverage of two PLMUs

Figure 3-12. Heterogeneous coverage model.

Hence, blocking only happens if there are $\Psi - 1$ or more full small-cell PLMUs and the blocking probability in this case can be calculated as

$$PB_{\Psi-1} = \sum_{n=1}^{(\mathrm{D}-1)C(\Psi-1)} P\,(j_I) \;\Big|\; \substack{I\subset\{1,\dots,D-1\} \\ |I|=\Psi-1, j_I=m}. \tag{3-25}$$

where the sum runs over all subsets I of the indices $1, \dots, D-1$ that contain $\Psi-1$ elements and has the value of $m.m$ is the number of resource block groups available at each PLMU.

$$j_I := \bigcap_{i\in I} j_i. \tag{3-26}$$

This denotes the intersection of all j_i with index I. Hence, the system blocking probability for (PB_{sc2}) can hence be calculated as

$$PB_{sc2} = \sum_{i=\Psi-1}^{D-1} \frac{BK_i \lambda_{UG}}{\lambda} PB_{\mathrm{i}}. \tag{3-27}$$

$$BK_i = N_{UG} - Cov_{D-1-i}. \tag{3-28}$$

whereBK_i is the number of blocked UGs when the AeNB and any iPLMUs are full, N_{UG} is the total number of user groups in the system, λ_{UG} is the UG arrival rate in the system and λ is the arrival rate of all UGs into the system (i.e., the system arrival rate) and Cov_n is the number of user groups served by any neNBs which is calculated from equation **Erreur ! Source du renvoi introuvable.** excluding the AeNB. The exclusion of the AeNB needs to be taken into account when using equation **Erreur ! Source du renvoi introuvable.** by subtracting $D-1$ and $\Psi-1$ as seen in the previous equations. D and Ψ were defined earlier.

3.3.3 Enabling technologies

The RRM techniques assessed here are the Load Balancing, Load Unbalancing, and the AeNB prioritisation. These are defined as follows:

Load Balancing (*LB*): *LB* tries to balance the traffic demand across the access network. It dynamically sets the priority of the eNBs depending on their loading status. The least loaded eNB has a higher priority over other eNBs in the access network. As seen in the previous sections, the probability of a given user with a candidate set of $eNBs\{eNB_1\ eNB_2\ \ eNB_3\}$to be directed to eNB_1 is given by $\rho_{1,\{123\}} = \bar{\delta}_{j_1 m_1}\left(\emptyset_{123} + \emptyset_{132} + \delta_{j_2 m_2}\emptyset_{213} + \delta_{j_3 m_3}\emptyset_{312} + \delta_{j_2 m_2}\delta_{j_3 m_3}(\emptyset_{231} + \emptyset_{321})\right)$. Generally, these probabilities can be written as $\rho_{x,xy} = \rho_{x,xyz} = \bar{\delta}_{j_x m_x}$; $\rho_{x,yx} = \rho_{x,yxz} = \bar{\delta}_{j_x m_x}\delta_{j_y m_y}$, and $\rho_{x,yzx} = \bar{\delta}_{j_x m_x}\delta_{j_y m_y}\delta_{j_z m_z}$, where $x, y, z \in \{1,2,3\}; x \neq y \neq z. LB$ changes the order of this UE's candidate set according to their loading status assigning highest priority to the least loaded AeNB/PLMU and the lowest to the most loaded AeNB/PLMU.

Load Unbalancing (*LUB*): This technique tends to cluster the traffic demand into a number of AeNB/PLMUs as small as possible. The *LUB* technique adopted here uses a fixed priority list to aid the decision of camping on a cell. The priority list, denoted byΩ, is as follows:$\Omega_1 > \Omega_2 > \cdots > \Omega_D$ for $eNB_1, eNB_2, \dots eNB_D$, respectively.

Macro-cell overlay priority (*MP*): This technique sets a priority figure to indicate whether the macro-cell AeNB has greater or lower priority than the small-cell PLMUs. This is used to identify the role of the AeNB in serving the traffic and how it can be used to optimise system performance. Two configurations are used. Assuming that eNB_5 is the AeNB, the first configuration sets the priority of eNB_D the highest (i.e., $\Omega_D > (\Omega_1,\ \Omega_2, \dots,\ \Omega_{D-1})$). The second configuration is to set the priority of

the AeNB the lowest (i.e., $\Omega_D < (\Omega_1, \Omega_2, \ldots, \Omega_{D-1})$). Please notice that this priority overruns any priority set by the LB or the LUB algorithms.

3.3.4 Results and discussion

The different RRM mechanisms and deployment strategies are assessed using the aforementioned mathematical model in a network of $D = 5$ AeNB/PLMUs. The analytical model assumes that users can only connect to Ψ =3 PLMUs out of the available 5 depending on their occupancy as interference is not taken into account. We assume a total number of 4 channels are available on 1 AeNB and 4 PLMUs in the area.

3.3.4.1 Role of the AeNB macro-cell overlay

In this subsection, the importance of the existence of a macro-cell overlay from AeNB and its effect on the RRM technique is studied in a wide range of terms: QoS, energy efficiency and system stability. Four different settings have been studied. These are the load balancing with the AeNB having the lowest priority (LB - AeNB low P), the load balancing with the AeNB having the highest priority (LB - AeNB high P), load unbalancing with the AeNB having the highest priority (LUB - AeNB high P), and lastly load unbalancing with the AeNB having the lowest priority (LUB - AeNB low P). These four settings have been chosen to have a clear insight into the potential of a heterogeneous deployment strategy to deliver the required QoS in a stable and energy efficient manner. Figure 3-13 illustrates the system QoS in terms of blocking probability for the aforementioned settings as marked on the legend. The figure indicates that system performance depends heavily on the priority of the macro-cell overlay and that this needs to be configured properly. There are roughly 25% more files blocked by changing the priority of the macro AeNB from lowest to highest when using the load unbalancing RRM. This percentage can be further enhanced to surpass the 30% mark when balancing the load at medium and high offered traffic and keeping the AeNB with lowest priority.

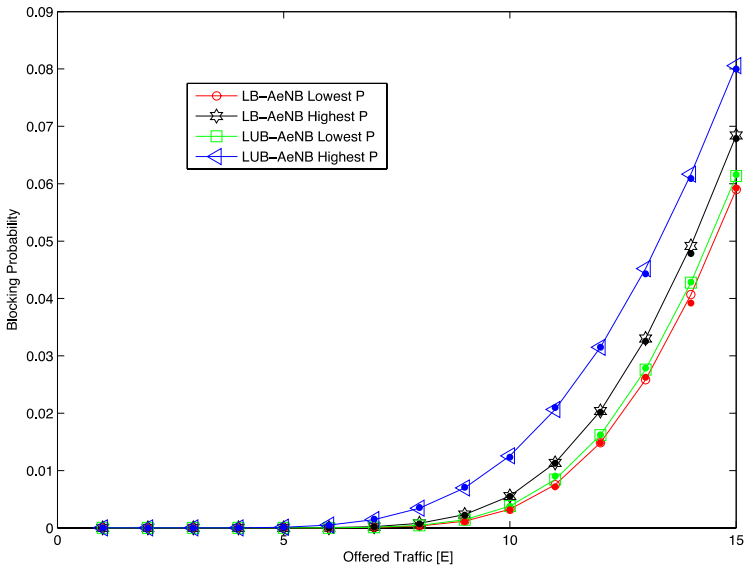

Figure 3-13: System blocking probability.

The number of AeNBs and PLMUs required in the network to provide adequate capacity is shown in Figure 3-14 below. Again, the importance of the prioritisation of the AeNB is evident. When load balancing is adopted, the alteration of the priority of the AeNB from highest to lowest decreases the

changes for network nodes of being in the idle state by an average of 20% at low traffic loads. Generally, load unbalancing seems to be the most beneficial approach in terms of energy efficiency at all traffic loads. However, taking Figure 3-13 into account, it is obvious that load unbalancing is not the optimal technique to avoid congestion at high traffic loads.

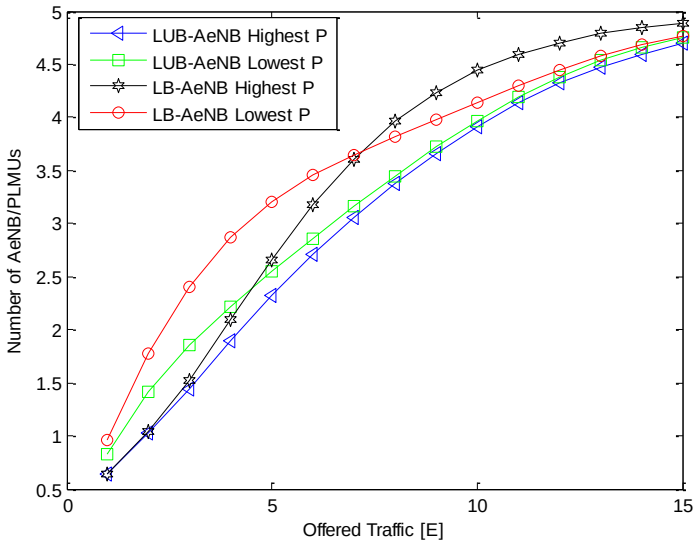

Figure 3-14. Number of AeNBs/PLMUs.

3.3.4.2 **Aerial-Terrestrial Heterogeneous vs. Terrestrial Homogeneous network**

Based on the performance of different settings of the heterogeneous deployment strategy, the load unbalancing with high priority AeNB and the load balancing with low priority AeNB are chosen for the comparison against homogenous deployment strategy. Figure 3-15 illustrates the blocking probability. Even though the homogenous deployment strategy performs well, it is still outperformed by the heterogeneous strategy in which the AeNB is set to have a low priority. The heterogeneous deployment still performs much better than its homogenous counterpart also in terms of network stability keeping the frequency of transiting from the idle to the active state as low as zero at very low traffic loads. Similar behaviour is noticed in terms of the network topology as shown in Figure 3-16 having the load balancing technique in homogenous deployments performing by far the worst.

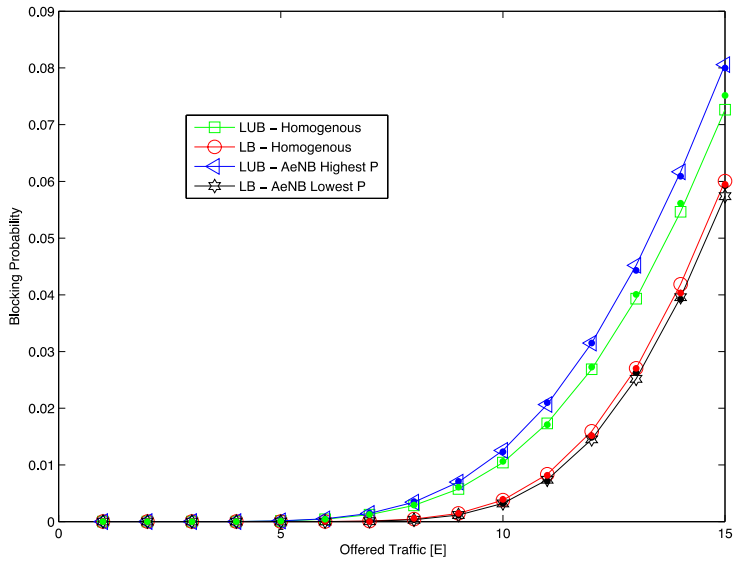

Figure 3-15: System Blocking Probability.

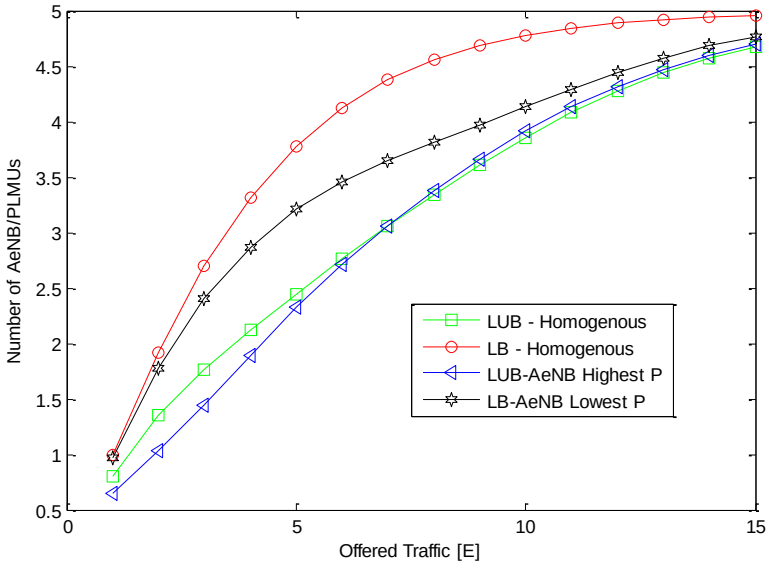

Figure 3-16: Number of AeNBs/PLMUs.

3.4 Conclusions

In this section, we have presented the access network capacity assessment of the heterogeneous aerial-terrestrial public safety network for disaster relief scenario. System level simulations of a practical urban disaster area have been conducted, which also validates various radio resource management techniques developed in Task 3.3 and 4.1. Moreover, mathematical capacity analysis has been carried out using Markov model, which validates the importance of AeNB in provisioning network capacity.

In the simulation based capacity assessment, we demonstrate two spectrum management policies for aerial and terrestrial network, namely multi-carrier and co-channel deployment. Transfer learning technologies have been used for interference management and load balancing. It has been shown that the co-channel deployment achieves significantly higher user throughput than the multi-carrier deployment, by using cognitive technologies to control interference. Transfer learning effectively

improves throughput compared to Q learning, by using inter-cell coordination to improve the Q-table for resource allocation. Effective convergence performance is achieved in transfer learning, which improves user throughput at initial stage. Moreover, load balancing is shown to significantly enhance AeNB throughput and system capacity at high traffic loads, by improving spectrum utilization in terrestrial networks.

In the mathematical based capacity assessment, the performances of AeNB heterogeneous deployment scenario were calculated using queuing theory. Two main RRM techniques, namely Load Balancing and Load Unbalancing, were also evaluated for the aforementioned deployment strategies. The importance of having an AeNB was also assessed. It is concluded that even though the RRM technique is important, system performance in all terms relies heavily on the AeNB prioritisation settings. It not only enhances system performance but it also adds flexibility to the underlying capacity boosters from PLMUs. Homogenous terrestrial networks also perform close to their heterogeneous counterparts, but more AeNB/PLMUs are required in order to reach the performance level of heterogeneous deployments. For this reason, homogenous deployment strategies are more suitable in areas that have a semi-constant traffic demand or traffic with small fluctuations over time. This could be high, medium or low traffic demand, or a mix of these, but with a slow changing nature, such as busy city centres where traffic exhibits constant intensity even overnight. Heterogeneous deployment strategies on the other hand are proven to have extended capabilities especially in terms of energy efficiency. It is recommended that these types of strategies are used in areas with unpredictable traffic demand, with a medium to high fluctuating nature.

4 Network Layer capacity Assessment based on Radio Environment Map

Within this chapter, we evaluate the system capacity of a LTE network covering a large rural area. The case scenario was selected in the area where ABSOLUTE emergency communications would be most beneficial when there is lack of a communication infrastructure. This is the case of a forest which is potentially endangered with wildfires. Selected scenario relates to the ABSOLUTE Public Safety use cases (*D2.1 Use cases definition and scenarios description)*: ABS.UC.01 (AeNB, PLMU and M-UE for Unitary call and data transfer) and ABS.UC.02 (AeNB, PLMU and MM-UE for Unitary call with a terrestrial backhaul).

In the observed scenario, we are primarily interested in the overall system capacity which is for this case defined as the amount of information that can be transmitted over a period of time. Since in LTE network capacity is defined in such a way that it depends on the end-users distribution, signal strengths, interference and user traffic demand, the answer for such estimation is fairly complex.

The framework for capacity assessment is based on two simulation environments (i.e. network layer simulation model and REM module) which interact with each other as also shown in **Erreur ! Source du renvoi introuvable.**.

4.1 Evaluation environment

The framework for capacity assessment is based on two simulation environments which interact with each other. The *network layer* simulation model acquires information about the physical environment from the REM module which has been presented in Deliverable D2.6.2.

A custom network layer simulation model has been developed using OPNET Modeler simulation tool. Its purpose is to develop and evaluate mobility management load balancing, routing, Quality of Service, scheduling and queue management solutions in a dynamic heterogeneous network, taking into account the environment (e.g. elevation maps, clutter data, other GIS information, …) in which radio access network technologies operate.

The REM and network level simulator interact via the hypertext transfer protocol (http), an application protocol for distributed, collaborative, hypermedia information systems. The network level simulator sends get-command within the region describing the geographical area in which a disaster occurs. The interaction between network level simulator and REM is illustrated in **Erreur ! Source du renvoi introuvable.**.

REM calculates the coverage maps, one for each active radio cell and packs them into a single coverage file per communication system. The files contains: most probable received signal levels for each pixel on the map in dBm per wireless network cell, information about the location of the cell transmitting antennas and its height (level above the ground). The network level simulator can access the coverage file in the agreed location and can use this information as input for the simulation.

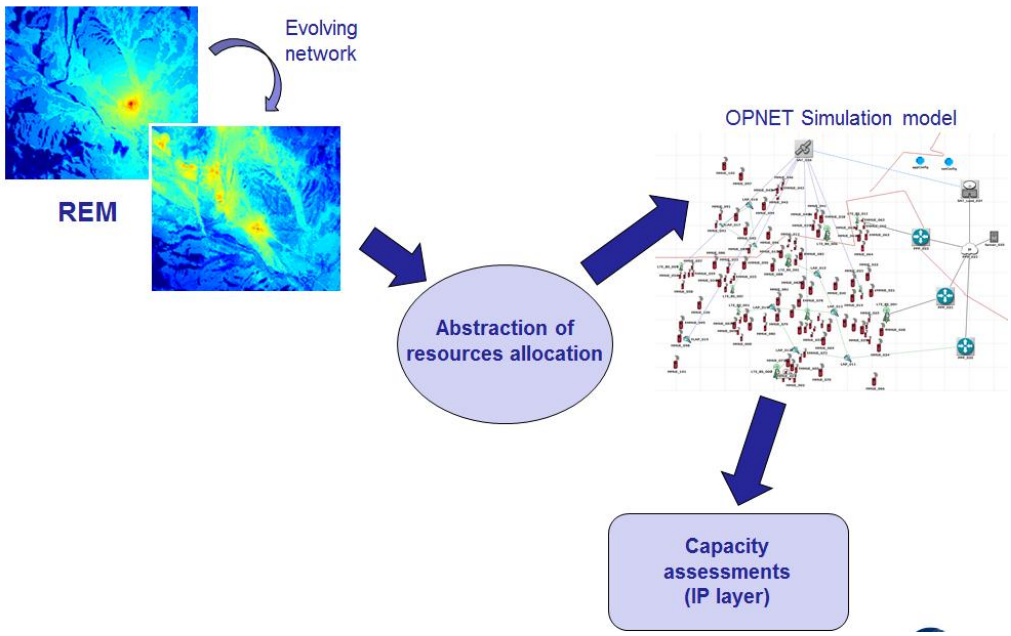

Figure 4-1: Information flow in the framework for capacity assessment.

The Network layer simulation model can functionally be described with four main modules, namely: (i) Application management module, (ii) Network module, (iii) Wireless module, and (iv) Topology management module.

Application management module is responsible for injecting traffic in the network. It allows evaluation of the QoS through measuring the delay and the amount of lost packets, as well as the quantity of service through goodput measurements. Traffic flow load intensities, packet sizes, packet inter-arrival times, type of service and source – destination selection depend upon the application selection (e.g. VoIP call inside the network or through SIP server). The overall amount of traffic in the network can be changed by deploying additional users in the network or by adjusting the individual user's behaviour (e.g. average duration of calls, average inter-arrival time between two calls, type of application e.g. Video, etc.).

Since we are focusing on dynamic heterogeneous networks, which serve as IP-CAN (IP Connectivity Access Network), we implemented also the Session Initiation Protocol (SIP) functionality. This serves, on one hand, for session initiation (e.g. VoIP, Multimedia) and on the other hand also as a candidate protocol for application layer mobility management and context aware interface selection [4].

Network module handles several functionalities. Primarily it routes packets through the network. Looking at the packet's destination and given current location the module sets the packets next hop. To do so, it needs to keep also the information about the current state of the network (e.g. link failures, nodes connectivity changes). This module autonomously makes decisions (if not already defined by the application) over which communication interface the MM-UE unit is accessed.

Wireless module takes care of successfully transmitting packets over the wireless medium. Wireless module comes in several instances i.e. LTE, Wi-Fi and Satellite links, where each instance differs also for base station (AeNB, PLMU) and MM-UE. Wireless modules also handle all the outgoing queues and according to the scheduling (e.g. real-time Polling Service (rtPS), Unsolicited Grant Service

(UGS), etc.) and queue management type (e.g. round robin, weighted round robin, FIFO, etc.) sets the packet running order. LTE instances also take into account the inputs provided by the REM.

Topology management module models the dynamic behaviour of the topology (roll in or roll out phases) and MM-UE mobility. Current topology is highly dependent on the REM provided by the REM module, which is one of the cornerstones of the proposed simulation.

In the network layer simulation model the REM is used for assigning the MM-UE to the serving LTE cell, calculating the achievable throughput for the MM-UE, estimating the interference and for the resources block assignment process. Each base station (e.g. AeNB, PLMU) can cover one area or it may cover several areas at once (where area is referred to as cell). Hence, in the following we usually refer to cells (e.g. LTE cell) rather than to base stations as they are more meaningful.

The MM-UE connects to the LTE cell with the highest received signal strength i.e. best serving LTE cell. The MM-UE generates resource demands based on the current traffic conditions. Knowing the serving LTE cell for each MM-UE the resource blocks can be scheduled.

The smallest assigned resource is a scheduling block (i.e. two Resource Blocks). The LTE cell resources in a scheduling frame (i.e. it corresponds to an LTE radio frame which lasts 10 ms (or 10 TTIs) are presented as a table whose size depends on the LTE bandwidth. Resources in the cell are available if the cell can assign a scheduling block to the user demand. In case when a demand is coming from the user that is positioned at the border between two cells, the resource block on both cells is reserved due to the interference problems.

In the following, we provide the explanation for the downlink channel resources assignment since the uplink concept is fairly similar. In order to model Inter-Cell Interference Coordination (ICIC) mechanism of the LTE system, all the LTE resources are delegated to the central global process module that has the perfect knowledge on the locally and globally available resources and demands for all the base stations and MM-UEs. The resource assignment algorithm is shown in Algorithm 3. If the resources are available at the cell, the demand is assigned to the scheduling block. The number of bits in a demand depends on the type of traffic source and it can vary from 470 bits for VOIP calls to 10.000 bits for FTP traffic. In addition, the number of bits per scheduling block varies from 117 to 756 bits depending on the SINR. Consequently, the demand could be served by a single scheduling block, or vice versa several scheduling blocks could be needed to fulfil demand requirements.

Algorithm 3: Assign resources to new demands.

```
1  resourcesAvailable = 1;
2  while (resourcesAvailable) do
3     resourcesAvailable = 0;
4     for i = 1 : numberOfBaseStations do
5        if (localResourcesRequired (i) && localResourcesAvailable (i)) do
6           sb = assignSchedulingBlock();
7           if (sb > 0) do
8              resourcesAvailable = 1;
9              setThroughput(i, sb)
10          end if
11       end if
12    end for
```

13 End while

The throughput per scheduling block of a particular MM-UE is evaluated applying the function set *Throughput*. This function takes into account signal strength (as acquired from the REM) from the best serving LTE cell, the sum of the powers from all cells transmitting in a selected resource block, the LTE system bandwidth, channel type (e.g. Gaussian or Rayleigh), the number of physical downlink control channels and the cyclic prefix (i.e. normal or extended). Scheduling blocks are allocated according to following three priorities:

1. First, resources are assigned according to the demands that are already in the air (e.g. the demand has received resources already in a previous frame). In this way, we assure that first the resources are scheduled amongst demands that are already being served. Nevertheless, if the network operates already at its maximum these demands will receive only one scheduling block per demand.

2. If after the first step there are still resources available new demands are considered. This process is iterative and is presented in Algorithm 3. The process considers serving new demands as long as we are able to assign resources to at least one demand from the pool of all the cells.

3. Up to this point all the demands have been assigned one scheduling block. If there are still available resources they are given to demands with already assigned resources. This process is also iterative, assigning to each demand one scheduling block (if available) per iteration. By doing this the process tries to assign all the available LTE resources to the currently served demands.

4.2 Evaluation scenario in the remote Slovenian region

The area of interest was selected in the remote Slovenian area Kocevje that is mostly covered by forest. The area screen shot can be seen from Figure 4-2 in which also LTE maximal signal strength received from the LAP is represented. The map under observation is 17 x 35 km^2 and the pixel size is a square of 100 x 100 m^2. We considered a scenario where a large area is under the wildfire and rescue teams go to the area to bring rescue.

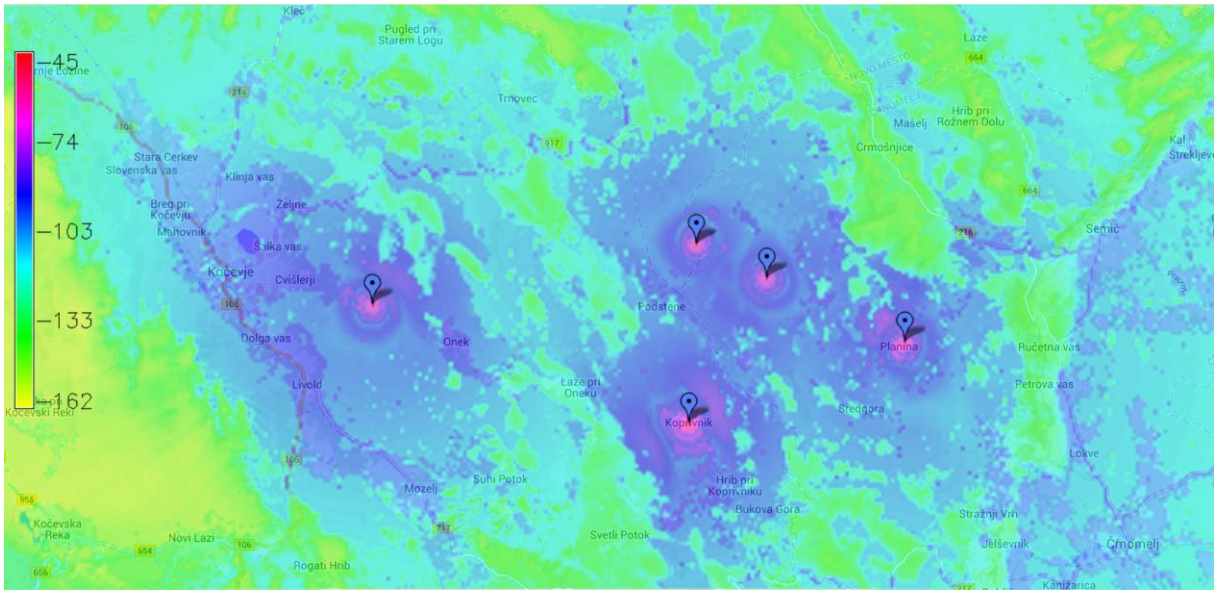

Figure 4-2: Map of the area used for the evaluation scenario. Map also shows exact placement of LAPs and expected received signal strength.

Three different LTE networks were deployed over the area: (i) LTE network from the commercial operator which in the observed area consists of 25 LTE cells. Five (ii) PLMU units and (iii) five LAPs. LAP and PLMU positions were selected to provide coverage in the area and to take into account the position altitude, availability of electrical power and road proximity. For the purposes of the system capacity assessment parts of the network are turned off and on to evaluate the contribution of the specific approach. Main network parameters related to LTE are summarised in Table 4-1. The 800 MHz carrier frequency is used in study in order to achieve a larger coverage on the ground. A total of 99 MM-UEs (end users) were deployed alongside road connecting towns Kocevje and Crnomelj (initial user placement, one-cell base stations, PLMUs, LAPS and routers can be seen from Figure 4-3). All users are assumed mobile and moving towards North East ± 30 º. The direction was reset every 20 seconds in the simulation. MM-UEs velocity was set to 1m / s ± 0.3 m / s offset. The speed was reset also every 20 seconds.

Table 4-1: Main LTE parameters.

Parameter	**Value**
System bandwidths (*W*)	10 MHz
Number of RBs	100
Carrier frequency (*f*)	800 MHz
RB bandwidth	180 kHz
TTI	1 ms
Modulations	QPSK, 16–QAM, 64–QAM
Transmission Power (P_{TX})	23 [dBm] LAP nd PLMU, 43 [dBm] Operator network
Temperature (*T*)	20 ºC
Channel Model	Ericsson channel model for PLMU [20]
Environment Properties	rural
Scheduler	Round robin
Receiver Antenna altitude	1.5 m
Base Station altitude	300m for the LAP, 3m for PLMU and as in the real deployment for the regular network

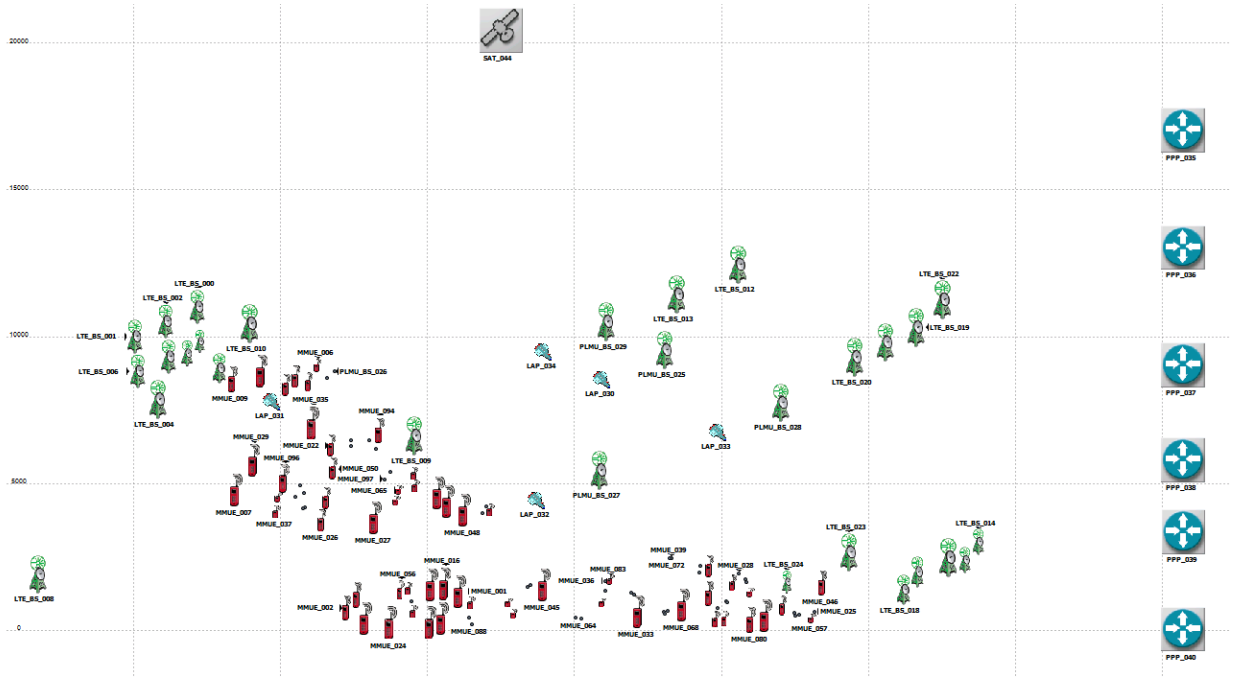

Figure 4-3: Screen shot of the scenario in OPNET Modeler simulation environment from which MM-UE positions LAPs and PLMUs can be identified.

For the purpose of running simulations, we assumed that MM-UEs were using four applications in a random fashion. The settings for applications are summarised in Table 4-2. The packet sizes are constant for all applications. The entries in the table denote the raw packet size without taking into account the required overhead (e.g. destination address, ToS, etc.). Inter-arrival time between packets is constant. Application duration and Inter-arrival time between applications denote average values for which they are calculated using exponential distribution. Video conference is a symmetric application that runs between the MM-UE and a server that is placed outside the disaster area and is accessible via the Internet (e.g. control centre).

VoIP application comes in two varieties: VoIP call to the server (same as Video conference application to the external network such as control centre, marked as VoIP) and between two MM-UEs (marked as VoIP direct). In the second case one of the MM-UEs initiates the call, where destination is selected through a random uniform process. If the selected recipient is available the connections is established, otherwise the call generating MM-UE searches for an alternative destination. The process has a threshold for the repetition.

Since we are interested in the capacity of the LTE network only, users that have the connectivity to one of the LTE base stations generate traffic.

Table 4-2: Main application settings.

Application name	Video Conference	VoIP direct	VoIP	FTP (from server)
Packet size (Kbits)	0.96	0.47	0.47	10
Packet interarrival time (s)	0.025	0.02	0.02	0.02
Application duration (s)	40	15	30	60

Interarrival time between applications (s)	40	240	240	30
Type of Service	2	1	1	3

4.3 Capacity assessment of a network, covering remote Slovenian region

Results are grouped into four cases: (i) the case where all the base stations are in operations (Full network scenario), (ii) only LAP stations are off (LAPs off scenario), (ii) only PLMU stations are off (PLMUs off scenario), and (iv) operator's network is off (Operators network off scenario). In such a way we can evaluate what can be attained using a specific technology in a scenario in which the developed technology might have a potential use.

In Figure 4-4 the number of MM-UEs with connectivity to LTE over time is showed. We consider that a MM-UE unit has LTE connectivity if the most probable received signal strength in the current position is above the threshold (i.e. -120 dBm). The area under observation has scarce communication possibilities and even with 5 LAPs deployed over the area results show that, at the most, approximately 60 % of MM-UE users would have LTE connectivity. As expected the highest impact on connectivity comes from the LAP stations as they cover a large area and thus provide opportunity for connectivity to most of MM-UEs. PLMUs offer unique LTE connectivity only occasionally. This result is also expected as the coverage area of such a device is small, but of course can provide other benefits. We can also see that Operator provides weak coverage with the LTE signal over the region selected for the simulations. Areas that are interesting from the commercial point of view do not necessarily overlap with possible emergency scenarios, such as in our case and where coverage would be of utmost importance.

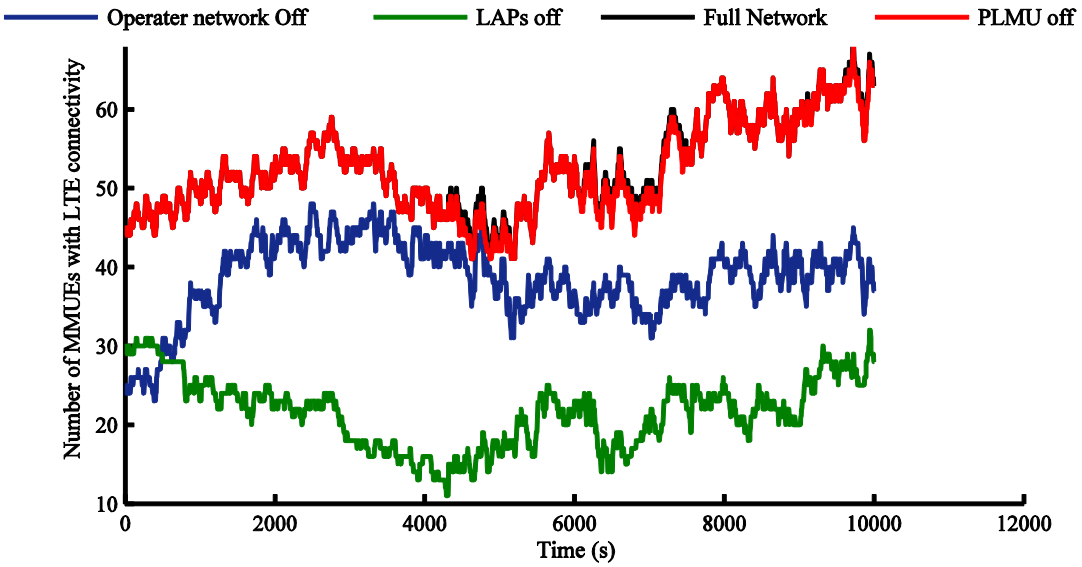

Figure 4-4: Number of MM-UEs with LTE connectivity over time

In Figure 4-5 we show the capacity made available to the MM-UE (i.e. traffic without the overhead on the application layer) in the overloaded network where only few users occasionally receive the required amount of resources. On average approximately 40 % of traffic has been dropped due to full queues in the system. Throughout the simulation there are poorly served demands or even not served

at all. Results show that received Capacity Goodput varies, which can be explained through several factors. First, users are mobile and their received signal strength varies through the simulation, thus affecting the coding and modulation scheme. Second, user demands change dynamically in terms of location (which corresponds to the MM-UE) and intensities (which correspond to the different applications). This affects interference and distribution of available scheduling blocks among LTE cells. In a network placed in such an ad-hoc fashion without pre-simulations or / and calculations, the interference between LTE cells is very likely to have a large impact on the throughput.

In Figure 4-6 capacity assigned to the end-users for all the scenarios with the results averaged over 500 s time intervals. We show that the full network scenario, where in cooperation with operators network is also in use, provides the highest capacity in most of situations. Interestingly, improper placement of PLMU units might cause reduction in total achievable capacity due to interference arising from collocated networks (LTE is a frequency reuse 1 technology). It worth pointing out is also that even though the operator network provides limited connectivity it can still provide the capacity for communications. This can be explained simply considering that the operator's cells are well planned and cover smaller areas with very limited interference, thus assuring that resource blocks are well used and really shared between base stations LTE cells.

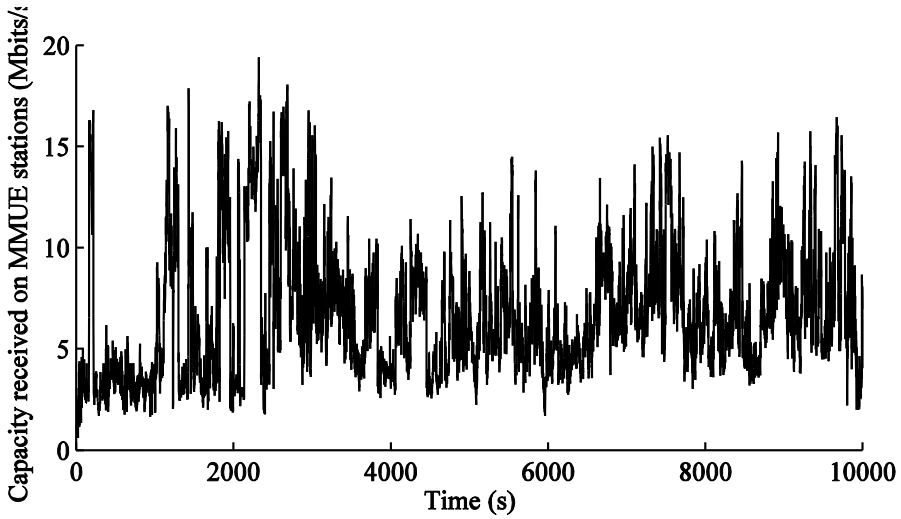

Figure 4-5: Capacity as a sum of Good put on all the MM-UEs for the Full Network scenario.

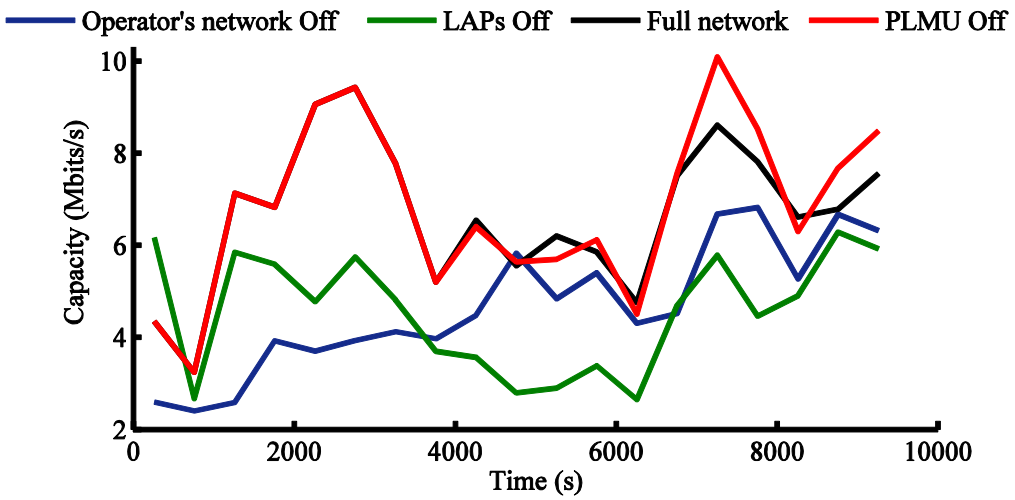

Figure 4-6: Average Capacity on all the MM-UE for different scenarios.

4.4 Conclusions

In this chapter we have analysed scenarios for public safety that are crucially important in ABSOLUTE project. Results have been collected for a remote Slovenian area where such a scenario might well represent a real challenge for the ABSOLUTE system in the future. We have shown that ABOLUTE technologies such as LTE AeNBs are crucial network elements in order to establish a communication network that covers large areas and provide means of communication for many end users. One may argue that the capacity that can be provisioned to the users in terms of throughput does not support stable broadband connectivity and it does not enable multimedia massaging on a larger scale. Anyway, voice calls and FTP applications can still be used as base line services for coordinating the action of PPDR organizations.

5 Capacity of WSN Data Collection with Multiple Gateways

Within this chapter, a scenario where multiple PLMUs are collecting data generated by a set of MM-UEs is considered, and the task in this case consists in designing an efficient access scheme for the MM-UEs in order to transmit and receive data reliably. We model the problem as a sensor network consisting of sensors (or MM-UEs in this particular case) trying to communicate with PLMU units (gateways to the remaining ABSOLUTE network). The channel is accessed by all terminals (i.e. MM-UEs) resorting to a random access scheme to access the gateway (i.e. PLMU) and the diversity gain brought by having more than one receiver available is analysed. A mathematical framework will be developed to investigate this problem, providing insights on the achievable improvements as well as identifying the key trade-offs and system design drivers. The results are relevant to all scenarios where collection of sensor data is critical to help or improve the perception of the emergency scene gathered by PPDR organizations.

In ABSOLUTE context, the LTE system capacity investigated here applies to both post-disasters and temporary events scenarios. Specifically, Table 5-1 below summarizes the scenarios and use cases with involved LTE equipment/subsystems. For more details refer to *D2.1 (Use cases definition and scenarios description)*. Notice that the use case in which the ABSOLUTE network is rolled out or rolled back brings the design of medium access together with the channel detection and estimation covered in D3.2 and D3.3. Furthermore, during the roll-out phase, once the channel is estimated using the algorithms presented in WP3 (in particular D3.1 and D3.3) and the topology management has taken place (using schemes in D4.1), the channel information may be used to select a random access scheme in order to provide an initial communication between MM-UEs and PLMUs.

Table 5-1: Scenarios and use cases with involved equipment/subsystems.

	Use case	Primary equipment	Secondary equipment	Description
	ABS.UC.04	PLMU		Media upload to the PLMU
	1 ABS.UC.05	2 PLMU	3 MM-UE	4 Unified group call
	ABS.UC.10	MM-UE	AeNB, PLMU, Ka-band satellite	Communication from MM-UEs to a remote peer through satellite link
	ABS.UC.11	MM-UE	AeNB, PLMU, Ka-band satellite	Inter-cell communications via the MM-UE's Ka-band links
	5 ABS.UC.17	6 AeNB		Roll-out phase of an AeNB in the context of a disaster
	ABS.UC.22	MM-UE		Direct communications with MM-UEs in relay-mode
Temporary	ABS.UC.12	MM-UE	AeNB, PLMU, Ka-band satellite	Inter-cell communications via the MM-UE's Ka-band links for temporary events
	ABS.UC.15	PLMU/WSN	MM-UE	WSN-assisted crowd monitoring and staff coordination

	ABS.UC.16	PLMU/WSN	MM-UE	Use of body area wireless sensor network in moving events
	ABS.UC.19	AeNB		Rolling-out an AeNB in the context of a temporary event
	ABS.UC.20	AeNB		Rolling-back an AeNB in the context of temporary event

5.1 Scenario

In general, sensor networks are constituted by a number of sensor devices with limited computational power, antenna gain and limited transmission capabilities and a receiver that collects the information sent by the sensors. In the aftermath of a crisis or even during special events both first responders and citizens can be equipped with sensor devices which monitor different vital parameters for example, in a similar fashion to a Body Area Network (BAN). Furthermore, sensors might be deployed inside a specific area to raise the awareness related to an environment-dependent situation (e.g. radiation levels after the Fukushima nuclear power plant breakdown). In both cases in the emergency situations addressed in ABSOLUTE, fast and reliable access to the information transmitted by the sensors can improve the efficiency of the rescue teams and improve tactical knowledge of the emergency scenario. It is hence important to address also this particular component of the ABSOLUTE system and to devise suitable communication protocols which enable the sensors to transmit information reliably over the shared wireless medium even in critical conditions in which the AeNB is either rolled out or rolled back.

There are different Medium Access Control (MAC) protocol solutions to tackle the problem of enabling sensors to share the common transmission medium: Time Division Multiple Access (TDMA), Frequency Division Multiple Access (FDMA) or Code Division Multiple Access (CDMA). These approaches are particularly efficient when the resources requested by the transmitters are relatively constant over the time and if the transmitter's population does not change in size or position. Another class of MAC protocols allow interference reduction among the transmitters and is commonly known as Random Access (RA) protocols such as the ALOHA channel [46]. The main advantages of RA are: flexibility to changes in the population size, location and traffic and in its simplicity from the perspective of a practical implementation. It is clear that, depending on the specific nature of the sensed data, it is necessary to reconstruct the information at the receiver side under different delay constraints. For example, packets containing information such as heart rate or even an ECG trace must comply with specific delay and jitter constraints. Temperature information however can be treated as best effort traffic. Even the sampling time of different observed phenomena shall be different, thus implying different traffic loads. Given the different nature of the sensed information, study the capacity of the sensor network in the context of ABSOLUTE is a way of quantifying the efficiency of selected MAC protocols.

Due to their simplicity and flexibility, RA protocols shall be preferred in sensor network scenarios and therefore this will be the approach for this study. In the following, we will concentrate on showing the benefit of introducing more than one receiver and what capacity gains can be expected compared to the classical scenario with single receiver, where the receivers is in this case are the PLMU units. The scenario can be composed by one or more PLMUs, and/or one or more satellite-enabled MM-UEs.

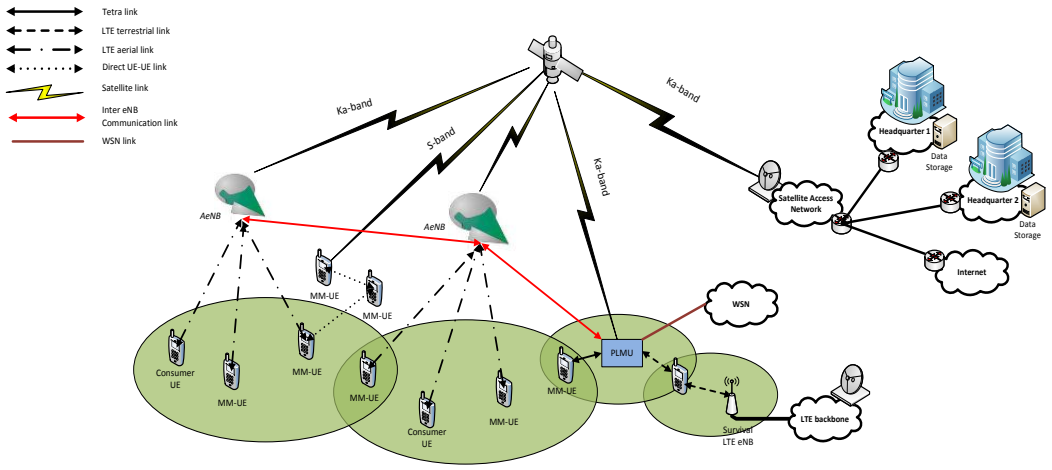

Figure 5-1: ABSOLUTE architecture for a multi-PLMU scenario where PLMUs act as gateways and MM-UEs as generators of sensor traffic.

5.2 Introduction to Random Access and Recent Protocols

A renewed interest for Aloha-like random access (RA) protocols led recently to the development of new high-throughput uncoordinated multiple-access schemes [30]-[39]. These schemes share the feature of cancelling the interference caused by a packet whenever (a portion of) it is successfully decoded. Among the aforementioned works, a specific class is based on the Diversity Slotted ALOHA (DSA) protocol introduced in [40] enhanced by successive interference cancellation (SIC) technique. In [33], [34] it was shown that the SIC process can be well modelled by means of a bipartite graph. By exploiting the graph model, a remarkably-high capacity (e.g., up to 0.8 packets/slot) can be achieved in practical implementations, whereas for large MAC frames it was demonstrated that full efficiency (1 packets/slot) can be substantially attained [37], [39], [41]. A further key ingredient to attain large throughput gains deals with the exploitation of diversity. As an example, the approaches proposed in [30], [33]-[35], [38]-[40] take advantage of time diversity to resolve collisions.

In this section, we focus on developing and analysing a simple yet powerful SA scheme which enjoys space diversity. More specifically, K independent observations of a slot are supposed to be available. The different observations are associated to K PLMUs, and, for each of them, the transmitted packets are subject to independent fading coefficients. Collisions are regarded as destructive, while collision-free received packets are always assumed to be perfectly decoded due to a powerful enough code that can counteract channel impairments. SA with space (antenna) diversity was analysed in [42] under the assumption of Rayleigh fading and shadowing, with emphasis on the two-antenna case. With respect to that work, we introduce in our analysis a simplified channel model. In particular, the uplink wireless link connecting sensor node i and PLMU j is described by a packet erasure channel with erasure probability $\varepsilon_{i,j}$, following the on-off fading model [43][44][45]. The fading is assumed to be independent for each sensor-PLMU pair. Despite its simplicity, the model is accurate enough for many cases of interest. As an example, it captures the main features of an interactive satellite network with satellite located in different orbits and where the line-of-sight link between MM-UEs and PLMUs may be blocked whenever an obstacle lies between a user and a satellite (in this case the satellites replace the PLMUs). Under this fading model, elegant exact expressions for the system throughput as a function of the number of PLMUs are derived, yielding deep insights in the gains provided by diversity in SA protocols.

5.2.1 System Model

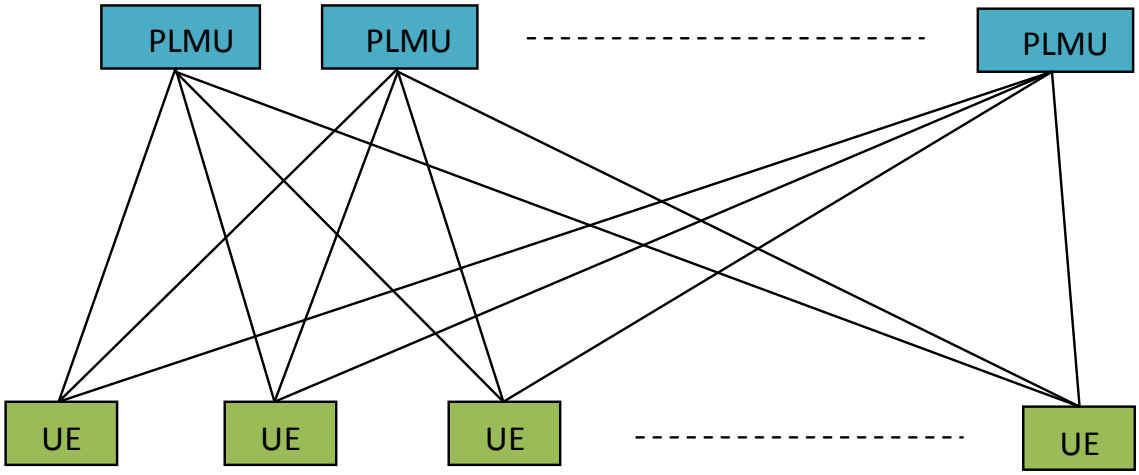

Figure 5-2: Reference topology for studying sensor communications.

Throughout this work, we focus on the topology, where an infinite population of users (MM-UEs) want to deliver information in the form of data packets to a collecting gateway, which in our case is a PLMU. The transmission process is divided in two phases, referred to as uplink and downlink, respectively. During the former, data is originated in a set of KMM-UEs, which in turn, forward collected information to the PLMU in the downlink. In relation to our specific scenario, the uplink phase is the phase that considers the transmission between the MM-UEs and the several PLMUs. This phase consist of the communication between the MM-UEs and PLMUs, and the satellite. Instead, the downlink phase, which is not depicted in the figure, consists of the communication from the PLMUs to a central unit that gathers all the information, and will be considered in the following ideal and without capacity constraints.

As to the uplink, time is divided in successive slots, and transmission parameters in terms of packet length, coding and modulation are fixed such that one packet can be sent within one time unit. Users are assumed to be slot-synchronized, and SA [46] is employed as medium access policy. Furthermore, the number of users accessing the channel in a generic slot is modelled as a Poisson-distributed random variable (r.v.) U of intensity ρ, with:

$$\Pr\{U = u\} = \frac{\rho^u e^{-\rho}}{u!} \tag{5-1}$$

The uplink wireless link connecting MM-UE i and PLMU j is described by a packet erasure channel with erasure probability $\varepsilon_{i,j}$, where each packet transmission between an (i, j) pair (i.e., MM-UE-PLMU pair) is stochastically independent from any other transmission between that pair. For the sake of mathematical tractability, we set $\varepsilon_{i,j} = \varepsilon, \forall\, i, j$. Following the on-off fading description used in [43], we assume that a packet is either completely shadowed, not bringing any power or interference contribution at a receiver, or it arrives not corrupted. While on the one hand such a model is especially useful to develop mathematically tractable solutions which allows highlighting the key trade-offs in the considered scenario, it also effectively captures effects like fading and short-term receiver unavailability due, for instance, to the presence of obstacles. Throughout our investigation, no multi-user detection capabilities are considered at the PLMUs, so that collisions among non-erased data units are regarded as destructive and prevent decoding at a PLMU side.

Within this framework, the number of non-erased packets that arrive at a PLMU when u concurrent transmissions take place follows a binomial distribution with parameters $(u, 1-\varepsilon)$ over one slot. Therefore, a successful reception occurs with probability $u(1-\varepsilon)\varepsilon^{u-1}$ and the average throughput experienced at each of the K PLMUs, in terms of decoded packets per slot can be computed as

$$T_{sa} = \sum_{u=0}^{\infty} \frac{\rho^u e^{-\rho}}{u!} u(1-\varepsilon)\varepsilon^{u-1} = \rho(1-\varepsilon)e^{-\rho(1-\varepsilon)}, \quad (5\text{-}2)$$

which corresponds to the performance of a SA system with erasures.

On the other hand, spatial diversity gain can occur when the PLMUs are considered jointly since independent channel realizations may lead them to retrieve different information units over the same time slot. In order to quantify this beneficial effect, we label a packet as *collected* when it has been received by at least one of the PLMUs and we introduce the uplink throughput $T_{up,K}$ as the average number of collected packets per slot. Despite its simplicity, such a definition offers an effective characterization of the beneficial effects of diversity, by properly accounting for both the possibility of retrieving up to $\min\{u, K\}$ distinct data units or multiple times the same data unit over a slot, as will be discussed in details in the next section. On the other hand, $T_{up,K}$ also quantifies the actual amount of information that can be retrieved by the set of PLMUs, providing an upper bound for the overall achievable end-to-end performance, and setting the target for the design of any user to PLMU delivery strategy.

5.2.2 Notation

Prior to delving into the details of our mathematical framework, we introduce in the following some useful notation. All the variables will be properly introduced when needed in the discussion, and the present section is simply meant to offer a quick reference point throughout the reading.

K PLMUs are made available in the scenario, and, within time slot t, the countably infinite set of possible outcomes at each of them is labeled as $\Omega_t \coloneqq \{\omega_0^t, \omega_1^t, \omega_2^t, \dots, \omega_\infty^t\}$ for each $t = 1,2,\dots,n$. Here, ω_0^t denotes the erasure event (given either by a collision or by an idle slot), while ω_j^t indicates the event that the packet of the j-th user arriving in slot t was received. According to this notation, we define as X_k^t the random variables with alphabet $\mathbb{N}$, where $X_k^t = j$ if ω_j^t was the observation at PLMU k.

When needed for mathematical discussion, we let the uplink operate for n time slots. In this case, let $\mathcal{A}_k^n$ be the set of collected packets after n time slots at PLMU k, where $\mathcal{A}_k^n \subseteq \bigcup_{t=1}^n \{\Omega_t \backslash \omega_0^t\}$. That is, we do not add the erasure events to $\mathcal{A}_k^n$. The number of received packets at PLMU k after n time slots is thus $|\mathcal{A}_k^n|$.

In general, the complement of a set $\mathcal{A}$ is indicated as $\bar{\mathcal{A}}$. We write vectors as lowercase underlined variables, e.g., $\underline{w}$, while matrices and their transposes are labeled by uppercase letters, e.g., G and G^T.

5.3 Capacity of the data collection with multiple PLMUs

With reference to the topology, we now consider the uplink phase. In order to gather a comprehensive description of the improvements enabled by PLMU diversity, we characterize the system by means of two somewhat complementary metrics: uplink throughput and packet loss rate.

5.3.1 Uplink Throughput

Let us focus on the random access channel, and, following the definition introduced previously let C be the number of packets collected by the PLMUs over one slot. C is a r.v. with outcomes in the set $\{0,1,2,\dots,K\}$, where the maximum value occurs when the K receivers decode distinct packets due to different erasure patterns. The average uplink throughput can thus be expressed by conditioning on the number of concurrent transmissions as:

$$T_{up,K} = \mathbb{E}_U\big[\mathbb{E}[C|U]\big] = \sum_{u=0}^{\infty} \frac{\rho^u e^{-\rho}}{u!} \sum_{c=0}^{K} cPr\{C = c|U = u\}\,. \tag{5-3}$$

While equation holds for any K, the computation of the collection probabilities intrinsically depends on the number of available PLMUs. In this perspective, we articulate our analysis by first considering the two-receiver case, to then extend the results to an arbitrary topology.

The Two-PLMU Case

Let us first then focus on the case in which only two PLMUs are available. Such a scenario allows a compact mathematical derivation of the uplink throughput, as the events leading to packet collection at the PLMUs set can easily be expressed. On the other hand, it also represents a case of practical relevance.

When $K = 2$, the situation for $C = 1$ can easily be accounted for, since a single packet can be collected as soon as at least one of the PLMUs does not undergo an erasure, i.e., with overall probability $1 - \varepsilon^2$. On the other hand, by virtue of the binomial distribution of U, the event of collecting a single information unit over one slot occurs with probability

$$\Pr\{C = 1|U = u\} = 2u(1-\varepsilon)\varepsilon^{u-1}[1 - u(1-\varepsilon)\varepsilon^{u-1}] + u(1-\varepsilon)^2\varepsilon^{2(u-1)}\,, \tag{5-4}$$

where the former addend accounts for the case in which one PLMU decodes a packet while the other does not (either due to erasures or to a collision), whereas the latter tracks the case of having the two PLMUs decoding the same information unit. Conversely, a reward of two packets is obtained only when the receivers successfully retrieve distinct units, with probability

$$\Pr\{C = 2|U = u\} = u(u-1)(1-\varepsilon)(1-\varepsilon)^2\varepsilon^{2(u-1)}\,, \tag{5-5}$$

Plugging these results into equation 5.3 we get, after some calculations, a closed-form expression for the throughput in the uplink and thus:

$$T_{up,2} = 2\rho(1-\varepsilon)e^{-\rho(1-\varepsilon)} - \rho(1-\varepsilon)^2 e^{-\rho\left(1-\varepsilon^2\right)} = 2T_{sa} - \rho(1-\varepsilon)^2 e^{-\rho\left(1-\varepsilon^2\right)}, \tag{5-6}$$

The trend of $T_{up,2}$ is shown in 5-6 against the channel load ρ for different values of the erasure probability and compared to the performance in the presence of a single receiver, i.e., T_{sa} (i.e., equation (5-2)). Equation 5-6 conveniently expresses $T_{up,2}$ as twice the throughput of SA in the presence of erasures, reduced by a loss factor which accounts for the possibility of having both PLMUs decoding the same packet. In this case, it is interesting to evaluate the maximum throughput $T^*_{up,2}(\varepsilon)$ as well as the optimal working point $\rho^*(\varepsilon)$ that can be achieving by the system in uplink. The transcendental nature of the equation does not allow obtaining a closed formulation of these quantities, which, on the other hand, can easily be estimated by means of numerical optimization techniques.

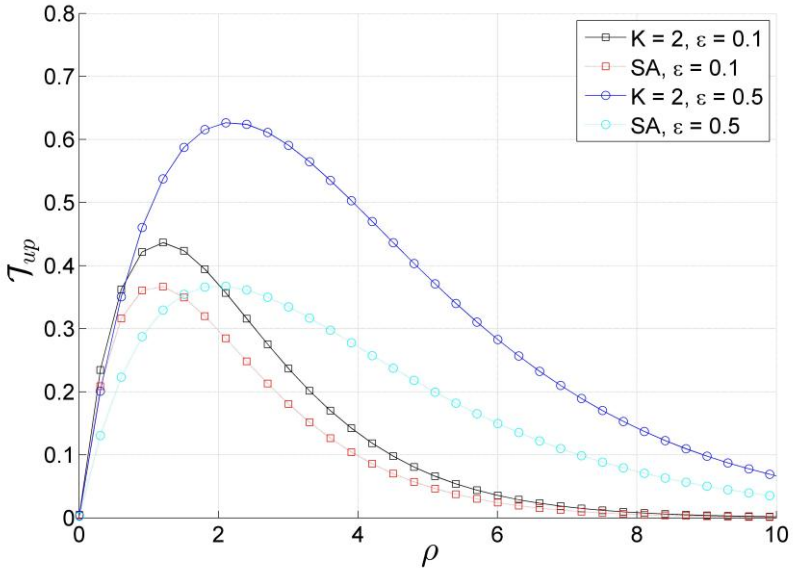

Figure 5-3: Average uplink throughput vs. channel load under different erasure probabilities for one and two PLMU case. Red and light blue markers indicate the performance of SA for the single PLMU case with different packet erasure probabilities. Black and dark blue markers indicate the performance of SA for the two-PLMU case with different erasure probabilities.

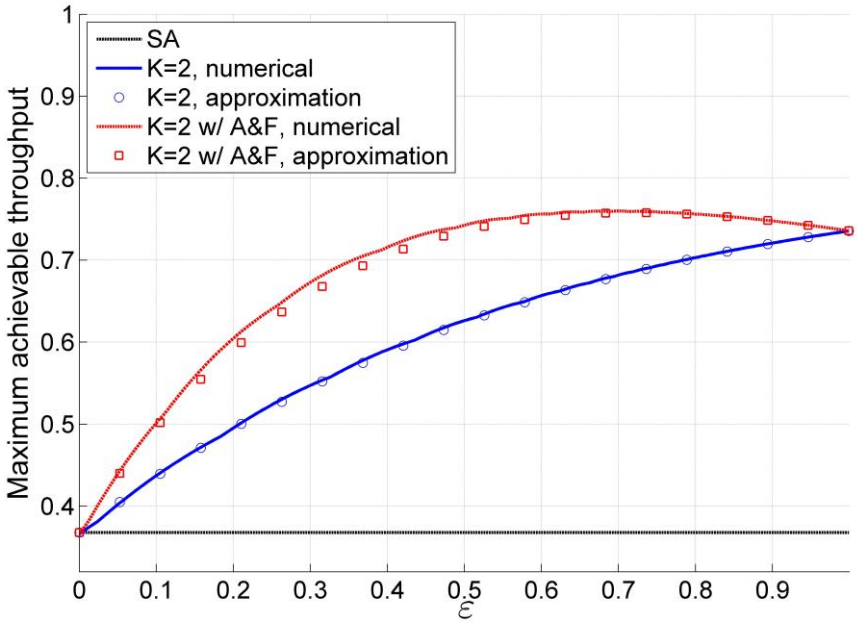

Figure 5-4: Maximum uplink throughput vs. erasure rate. The blue curve reports the performance $T^*_{up,2}$ of a two-PLMU case, while the red curve indicates $T^*_{up,2}(1/(1-\varepsilon))$, and the black straight line shows the behaviour of pure SA.

The results of this analysis are showed in Figure 5-4, where the peak throughput T^*_{up} is depicted by the black curve as a function of ε and compared to the performance of SA, which clearly collects on average at most 0.36 pkt/slot regardless of the erasure rate. In ideal channel conditions, i.e., $\varepsilon = 0$, no benefits can be obtained resorting to multiple PLMUs, as all of them would see the same reception set across the slots. Conversely, higher values of (ε) implies lower collisions and higher probability of

reception of unique packets at different PLMUs, which results in improved throughput. The result is a monotonically increasing behaviour for $T^*_{up,2}(\varepsilon)$, prior to plummeting with a singularity to a null throughput for the degenerate case $\varepsilon = 1$. Figure 5-3 also reports (red curve) the average throughput obtained for $\rho = 1/(1-\varepsilon)$, i.e., when the uplink of the system under consideration operates at the optimal working point for a single-PLMU SA, showing a tight match. In fact, even though the abscissa of maximum $\rho^*(\varepsilon)$ may differ from this value (they coincide only for the ideal case $\varepsilon = 0$), the error which is committed when approximating $T^*_{up,2}$ with $T^*_{up,2}(1/(1-\varepsilon))$ can easily be shown numerically to never exceed 0.6%, due to the very small slope of the function in the neighbourhood of $\rho^*(\varepsilon)$. We can thus provide a very precise estimate of the peak uplink performance for a specific erasure rate as:

$$T^*_{up,2}(\varepsilon) \simeq \frac{2}{e} - (1-\varepsilon)e^{-1-\varepsilon}, \qquad 0 \le \varepsilon \le 1$$

which once again compactly captures the behaviour of a two-user scenario by quantifying the loss with respect to twice the performance of SA.

Two remarks shall be done at this point. First of all, in order to approach the upper bound, the system has to be operated at very high load, as $\rho^* \simeq 1/(1-\varepsilon)$. These working points are typically not of interest, since very low levels of reliability can be provided by a congested channel with high erasure rates. Nevertheless, the presence of a second PLMU triggers remarkable improvements already for loss probabilities that are of practical relevance, e.g., under harsh fading conditions or for satellite networks. Indeed, with $\varepsilon = 0.1$ almost a 15% raise can be spotted, whereas a loss rate of 20% already leads to a 50% throughput gain. Second, the number of MM-UEs that can be supported by a single PLMU does not change when another PLMU is added. Such a result is particularly interesting, as it suggests that a second PLMU can be seamlessly and efficiently added to an already operating PLMU, triggering the maximum achievable benefit without the need to undergo a re-tuning of the system, which might be particularly expensive in terms of resources.

The General Case, $K > 2$

Let us now focus on the general topology, where K PLMUs are available. Notice that we do not normalize the throughput with respect to the number of PLMUs. While conceptually applicable, the approach presented to compute the uplink throughput in the two-PLMU case becomes cumbersome as K grows, due to the rapidly increasing number of events that have to be accounted for. In order to characterize $T_{up,K}$, then, we follow a different strategy. With reference to a single slot t, let $\Omega_t \coloneqq \{\omega_0^t, \omega_1^t, \omega_2^t, \dots, \omega_\infty^t\}$ for each $t = 1,2,\dots,n$ be the countably infinite set of possible outcomes at each PLMU, where ω_0^t denotes the erasure event while ω_j^t indicates the event that the packet of the j-th MM-UE arriving in slot t was received. Let us furthermore define as X_k^t the random variables with alphabet $\mathcal{X} = \{0,1,2,\dots,\infty\}$, where $X_k^t = j$ if ω_j^t was the observation at PLMU k, so that $X_k^1, X_k^2, \dots, X_k^n$ is an i.i.d. sequence for each PLMU k. We let the uplink operate for n time slots, and indicate as $\mathcal{A}_k^n$ the set of packets collected at PLMU k over this time-span, where $\mathcal{A}_k^n \subsetneq \bigcup_{t=1}^n \{\Omega_t \setminus \omega_0^t\}$ (i.e., we do not add the erasure events to $\mathcal{A}_k^n$). The number of received packets at PLMU k after n time slots is thus $|\mathcal{A}_k^n|$ and, it is possible to prove the following result:

Proposition 5-1

For an arbitrary number of K relays, the throughput $T_{up,K}$ is given by

$$T_{up,K} = \sum_{k=1}^{K}(-1)^{k-1}\binom{K}{k}\rho(1-\varepsilon)^k e^{-\rho(1-\varepsilon^k)}\,, \tag{5-7}$$

The complete proof can be found in [47].

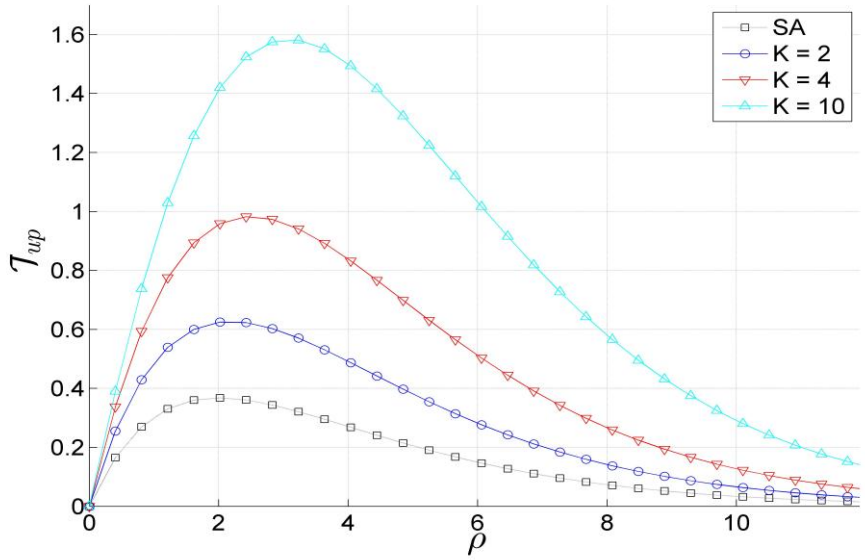

Figure 5-5: Average uplink throughput vs. channel load for different number of PLMUs K. The erasure probability has been set to $\varepsilon = 0.5$.

The performance achievable by increasing the number of PLMUs is reported against the channel load in Figure 5-5 for a reference erasure rate $\varepsilon = 0.5$. As expected, $T_{up,K}$ benefits from a higher degree of spatial diversity, showing how the system can collect more than one packet per uplink slot as soon as more than four PLMUs are made available, for the parameters under consideration. Such a result stems from two main factors. On the one hand, increasing K enables larger peak throughput over a single slot, as up to K different data units can be simultaneously retrieved. On the other hand, broader PLMU sets improve the probability of decoding packets in the presence of collisions even when less than K users accessed the channel by virtue of the different erasure patterns they experience.

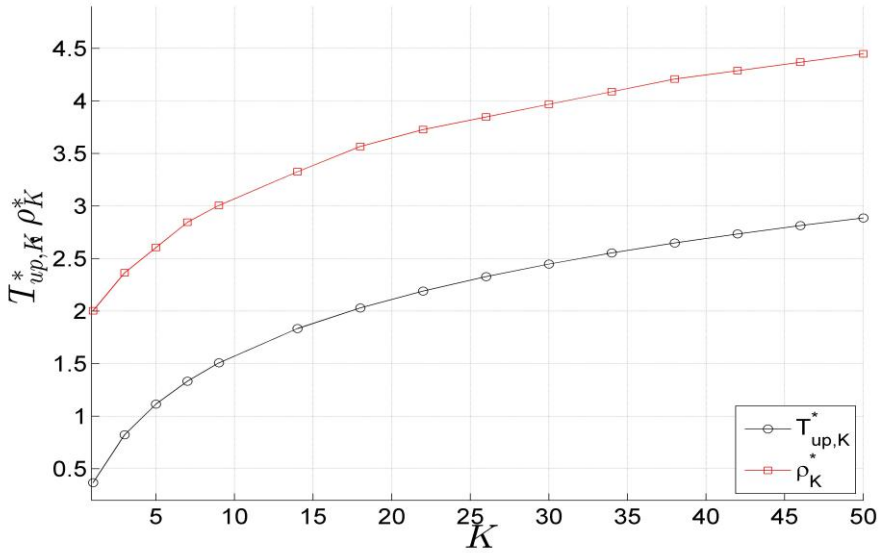

Figure 5-6: Maximum achievable throughput $T^*_{up,K}$ as a function of the number of PLMUs K for an erasure rate $\varepsilon = 0.5$. The gray curve reports the load on the channel ρ^*_K needed to reach $T^*_{up,K}$.

The uplink throughput characterization is complemented by Figure 5-6 which reports the peak value for $T^*_{up,K}$ (solid black curve), obtained by properly setting the channel load to ρ^*_K (whose values are shown by the gray dashed curve) for an increasing size of the PLMU population. The figure clearly highlights how the benefit brought by introducing an additional PLMU to the scheme, progressively reduces, leading to a growth rate for the achievable throughput that is less than linear and that exhibits a logarithmic-like trend in K. This behaviour is captured in equation **Erreur ! Source du renvoi introuvable.**.

$$\Delta_{T_{up}} = T_{up,K} - T_{up,K-1} = \sum_{k=1}^{K}(-1)^{k-1}\binom{K-1}{k-1}\rho(1-\varepsilon)^k e^{-\rho(1-\varepsilon^k)}, \quad (5\text{-}8)$$

5.3.2 Packet Loss Probability

The aggregate throughput derived in the previous section represents a metric of interest towards understanding the potential of SA with diversity when aiming at reaping the most out of uplink bandwidth. On the other hand, operating an Aloha-based system at the optimal load ρ^*_K exposes each transmitted packet to a loss probability that may not be negligible. In the classical single-PLMU case without fading for instance, the probability for a data unit not to be collected evaluates to $1 - e^{-1} \simeq 0.63$. From this standpoint, in fact, several applications may resort to a lightly loaded random access uplink, aiming at a higher level of delivery reliability rather than at a high throughput. This is the case, for example, of channels used control signalling in many practical wireless networks. In order to investigate how diversity can improve performance in this direction, we extend our framework by computing the probability ζ_K that a user accessing the channel experiences a data loss, i.e., that the information unit it sends is not received correctly, due to fading or collisions, by any of the K PLMUs.

To this aim, let O describe the event that the packet of the observed MM-UE sent over time slot t is not received by any of the PLMUs. Conditioning on the number of interferers$i$, i.e., of data units that were concurrently present over the uplink channel at t, the sought probability can be written as:

$$\zeta_K = \sum_{i=0}^{\infty} \Pr[O|I=i]\Pr[I=i]$$

Here, the conditional probability can easily be determined recalling that each of the K PLMUs experiences an independent erasure pattern, thus obtaining $\Pr[O|I=i] = \left(1-(1-\varepsilon)\varepsilon^i\right)^K$ for an individual packet and K PLMUs with independent erasures on individual links. By resorting to the binomial theorem, such an expression can be conveniently reformulated as:

$$\Pr[O|I=i] = \sum_{k=0}^{K} (-1)^k \binom{K}{k} \left((1-\varepsilon)\varepsilon^i\right)^k$$

On the other hand, the number of interferers seen by a user that access the channel at time t still follows a Poisson distribution of intensity ρ, so that, after simple calculations we finally obtain

$$\zeta_K = \textstyle\sum_{k=0}^{K} (-1)^k \binom{K}{k} (1-\varepsilon)^k e^{-\rho(1-e^k)}\,, \tag{5-9}$$

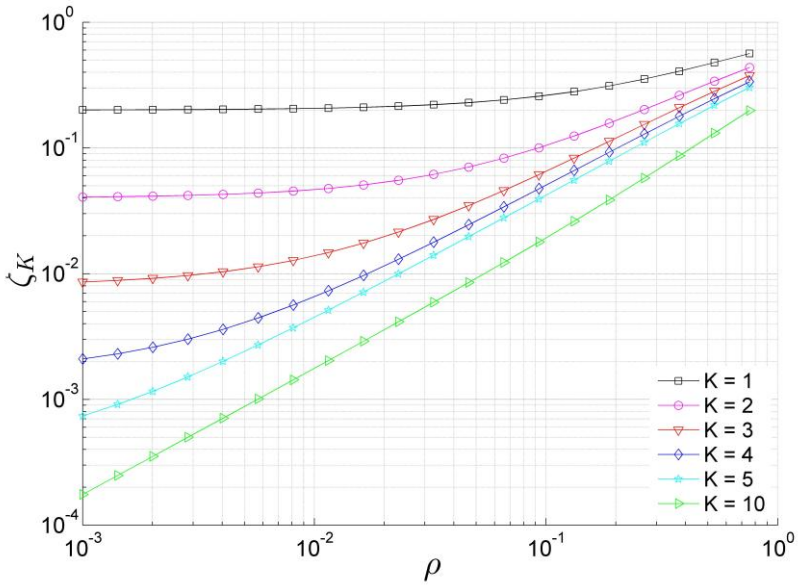

Figure 5-7: Probability ζ_K that a packet sent by a user is not received by any of the PLMUs. Different curves indicate different values of K, while the erasure probability has been set to $\varepsilon = 0.2$.

Figure 5-7 reports the behaviour of ζ_K as a function of ρ when the erasure rate over a single link is set to $\varepsilon = 0.2$. Different lines indicate the trend when increasing the number of PLMUs from 1 to 10. As possible to predict, when $\rho \to 0$, a user accessing the channel is not likely to experience any interference, so that failures can only be induced by erasures, leading to an overall loss probability of ε^k. In this perspective, the availability of multiple PLMUs triggers a dramatic improvement, enabling levels of reliability that would otherwise not be possible irrespective of the channel configuration. On the other hand, equation turns out to be useful for system design, as it allows determining the load which can be supported on the uplink channel while guaranteeing a target loss rate. Also in this case, diversity can significantly ameliorate the performance. As shown, for example, a target loss rate $\zeta = 5 \cdot 10^{-2}$ is achieved by a three and four PLMU scheme under 6- and 10-fold larger loads compared to the $K = 2$ case, respectively.

5.4 Conclusions

The context of public safety where the ABSOLUTE system is deployed requires the network to cope with extreme conditions in which PPDR organizations are demanded to intervene. The ABSOLUTE network is meant to relief most of the limitations of existing technologies for public safety and to help first responders in improving the quality of the rescue they can provide. This means that several different situations typical of public safety have to be taken into account. In this sense, a network of sensors either worn by the first responders (e.g. BAN) or deployed in the environment needs to be studied.

We modelled the communication link between MM-UEs and PLMUs deployed over the area of a crisis or of a temporary event in terms of a medium access problem between MM-UEs and PLMU units. We considered first the two-PLMU case and showed that the proposed framework highlights how no modification in terms of number of supported MM-UEs is needed with respect to plain SA for a two-PLMU system to be efficiently operated. Such a result is of particular interest since it suggests that PLMUs can be seamlessly and efficiently added to an already operating SA uplink when available, creating the maximum achievable benefit without the need to undergo a re-tuning of the system, which might be particularly expensive in terms of resources.

For more than two PLMUs, the throughput performance achievable by increasing the number of PLMUs benefits from a higher degree of spatial diversity, showing how the system can collect more than one packet per uplink slot as soon as more than four PLMUs are available. Such a result stems from two main factors. On the one hand, increasing PLMUs enables larger peak throughput over a single slot since up to K different data units can be simultaneously retrieved. On the other hand, a larger set of PLMUs improves the probability of decoding packets in the presence of collisions exploiting the independent erasure patterns of each link.

6 Conclusions

This deliverable has provided an exhaustive set of studies on system capacity attainable by the ABSOLUTE network in both post disaster and temporary event scenarios. Results have been obtained using system, packet level simulators and analytical tools. The main constituents of the ABSOLUTE network, the AeNB, the PLMU and the MM-UE, have been considered in different conditions of traffic, public safety scenarios where first responders have to intervene and type of services requested by PPDR organizations. In particular, the network constituents of the ABSOLUTE system were considered either individually or mixing them in order to conduct a study as general as possible. This approach is functional to evaluate the capabilities of the overall ABSOLUTE architecture and create the necessary understanding of the performance which can be achieved in realistic public safety scenarios. The satellite link has been assumed always present to provision a radio signal over a wide geographical area. Furthermore, the studies on capacity have been complemented with a study on sensor networks in which first responders could wear a BAN that monitors their life parameters or it could monitor the conditions in the surrounding environment.

The studies have shown that per MM-UE and per cell capacity are largely affected by the selection of the scheduling discipline. Few megabits per second can be provisioned on average to a MM-UE inside the ABSOLUTE network depending also on the channel conditions. A reinforcement learning approach to manage the frequency spectrum has showed to be crucial for the sake of provisioning the necessary resources in the network. Along the same line, load balancing and unbalancing with different associated priorities has allowed to quantify the number of base stations which would be needed as the traffic load increases. Simulation studies on the capacity which can be provisioned to the first responders over time have showed a strong dependence on the environment and the type of services requested by the first responders (e.g. VoIP or FTP). Furthermore, the capacity provisioned by AeNB shows to be the most important for the MM-UEs and even if the PLMU units would be deployed in minimal part, the throughput degradation would anyway be marginal. The PLMU can still provide benefits and in particular in several different scenarios and it can be the gateway to transfer sensor data to the command centre (either local or remote) in order to better coordinates the actions of the PPDR organizations.

In conclusions, the results presented in this deliverable show that the innovative ABSOLUTE architecture is capable to unfold the necessary capacity required in both post disaster and temporary event scenarios by the first responders. Since scenarios for public safety are complex it is imperative to use intelligently all the network resources and in this respect a cognitive approach to the problem shows to be very important.

References

[1] URL of ABSOLUTE project: http://www.absolute-project.eu

[2] The 3rd Generation Partnership Project (3GPP). Available at: http://www.3gpp.org.

[3] T. Doumi, M. Dolan, S. Tatesh, A. Casati, G. Tsirtsis, K. Anchan, and D. Flore, "LTE for public safety networks," IEEE Comm. Mag., vol. 51, no. 2, 2013.

[4] L. Ruiz de Temino, G. Berardinelli, S. Frattasi, and P. Mogensen, "Channel-aware scheduling algorithms for SC-FDMA in LTE uplink," in IEEE PIMRC, Sept 2008, pp. 1–6.

[5] B. Sadiq, R. Madan, and A. Sampath, "Downlink scheduling for multiclass traffic in LTE," EURASIP J. Wirel. Commun. Netw., vol. 2009, pp. 14:9–14:9, Mar. 2009.

[6] O. Osterbo, "Scheduling and capacity estimation in LTE," in IEEE ITC, 2011, pp. 63–70.

[7] G. Araniti, M. Condoluci, L. Militano, and A. Iera, "Adaptive resource allocation to multicast services in LTE systems," IEEE Trans. on Broadcasting, vol. 59, no. 4, pp. 658–664, 2013.

[8] "Technical Specification Group Radio Access Networks; Deployment aspects (Release 8)," Available at: http://www.3gpp.org/ftp/Specs/html-info/25943.htm.

[9] S. Schwarz, C. Mehlfuhrer, and M. Rupp, "Throughput maximizing multiMM-UE scheduling with adjustable fairness," in IEEE ICC, 2011.

[10] R. Kwan, C. Leung, and J. Zhang, "Proportional fair multiMM-UE scheduling in LTE," IEEE SPL, vol. 16, no. 6, 2009.

[11] S. Schwarz, C. Mehlfuhrer, and M. Rupp, "Low complexity approximate maximum throughput scheduling for LTE," in IEEE ASILOMAR, Nov 2010.

[12] E. Yaacoub and O. Kubbar, "On the performance of distributed base stations in LTE public safety networks," in IEEE IWCMC, Aug 2012.

[13] R. Hallahan, J. M. & Peha, (2011) The Business Case of a Network that Serves both Public Safety and Commercial Subscribers. *Telecommunications Policy*, Volume 35, Issue 3, April 2011, Pages 250-268,doi:10.1016/j.telpol.2010.12.006.

[14] S, Borkar, D. Roberson and K. Zdunek, "Priority Access for public safety on shared commercial LTE networks," Telecom World (ITU WT), 2011 Technical Symposium at ITU, vol., no., pp.105,110, 24-27 Oct. 2011.

[15] J. C. Ikuno, M. Wrulich, and M. Rupp, "System level simulation of LTE networks," in Proc. 2010 IEEE VTC, Taipei, Taiwan, May 2010.

[16] R. Jain, D.-M. W. Chiu, and W. R. Hawe, "A Quantitative Measure of Fairness And Discrimination For Resource Allocation In Shared Computer Systems," Digital Equipment Corp., Tech. Rep., Sep. 1984.

[17] M. Lerch, S. Caban, M. Mayer and M. Rupp, "The Vienna MIMO Testbed: Evaluation of Future Mobile Communication Techniques," Intel Technology J. (Invited), 4G Wireless Communications: Real World Aspects and Tools, vol. 3, pp. 58-69, 2014.

[18] J. Rodriguez-Pineiro, M. Lerch, J. A. Garcia Naya, S. Caban, M. Rupp and L. Castedo, "Emulating Extreme Velocities of Mobile LTE Receivers in the Downlink," EURASIP J. on Wireless Communications and Networking, Experimental Evaluation in Wireless Communications, vol. 1, pp. 1-14, 2015.

[19] A. Al-Hourani, S. Kandeepan, and A. Jamalipour, "Modeling air-to-ground path loss for low altitude platforms in urban environments," in IEEE GLOBECOM, Dec 2014, pp. 2898-2904.

[20] Sami A Mawjoud. Path Loss Propagation Model Prediction for GSM Network Planning. International Journal of Computer Applications 84(7):30-33, December 2013.

[21] A. Papadogiannis and A. G. Burr, "Multi-beam assisted MIMO - A novel approach to fixed beamforming," in Future Network & Mobile Summit (FutureNetw), 2011, pp. 1-8.

[22] J. D. Chimeh, M. Hakkak, and S. A. Alavian, "Internet Traffic and Capacity Evaluation in UMTS Downlink," in Future Generation Communication and Networking, 2007, pp. 547-552.

[23] A. Hrovat, A. Vilhar, I. Ozimek, T. Javornik, and E. Kocan, "GRASS-RaPlaT - Radio planning tool for GRASS GIS system," in International Conference on Applied Electromagnetics and Communications, 2013.

[24] Q. Zhao, D. Grace, and T. Clarke, "Transfer learning and cooperation management: balancing the quality of service and information exchange overhead in cognitive radio networks," *Transactions on Emerging Telecommunications Technologies*, vol. 26, pp. 290-301, 2015.

[25] Q. Zhao, T. Jiang, N. Morozs, D. Grace, and T. Clarke, "Transfer Learning: A Paradigm for Dynamic Spectrum and Topology Management in Flexible Architectures," in IEEE 78th Vehicular Technology Conference September 2013.

[26] Q. Zhao and D. Grace, "Transfer learning for QoS aware topology management in energy efficient 5G cognitive radio networks," 5G for Ubiquitous Connectivity (5GU), 2014 1st International Conference on , vol., no., pp.152,157, 26-28 Nov. 2014

[27] R. B. Cooper, Introduction to Queueing Theory: Elsevier North Holland, Inc, 1981.

[28] A. Mohammed, A. Mehmood, F. N. Pavlidou, and M. Mohorcic, "The Role of High-Altitude Platforms (HAPs) in the Global Wireless Connectivity," Proceedings of the IEEE, vol. 99, pp. 1939-1953, 2011.

[29] Transparency Market Research, "High Altitude Platforms (HAPs) Technologies Market - Global Industry Analysis, Size, Share, Growth, Trends and Forecast (2012 - 2018)," ed: Transparency Market Research

[30] E. Casini, R. D. Gaudenzi, and O. del Rio Herrero, "Contention Resolution Diversity Slotted ALOHA (CRDSA): An Enhanced Random Access Scheme for Satellite Access Packet Networks." IEEE Trans. Wireless Commun., vol. 6, pp. 1408–1419, Apr. 2007.

[31] Y. Yu and G. B. Giannakis, "High-Throughput Random Access Using Successive Interference Cancellation in a Tree Algorithm," IEEE Trans. Inf. Theory, vol. 53, no. 12, pp. 4628–4639, Dec. 2007.

[32] S. Gollakota and D. Katabi, "Zigzag Decoding: Combating Hidden Terminals in Wireless Networks," in Proceedings of the ACM SIGCOMM 2008 Conference on Data communication, ser. SIGCOMM '08, 2008, pp. 159–170.

[33] G. Liva, "Graph-Based Analysis and Optimization of Contention Resolution Diversity Slotted ALOHA," IEEE Trans. Commun., vol. 59, no. 2, pp. 477–487, Feb. 2011.

[34] E. Paolini, G. Liva, and M. Chiani, "High Throughput Random Access via Codes on Graphs: Coded Slotted ALOHA," in Proc. 2011 IEEE Int. Conf. Commun., Kyoto, Japan, Jun. 2011.

[35] C. Kissling, "Performance Enhancements for Asynchronous Random Access Protocols over Satellite," in Proc. 2011 IEEE Int. Conf. Commun., Kyoto, Japan, Jun. 2011.

[36] A. Tehrani, A. Dimakis, and M. Neely, "SigSag: Iterative Detection Through Soft Message-Passing," vol. 5, no. 8, pp. 1512 –1523, Dec. 2011.

[37] G. Liva, E. Paolini, M. Lentmaier, and M. Chiani, "Spatially-Coupled Random Access on Graphs," in Proc. IEEE Int. Symp. on Information Theory, Cambridge, MA, USA, Jul. 2012.

[38] C. Stefanovic, P. Popovski, and D. Vukobratovic, "Frameless ALOHA Protocol for Wireless Networks," IEEE Commun. Lett., vol. 16, no. 12, pp. 2087–2090, 2012.

[39] K. Narayanan and H. D. Pfister, "Iterative Collision Resolution for Slotted ALOHA: An Optimal Uncoordinated Transmission Policy," in Proc. 2012 7th International Symposium on Turbo Codes and Iterative Information Processing (ISTC), Gothenburg, Sweden, Aug. 2012.

[40] G. L. Choudhury and S. S. Rappaport, "Diversity ALOHA - A Random Access Scheme for Satellite Communications," IEEE Trans. Commun., vol. 31, pp. 450–457, 1983.

[41] E. Paolini, G. Liva, and M. Chiani, "Graph-Based Random Access for the Collision Channel without Feed-Back: Capacity Bound," in Proc. 2011 IEEE Global Telecommun. Conf., Houston, Texas, Dec. 2011.

[42] M. Zorzi, "Mobile Radio Slotted ALOHA with Capture, Diversity and Retransmission Control in the Presence of Shadowing," Wireless Networks, vol. 4, pp. 379 –388, Aug 1998.

[43] E. Perron, M. Rezaeian, and A. Grant, "The On-Off Fading Channel," in Proc. IEEE Int. Symp. on Information Theory, Yokohama, Japan, Jul. 2003, p. 244.

[44] A. F. Dana, R. Gowaikar, R. Palanki, B. Hassibi, and M. Effros, "Capacity of Wireless Erasure Networks," Information Theory, IEEE Transactions on, vol. 52, no. 3, pp. 789–804, 2006.

[45] T. Ho, M. Medard, R. Koetter, D. R. Karger, M. Effros, J. Shi, and B. Leong, "A Random Linear Network Coding Approach to Multicast," Information Theory, IEEE Transactions on, vol. 52, no. 10, pp. 4413–4430, 2006.

[46] N. Abramson, "The ALOHA System - Another Alternative for Computer Communications," in Proc. 1970 Fall Joint Computer Conference, vol. 37. AFIPS Press, 1970, pp. 281–285.

[47] A. Munari, M. Heindlmaier, G. Liva and M. Berioli, "The Throughput of Slotted Aloha with Diversity" in Proc. of 51st Allerton Conference, Allerton House, Illinois USA, pp. 698-706, 2013.

Acknowledgement

(Mandatory Text) This document has been produced in the context of the ABSOLUTE project. ABSOLUTE consortium would like to acknowledge that the research leading to these results has received funding from the European Commission's Seventh Framework Programme (FP7-2011-8) under the Grant Agreement FP7-ICT-318632.